Sede Amministrativa: Università degli Studi di Padova

Dipartimento di Biologia

SCUOLA DI DOTTORATO DI RICERCA IN : Bioscienze e Biotecnologie

INDIRIZZO: Biotecnologie

CICLO: XXV

The role of specific serum/plasma proteins in the modulation of the cellular response to amorphous silica nanoparticles

Direttore della Scuola: Ch.mo Prof. Giuseppe Zanotti

Coordinatore d'indirizzo: Ch.mo Prof. Giorgio Valle

Supervisore: Ch.mo Prof. Emanuele Papini

Dottorando: Chiara Fedeli

ai miei genitori

Table of contents

Abstract

Nanoparticles are structures of different dimensions (1-100 nm) and composition (metal oxides, organic acid polymers, silica polymers) present in the environment as a consequence of natural processes (such as volcanic eruptions or dusts erosion) or anthropogenic activities (industrialization or pollution). In the last decades they have been intensely studied and engineered for industrial applications (as additive of food, cosmetics and building materials) and medical purposes, where they can be employed as drug carriers or imaging agents. Thanks to its abundance, cheapness and resistance to a variety of environmental perturbations, silicon dioxide (SiO_2) is one of the most widely used materials in both industrial and biomedical fields in its amorphous form (contrary to crystalline silica that causes silicosis, a chronic pulmonary disease common in occupational categories largely exposed to silica crystals, such a miners and ceramic workers). Despite amorphous silica is considered much less dangerous than crystalline silica, recent evidences have shown cytotoxic and pro-inflammatory potential in *in vitro* and animal models. To shed more light on this topic, in the first part of my PhD work I have characterized amorphous silica toxicity and inflammatory effects in primary human monocytes and macrophages (myeloid professional phagocytic cells) and on primary human lymphocytes and HeLa cells (lymphoid and epithelial non-phagocytic cells), using as nanoparticles model the commercial non labeled Ludox TM40 (29 nm Ø) and the fluorescein labeled Stöber (35 nm Ø). In particular, the influence of serum and the possible mechanisms determining silica nanoparticles (SiO_2-NPs) effects have been investigated. I have found that SiO_2-NPs toxicity (evaluated as mitochondrial dysfunction and plasma membrane permeabilization) was stronger in phagocytes (LD50 after 18 h exposure ~ 40 µg/ml) and, in these cells, associated to the production of the three main inflammatory cytokines (IL-1β, TNF-α and IL-6). On the contrary, non phagocytic cells were much more resistant (LD50 after 18 h exposure ~ 300-500 µg/ml) and, curiously, HeLa cells were subjected apoptosis after SiO_2-NPs treatment (while monocytes, macrophages and lymphocytes became necrotic). Cytofluorimetric and confocal microscopy analysis have shown that SiO_2-NPs were engulfed in acidic compartments (phagolysosomes) in monocytes and macrophages, while they mostly localized onto plasma membrane in HeLa cells. This suggested that the higher sensitivity of the two phagocytic models could be due to the more efficient internalization of the particles, followed by lysosomal rupture (as indicated by experiments showing the decrease of the

fluorescence associated to the lysosomotropic agent Lysotracker upon cellular exposure to high NPs doses) and the consequent liberation of lysosomal proteases (as reported in literature for crystalline silica). To investigate if acidic lysosomal pH could influence SiO_2-NPs cytotoxicity in phagocytes, cells were treated with silica in the absence or in the presence of two pH neutralizing agents (NH_4Cl and Bafilomycin AI), resulting in a significant protective effect in monocytes and in a negligible protection in macrophages. As mentioned above, we found that in myeloid cells SiO_2-NPs induced an inflammatory response (more pronounced in monocytes), starting in the correspondence of the beginning of cytotoxicity, reaching a peak and decreasing at high NPs doses because of the strong and anticipated cellular death. In particular, IL-1β was the cytokine most represented in both cellular types, while TNF-α and IL-6 levels were lowers. Moreover, in monocytes (and, in less degree in macrophages) IL-1β production was synergized by the co-stimulation with silica and lypopolisaccharide (LPS). Since crystalline silica is known to activate the NLRP3 inflammasome (a cytosolic multiprotein complex responsible of the production of some inflammatory cytokines, primarily IL-1β) we investigated NLRP3 activation by amorphous SiO_2-NPs in our myeloid cellular models. We found that monocytes and macrophages treatment with SiO_2-NPs increased pro-IL1β levels, and that its conversion into mature IL-1β involved caspase 1 activation, intracellular ATP release and subsequent binding to ATP receptor P2X7. Interestingly, P2X7 blockage did not affect SiO_2-NPs induced cellular death in both cells, and caspase 1 inhibition did not reduce SiO_2-NPs toxicity in macrophages but showed a protective effect in monocytes, suggesting that amorphous silica might induce pyroptosis (a caspase 1 dependent cellular death) in these cells.

Afterwards, I have studied how serum could modulate SiO_2-NPs toxicity and pro inflammatory effects. In the presence of increasing FCS amount both SiO_2-NPs cytotoxicity threshold and LD50 were shifted to higher NPs doses, indicating a serum protective action (more pronounced in non-phagocytic cells in comparison to phagocytes). In parallel, also inflammatory cytokines production in myeloid cells occurred at higher NPs concentrations with the increment of FCS percentage. To investigate if the protective serum effect reflected a modification in NPs cellular association I have performed experiments with the fluorescent Stöber NPs, finding that the presence of serum strongly decreased NPs cellular binding in lymphocytes and HeLa, with a moderate reduction in monocytes and macrophages. This result was in accord with

the stronger serum protection in non phagocytic cells, and consolidated the hypothesis that SiO_2-NPs toxicity depends on their interaction level with cells. Also SiO_2-NPs cellular localization was affected by different serum concentrations. In particular, I have found that in the absence of serum SiO_2-NPs mostly localized onto the plasma membrane in monocytes and HeLa, while in macrophages they were still internalized into phagolysosomes, even if with a lower efficiency. Considering this different NPs sub-cellular localization, I have investigated if the protective effect of NH_4Cl, Bafilomycin AI and caspase 1 inhibitor observed in monocytes in standard culture conditions (10% FCS) was maintained also in the absence of serum. Interestingly, neither acidic compartments neutralization nor caspase 1 blockage were able to reduce SiO_2-NPs toxicity in serum free conditions, suggesting that monocytes cellular death mechanism was different with or without serum.

In the second part of my PhD work I have studied several aspects of nanoparticles interaction with plasma and serum proteins, since this is a very important point in nanomaterials biomedical applications. Indeed, when nanoparticles (functioning as drug-gene vectors or imaging agents) are introduced in the human body (primary, into the bloodstream), they are rapidly coated by a series of specific proteins, forming the so called " nanoparticles corona" and mediating cellular response to nanomaterial. This problematic was approached by using Ludox TM40 as nanoparticles model (to maintain the continuity with the previous characterization work), and performing a comparative analysis between fetal calf serum and human plasma. I have found that the main proteins adsorbed to NPs surface were plasminogen, albumin, apolipoprotein AI (ApoAI), hemoglobin and apolipoprotein AII (ApoAII) from FCS, and immunoglobulins (IgG), histidine rich glycoprotein (HRG), albumin, apolipoprotein AI, apolipoprotein AII and apolipoprotein CIII (ApoCIII) from human plasma. In both situations, albumin (the most abundant plasma/serum protein) was the principal polypeptide bound to NPs at very low serum/plasma concentrations, while at greater serum/plasma doses it was displaced by less plentiful proteins (over all, apolipoproteins), indicating an higher affinity of these latter for SiO_2-NPs surface. Congruent with this, NPs firstly absorbed plasminogen, apolipoproteins and hemoglobin, while once these proteins were depleted from serum albumin started to bind NPs surface proportionally to NPs dose. I have also found that the serum proteins pattern associated to NPs surface was not rearranged from a neutral environment (representative of cytosol) to an acidic environment (representative of endo-

lysosomes). Finally, I have investigated how single plasma opsonines could influence SiO_2-NPs biological activity, finding that IgG and HRG did not protect cells against NPs toxicity, while albumin and, over all, high density lipoproteins (the complexes containing ApoAI, ApoAII and ApoCIII) strongly reduced NPs adverse effects by inhibiting NPs cellular association.

Part of this PhD work has been published on Nanomedicine (London) [186].

Riassunto

Le nanoparticelle sono strutture di diverse dimensioni (1-100 nm) e varia composizione (ossidi metallici, polimeri di silice, polimeri di acidi organici), presenti nell'ambiente come conseguenza di processi naturali (eruzioni vulcaniche, erosione di rocce) o antropogenici (inquinamento, attività industriale). Negli ultimi decenni esse sono state intensamente studiate e ingegnerizzate a scopo industriale (come additivi di cibi, cosmetici e materiali utilizzati nell'edilizia) e nell'ambito biomedico, in cui possono essere impiegate come vettori per farmaci o agenti di imaging. Grazie alla sua abbondanza, economicità e resistenza, il biossido di silicio (SiO_2) è, nella sua forma amorfa, uno dei materiali maggiormente usati sia in ambito industriale che biomedico (contrariamente alla forma cristallina che provoca l'insorgenza della silicosi, una malattia polmonare cronica molto diffusa nei minatori, lavoratori di ceramica e altre categorie occupazionali quotidianamente esposte a cristalli/fibre di silicio). Nonostante la silice amorfa sia considerata molto meno pericolosa di quella cristallina, studi recenti condotti *in vitro* e su modelli animali hanno messo in luce un potenziale citotossico e pro infiammatorio. Per chiarificare questo aspetto, nella prima parte del mio dottorato ho caratterizzato la citotossicità e l'induzione di una risposta pro infiammatoria di nanoparticelle di silice amorfa (la variante commerciale non fluorescente Ludox TM40 e la variante fluorescente Stöber) su due modelli di cellula fagocitica (monociti e macrofagi primari umani) e in due modelli di cellula non fagocitica (linfociti primari umani e la linea stabile epiteliale HeLa). In particolare, mi sono concentrata sui possibili meccanismi coinvolti nell'azione delle nanoparticelle e su come il siero possa influenzarli. Un primo risultato ha indicato una maggior tossicità delle nanoparticelle di silice (valutata in termini di disfunzione mitocondriale e permeabilizzazione della membrana) nelle cellule fagocitiche, associata anche alla produzione delle tre principali citochine pro infiammatorie (IL-1β, TNF-α and IL-6). Più in dettaglio, la dose di nanoparticelle in grado di uccidere il 50% delle cellule (LD50) dopo un trattamento di 18 h è risultata essere di ~ 40 µg/ml, mentre le cellule non fagocitiche hanno mostrato una maggior resistenza alle nanoparticelle (LD50 ~ 300-500 µg/ml). Analizzando il tipo di morte indotta dalle nanoparticelle di silice, le cellule HeLa hanno mostrato un fenotipo apoptotico, mentre i monociti, macrofagi e linfociti sono risultati andare incontro a necrosi. Da una valutazione al citofluorimetro e al microscopio confocale

dell'associazione e della localizzazione cellulare delle nanoparticelle è emerso che queste venivano internalizzate in compartimenti acidi nelle due cellule fagocitiche, mentre nelle cellule HeLa rimanevano legate alla membrana plasmatica. Questo risultato ha suggerito che la maggior sensibilità dei fagociti fosse dovuta a una maggior captazione delle nanoparticelle che, una volta accumulate all'interno di endo-lisosomi, potessero provocarne la rottura con la conseguente liberazione di enzimi litici (proteasi, idrolasi, lipasi) in grado di danneggiare la cellula. A questo proposito, è stato valutato il contributo dell'ambiente acido degli endo-lisosomi alla tossicità delle nanoparticelle di silice nei fagociti trattando le cellule in presenza o in assenza di due agenti neutralizzanti (NH_4Cl o Bafilomicina AI), ottenendo una diminuzione della citotossicità della silice nei monociti e solo un lieve effetto nei macrofagi.

Come anticipato precedentemente, le nanoparticelle di silice si sono mostrate in grado di indurre una risposta infiammatoria (più evidente nei monociti) caratterizzata da un'iniziale fase di latenza fino al raggiungimento della soglia di tossicità, un picco centrale e una fase finale decrescente (in corrispondenza delle dosi più alte di nanoparticelle) a causa della forte e anticipata morte cellulare. In particolare, l' IL-1β è risultata essere la citochina prodotta più abbondantemente, seguita dal TNF-α e dall'IL-6; inoltre, in copresenza di nanoparticelle e LPS essa veniva secreta in modo sinergico. Dal momento che la silice cristallina è in grado di attivare l'inflammasoma NLRP3 (un complesso multi proteico citosolico responsabile della produzione di alcune citochine pro infiammatorie, prima fra tutte l' IL-1β), una parte del lavoro di tesi è stata dedicata allo studio dell'attivazione di NLRP3 da parte di nanoparticelle di silice amorfa nei nostri due modelli di cellula fagocitica. Inizialmente è stata evidenziata sia in monociti che in macrofagi la capacità delle nanoparticelle di silice amorfa di aumentare i livelli di pro IL1-β e stimolarne la conversione nella forma matura IL-1β tramite un processo dipendente dall'attivazione della caspasi 1, della secrezione di ATP ed dal successivo legame di ATP al suo recettore P2X7. Inoltre, a seguito del blocco di P2X7 con uno specifico inibitore la mortalità indotta dalle nanoparticelle di silice non ha subito variazioni sia nei monociti che nei macrofagi, mentre i monociti hanno mostrato una maggior resistenza alle nanoparticelle in presenza di un inibitore della caspasi 1, segno di una possibile morte per piroptosi causata dalle nanoparticelle in queste cellule. Un altro aspetto importante presentato in questa tesi di dottorato riguarda l'influenza del siero (FCS) sugli effetti citotossici e pro infiammatori indotti dalle nanoparticelle di silice

amorfa. Innanzitutto, all'aumentare della concentrazione del siero sia la soglia di tossicità sia l'LD50 delle nanoparticelle di silice sono risultate spostate verso valori più alti, indicando un effetto protettivo dell' FCS (più evidente nei non fagociti rispetto ai fagociti), cosi come la produzione di citochine pro infiammatorie nei monociti e nei macrofagi. Per capire se questo spostamento fosse dovuto a una diversa associazione delle nanoparticelle alle cellule sono stati fatti esperimenti con le nanoparticelle fluorescenti Stöber, che hanno evidenziato come la presenza di siero fosse in grado di diminuire il legame fra la nanoparticelle e le cellule, in particolare nel caso dei linfociti e delle HeLa. Questo risultato è in accordo con la precedente osservazione di un maggior effetto protettivo del siero nei non fagociti, e rafforza l'ipotesi che la tossicità delle nanoparticelle sia in qualche modo legata al loro livello di interazione con le cellule. Inoltre, anche la localizzazione intracellulare delle nanoparticelle è risultata essere influenzata dalla concentrazione di siero. In particolare, in assenza di siero le nanoparticelle erano prevalentemente distribuite sulla membrana cellulare nei monociti e nelle HeLa, mentre nei macrofagi venivano internalizzate in fago-lisosomi, anche se meno efficientemente che con 10% FCS. Vista la diversa localizzazione subcellulare nelle due diverse condizioni di siero, ci si è chiesti se l'effetto protettivo dell' NH_4CL, Bafilomicina AI e dell'inibitore della caspasi 1 osservato nei monociti nelle condizioni di coltura standard (10% FCS) venisse mantenuto anche in assenza di siero. Né la neutralizzazione dei compartimenti acidi né l'inibizione della caspasi 1 si sono dimostrati efficaci nel prevenire la tossicità, indicando che nei monociti il meccanismo di morte cellulare fosse diverso in assenza o in presenza di siero.

Nella seconda parte della mia tesi di dottorato ho analizzato diversi aspetti dell'interazione delle nanoparticelle con le proteine del plasma e del siero, essendo questo un aspetto cruciale nell'applicazione dei nanomateriali in campo biomedico. Infatti, nanoparticelle introdotte nell'organismo (in particolare del circolo sanguigno come vettori per farmaci o agenti d'immagine) vengono rapidamente rivestite da una serie di proteine (costituenti la cosiddetta "corona di proteine") in grado di mediare l'interazione cellula-nanoparticella. Questa problematica è stata affrontata utilizzando come nanoparticelle modello le Ludox TM40 (per mantenere la continuità con la caratterizzazione fatta in precedenza) ed eseguendo esperimenti in parallelo con il siero fetale bovino ed il plasma umano. Le principali proteine del siero bovino legate alle nanoparticelle di silice sono risultate essere il plasminogeno, l'albumina, le

apolipoproteine AI e AII e l'emoglobina, mentre quelle del plasma umano le immunoglobuline, l'histidine rich glycoprotein, l'albumina e le apolipoproteine AI, AII e CIII. Il pattern di proteine adsorbite alle nanoparticelle di silice ha evidenziato che a basse concentrazioni di siero/plasma la principale proteina legata era l'albumina (la proteina più abbondante del siero/plasma), mentre all'aumentare della concentrazione di siero/plasma essa veniva "spiazzata" da proteine meno abbondanti (in primis dalle apolipoproteine), suggerendo una maggiore affinità di queste ultime per la superficie di nanoparticelle di silice amorfa. In accordo con questa ipotesi, le nanoparticelle inizialmente legavano il plasminogeno, l'emoglobina e le apolipoproteine, mentre solo quando queste proteine venivano esaurite dal siero (in presenza di alte dosi di nanoparticelle) iniziava a legarsi l'albumina, proporzionalmente alla quantità di nanoparticelle presenti. Dall'analisi del pattern di proteine legate alla silice in presenza di differenti pH è emerso che esso non subiva variazioni rilevanti in presenza di un ambiente neutro (rappresentativo del citoplasma) o di un ambiente acido (rappresentativo degli endo-lisosomi). Infine, esperimenti preliminari su come le singole proteine della corona potessero influenzare l'attività biologica delle nanoparticelle hanno indicato né le immunoglobuline né l'HRG erano in grado di diminuire gli effetti citotossici delle nanoparticelle, mentre l'albumina e, in particolare, le HDL erano fortemente protettive, riducendo l'associazione delle nanoparticelle alle cellule.

Una parte di questo lavoro di dottorato è stata pubblicata sulla rivista Nanomedicine (London) [186].

Aim of the thesis

The first objective of this PhD thesis is to characterize the cytotoxic and pro inflammatory potential of amorphous silica nanoparticles, since they are widely used in the industrial field for the manufacture of several products and they are very similar to the well known crystalline silica (responsible of the development of silicosis and other pulmonary pathologies). In particular, we focused on the differential mechanism of action of SiO_2-NPs on our cellular models (primary human monocytes and macrophages, representative of myeloid professional phagocytes population, and primary human lymphocytes and HeLa cells, representative of non phagocytic cells), considering also its modulation by serum. The evaluation of serum influence of SiO_2-NPs biological effects acquires big importance in view of the fact that nanoparticles used for biomedical purposes (as imaging agents or drug carriers) are mainly administered by intravenous injection so that, once in the bloodstream, they are coated by specific plasma proteins modulating nanomaterials biological effects. In the light of this, the second aim of my thesis is to identify the principal bovine serum and plasma proteins (representative of an *in vitro* and *in vivo* condition, respectively) absorbed on SiO_2-NPs surface, to characterize some important aspects of this interaction (such as the evolving of protein "corona", the affinity and the dependence on pH) and, finally, to investigate how the single absorbed proteins can modulate SiO_2-NPs biological activity (e.g. promoting NPs cytotoxicity or exerting protective effects on cells.).

1. Introduction

1.1 Nanoparticles

Nanomaterials are defined as particles or systems that have at least one dimension less than 100 nanometers (nm) in length. In particular they can be classified in nanoplates (nanoscale only in one dimension), nanofibers (nanoscale in two dimensions) and nanoparticles (nanoscale in all three dimensions) [1]. They can have different shapes (tubes, spheres, crystals, wires), composition (inorganic or organic compounds) and dimensions, depending on their origin [2]. Natural processes such as desert storms, volcanic eruptions, and ocean evaporations are the primary source of nanoparticles present in the environment [2]. In addition, the advent of the industrial revolution and technological progress has introduced new typologies of nanoparticles, called "anthropogenic" because they derive from human activities. A first category of these particles includes nanoparticles unintentionally generated by anthropogenic processes (unintentional nanoparticles) [3], like ultrafine particles released in diesel and other engines exhausts, fumes of industry and incinerators and indoor pollution derived from common activities (cooking, cleaning and smoking) [4]. A second large category is related to nanoparticles intentionally produced by humans and used in industrial and biomedical fields.

1.1.1 Nanoparticles for industrial applications

The main characteristic that has determined a wide use of nanoparticles in industry is the large ratio of surface area to volume (that increases exponentially with decreasing particle size) [3]. This means that an increasingly high percent of atoms are located on the surface in smaller and smaller nanoparticles, while in a bulk material they are virtually all in the inner part of the structure, and that the same mass unit is composed by a higher particles number with their large surface area, in comparison to macro or micro material (Figure 1). As a consequence, nanomaterials have much more point of interaction with environment (e.g., a solvent) or surrounding nanostructures, with a strong influence of physical – chemical properties (increased reactivity, solubility and stability). For example, gold is an inert element at a macroscale dimension, while gold nanoparticles (nanoscale) become reactive and can be used to catalyze reactions [5].

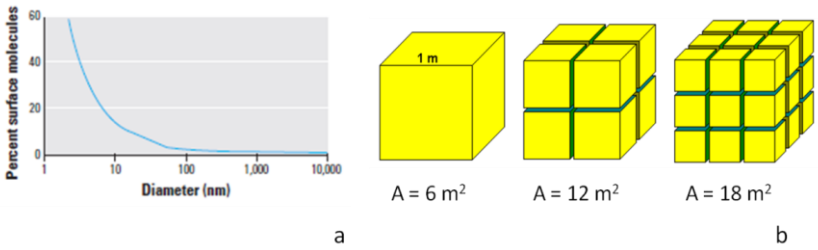

Figure 1: (a) Surface molecules as function of particle size [3]. (b) Exemplification of surface area increment in the presence of smaller objects keeping the same total volume.

An emerging field for nanoparticles applications is the food industry, where they are employed as coloring or clarifying agents for beverages, additives to enhance flavors, preservants and packaging materials [6]. Other common applications are cosmetic (e.g. titanium dioxide nanoparticles are used as sunscreen and silver nanoparticles are present in different products as antibacterial/antifungal agents), building trade (e.g., for thermal insulation) and others, as summarized in [2].

1.1.2 Nanoparticles for biomedical applications

The peculiar characteristics of nanomaterials have determined, in the past decades, an increasing interest around the use of nanotechnology in biological and medical fields. The new discipline concerning these purposes is nanomedicine, defined as an "application of nanotechnology for treatment, diagnosis, monitoring and control of biological systems" [7]. Traditional medicine presents many limits for the diagnosis and treatment of pathologies, for example, it acts at a "macro" level (losing sensitivity and specificity), and it is non-site-specific targeting (so high doses of therapeutic agent must be administrated to obtain the desired effect at the designated area, but several aspecific side effects may develop) [8,9]. Moreover, drugs have often poor solubility and short half life in the blood circulation, sometimes they cause undesired immune reactions and other adverse effects, so their administration can be problematic [7-10]. Nanomedical studies have developed a series of nanostructures of different dimensions and chemical composition that are expected to solve many problems related to canonical medicine (Figure 2). First of all, nanosystems have a size (1-100 nm) comparable to biological structures (DNA, proteins, macromolecular assemblies) and can easily interact with them. They can act as "carriers" for insoluble drugs, that are entrapped in the inner cavity or exposed on the surface of nanosystems and can reach the target area without losing their concentration and effectiveness (so, they can be administered at a lower dose). Moreover, nanocarriers can

be largely modified in their chemical composition, in order to acquire several advantages for drug delivery and imaging. For instance, to improve the specificity of target they are often conjugated with a specific molecule (e.g. a peptide or an antibody) that recognize, for example, a receptor present or over-expressed in a particular tissue (e.g., in neoplastic formations). Once reached the interested area, therapeutic and diagnostic agents can be selectively activated and released by changes in the environmental conditions (by modifying pH or applying a magnetic field or an external heat source) [7,11,12]. Another common modification is the attachment of units of polyethylene glycol (PEG), a non toxic and non-immunogenic polymer with an high hydrophilicity, that reduces the adsorption to nanoparticles surface of plasma proteins (the so called "opsonines"), usually promoters of the NPs clearance by macrophages of the reticuloendothelial system (RES) [9].

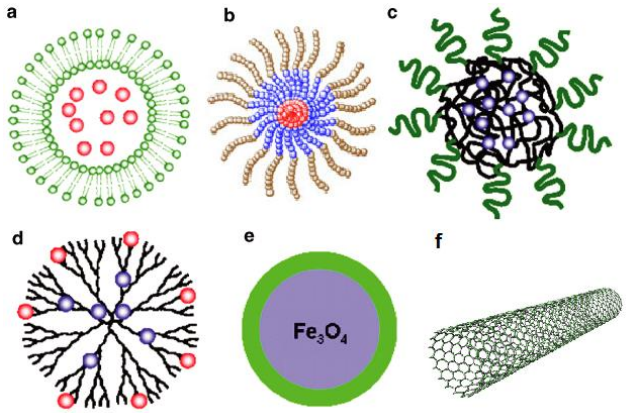

Figure 2: schematic illustration of nanoparticles used in medicine. (a) liposome: concentric bilayered vesicle in which an aqueous volume is entirely enclosed by one or more lipid bilayers mainly composed of natural or synthetic phospholipids. Drug molecules can be either entrapped in the aqueous space or intercalated into the layer. (b) polymeric micelle: spheroidal structure with an hydrophobic core shielded from the water by a mantle of hydrophobic groups. They are used for the delivery of water insoluble drugs that, once trapped within the hydrophobic core, can be dispersed in aqueous media such as bloodstream. (c) polymeric nanoparticle: spherical polymers of biodegradable materials, such as polylactic acid (PLA) or polylactic-glycolic acid (PLGA). Drugs are entrapped into the matrix, and functional groups can be conjugated to the surface. (d) dendrimer: highly branched macromolecule with a three dimensional architecture growing from a central core through a series of convergent or divergent polymerizations reactions. Drug molecules can be loaded inside the central core or attached to the surface groups. (e): ceramic nanoparticle: nanoparticle made up of inorganic (ceramic) compounds either metals (iron, gold, alumina, titanium) or non metals (silica). (f): carbon nanotube: sheets made of > 60 carbon atoms (fullerenes) rolled up into a tubular form (one sheet: single-walled nanotube; several concentric sheets: multi-walled nanotubes). Modified from [9].

1.2 Nanotoxicology

The present day increasing exposition of humans to nanoparticles has pointed the attention on the possible side effects of these systems (considering their high reactivity and "foreign nature" for human body). A new branch of toxicology, "nanotoxicology", has been proposed to address the gap in knowledge and specifically address the understanding of possible adverse health effects caused by nanomaterials [13]. Nanotoxicology purpose is to study physicochemical determinants, routes of exposure, biodistribution, molecular determinants and genotoxicity of nanomaterials, and to deliberate protocols for nanoparticles-associated risk assessment in humans and environment [14].

1.2.1 Route of exposure to nanomaterials and possible consequences

Because of their small-scale dimension, nanomaterials can easily cross biological barriers and enter into the body through several routes. The major portal for nanomaterials in body is the respiratory system, through inhalation. Once inside the respiratory tract, nanoparticles can be subjected to chemical or physical clearance processes [15]. The first case occurs when nanoparticles are biosoluble and involves their rapid dissolution in extracellular or intracellular fluids. On the contrary, if nanoparticles are insoluble, they are subjected to slow physical translocation in different ways, depending on their size and on the region they are located in. Bigger particles (> 2.5 μm) are usually cleared by the mucociliary escalator system [16] and enter the gastrointestinal tract, where they are usually excreted. Smaller particles can enter the blood or lymph and be distributed in other districts of the body, reaching the central nervous system via sensory neurons [17] or being phagocytized by resident alveolar macrophages, that are attracted in the site of particles deposition by specific chemotactic signals [18,19].

The way of exposure to nanoparticles present in the environment or in cosmetics is skin, a 1.5-2 m^2 organ composed of three main layers: epidermidis (external), dermis (intermediate) and subcutaneous (inner) [1,3,14]. The principal sites of dermal penetration are hair follicles [20] and broken skin [3], but it has been shown that very small nanoparticles (< 10 nm) are able to cross spontaneously epidermidis and dermis. Once inside the deepest layers of skin, nanoparticles can be recognized by the resident macrophages and dendritic cells (Langherans cells) with a possible consequent

inflammatory response [21], or reach other districts of the body through the lymphatic and blood vessels network [3]. In addition, they can exert toxic effects on epidermal cells (keratinocytes and fibroblasts) [22].

Another possibility is nanoparticles contact with the gastrointestinal tract after ingestion (if they are present in food or water) or after the mucociliary clearance from the respiratory tract [3,14]. Few data are currently available on this topic and it is generally assumed that the large majority of ingested NPs are rapidly eliminated via feces or urine [23]. However a limited, but biologically relevant, translocation at the level of the gastrointestinal mucosa, cannot be excluded, especially for nanostructured food-additives, like amorphous silica based ones [24].

Nanoparticles used in biomedical applications (as carriers of drugs or imaging agents) are mostly designed to be injected in the blood circulation and get distributed to several organs, where they can accumulate or be cleared more or less efficiently. An important aspect to consider is that, once in blood, NPs come in contact with several soluble molecules naturally present in circulation (e.g. coagulation factors or complements proteins), determining possible adverse effects (complement activation, thrombosis). Furthermore, the huge amount of proteins present in plasma can absorb to NPs surface (forming the so called "nanoparticles corona") and mediate many cellular processes in response to a foreign material introduced in the bloodstream [25-27, 180-181]. This central aspect, will be better considered in the next paragraph.

1.2.2 Nanoparticles interaction with plasma proteins

Plasma, the acellular portion of blood, is a very concentrated solution containing small and macromolecular solutes. Among these latter, we can find more than 3,700 different protein types [26] present in variable concentrations, ranging from < pg/ml to > mg/ml. Plasma proteins are involved in several essential physiological processes, such as coagulation, immune response and inflammation, lipid metabolism, proliferation, signaling, proteolysis and transport [28]. Since the majority of nanosystems for biomedical applications is developed for intravenous injection, many studies have concentrated on NPs interaction with plasma proteins and its possible influence of cellular/organism response. Indeed, it is universally accepted that the biological fate and biodistribution of NPs do not depend on nanoparticle *per se* but on the particle "dressed" with its protein corona, as this is the real system that cells see and respond to [26,29,181].

Physicochemical aspects

Plasma proteins adsorption to nanoparticles surface is driven by several interactions that are established at the nano-bio interface (hydrophobic, electrostatic, steric, Van der Walls forces and hydrogen bonds). Each nanoparticle type presents peculiar surface properties (determined by chemical composition, surface functionalization, shape and angle of curvature, porosity and crystallinity, hydrophobicity and hydrophilicity) that influence the nature of proteins that bind the surface, determining a specific protein pattern adsorbed to different NPs typologies [181]. However, it has been reported that the vast majority of nanoparticles studied so far binds apolipoproteins, which are proteins belonging to lipoprotein complexes (VLDL-LDL-HDL) responsible of lipid transport. In addition, Hellstrand *et al*. recently documented the presence of complete HDL in the biomolecular corona surrounding polymeric NPs [30], indicating that not only the proteic component but also the lipidic/saccharidic ones can compose NPs corona. This preferential binding of apolipoproteins/lipoproteins to different classes of nanoparticles can be explained considering that, similarly to nanostructures, lipoprotein complexes have dimension in the nanoscale (Figure 3) and so their reciprocal binding can be driven by size or curvature dependent interactions [30,180]. Other plasma polypeptides often found in the corona of several NPs are albumin, immunoglobulins and coagulation factors (e.g., fibrinogen) (Table 1), but their ubiquity is probably due to their high plasma concentration (> 10 mg/ml).

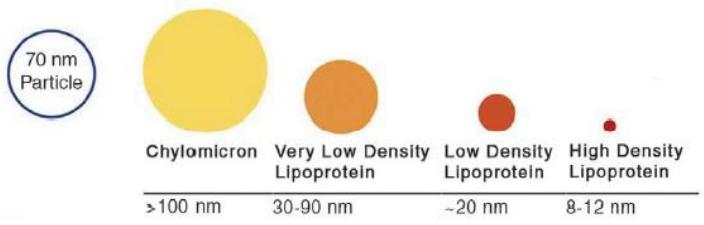

Figure 3: Size comparison of a 70 nm generic nanoparticle with lipoprotein complexes - chylomicrons, very low, low, and high density lipoproteins [180].

Nanoparticles	Identified proteins
Polystyrene with poloxamer 184, 188, 407	Factor B, transferrin, albumin, fibrinogen, IgG, apolipoproteins
Liposomes	Albumin, fibrinogen, apolipoproteins, IgG, α1-antitrypsin, α2-macroglobulin, IgM
Single-walled carbon nanotubes	Albumin
Solid lipid nanoparticles with Tween 80	Fibrinogen, IgG, IgM, apolipoproteins (including ApoE), transthyretin
Solid lipid nanoparticles with poloxamer 188	Fibrinogen, IgG, IgM, apolipoproteins (excluding ApoE), transthyretin, albumin
Poly(lactic acid) nanoparticles with PEG	Albumin, fibrinogen, apolipoproteins, IgG
Polyhexadecylcyanoacrylate nanoparticles	Albumin, apolipoproteins, IgG, transferrin
Poly(ε-caprolacton) nanoparticles	IgG, apolipoproteins
Polycyanoacrylate nanoparticles	Albumin, IgG, IgM, fibrinogen, apolipoproteins
Iron oxide nanoparticles	Albumin, IgG, IgM, fibrinogen Albumin, IgM, fibrinogen, C3b, apolipoprotein A-1 Albumin, IgG, IgM, fibrinogen, C3b IgG, IgM, fibrinogen
Various polymer/copolymer composition nanoparticles	Albumin, IgG, fibrinogen, apolipoproteins
Poly(D,l-lactic acid) nanoparticles	Albumin, IgG, fibrinogen, IgM, apolipoproteins, antithrombin III
Polystyrene with Rhodamine B	Albumin, IgG, fibrinogen, apolipoproteins, PLS:6
Various polymer/copolymer composition nanoparticles	Albumin, IgG, fibrinogen, IgM, apolipoproteins, PLS:6, U2
Poly(isobutylcyanoacrylate) with Dextran	Albumin, IgG, fibrinogen, apolipoproteins, serotransferrine, transthyretine
Single- and double-walled carbon nanotubes	Albumin, fibrinogen, apolipoproteins, C1q
Polybutylcyanoacrylate nanoparticles with polysorbate 80	Albumin, IgG, fibrinogen, IgM, apolipoproteins
Solid lipid nanoparticles with poloxamer or poloxamine coating	Albumin, fibrinogen, apolipoproteins

Table 1: Summary outlining various nanoparticles and the proteins they bind. Modified from [25].

Protein adsorption on NPs surface is a very rapid process occurring within seconds-minutes, and, most importantly, is highly dynamic, with continuous association and dissociation events over time. In particular, it has been found, as a general trend, that the more plentiful plasma proteins (like albumin) first absorb to NPs, independently on their affinity for NPs surface. However, subsequently these proteins are displaced by less abundant proteins endowed with a higher affinity for a certain nanoparticle type [31,32]. The whole process of competitive adsorption of proteins onto a limited surface based on abundance, affinities and incubation time is collectively known as "Vroman Effect" [25], from the name of the author that firstly documented these changes of NPs corona composition [33]. A consequence of the Vroman effect is that the pattern of protein bound to a given NP at low serum concentrations, corresponding to a situation in which

high affinity but scarce proteins are limiting and negligible, reflects the pattern present at early time, while the pattern in high serum concentrations reflects that occurring in the second, slower phase, in which there is a displacement of abundant low affinity binding components by less concentrated high affinity ones. The "Vroman Effect" can be explained considering the balance between association rate (k_{on}) and dissociation rate (k_{off}) of a protein to a nanomaterial, defined as the dissociation constant K*d* (normally varying from 10^{-4} M to 10^{-9} M). The value of k_{on}, which depends on the frequency of contact between the protein and the nanomaterial, is high in abundant plasma proteins that, thanks to their huge amount, have large probability to interact with NPs surface. Once binding is established, if proteins have a low k_{off} (which depends on the binding energy of the protein-nanomaterial complex) they remain attached to NPs while, in the opposite case (low binding energy), they dissociate within minutes leaving space for the binding of less plentiful proteins (low association rate) with higher affinity [29]. To distinguish these two series of proteins differently adsorbing onto NPs surface the terms "soft" and "hard" corona have been introduced, indicating respectively polypeptides that rapidly dissociate from NPs and high affinity proteins stable on NPs surface determining the final molecular signature of a particle in a certain environment [29,34,35]. As a confirmation that apolipoproteins present a large propensity for NPs binding, several studies have documented their ability to displace much more plentiful plasma proteins (albumin, fibrinogen, immunoglobulins) from the surface of different NPs types, finally constituting the "hard" NPs protein corona [31,32,36,37,181]. The process of protein exchange may also be important when particles redistribute from one compartment or organ to another. For example upon NPs i) diffusion from the bloodstream to the interstitial space; ii) cell uptake with possible transport to endocytic acidic compartments; iii) cytosol translocation possibly followed by organelle targeting (mitochondria, nucleus) [180].

Another important aspect concerning macromolecules interaction with NPs is that proteins can undergo conformational changes, leading to either a loss or a gain of the α-helix content at the expense of random coil structures without affecting their catalytic activity [38], while TiO_2-NPs induce a transition of α-helix into β-sheets resulting in a substantial inactivation of lysozyme [39]. In other cases, the interaction of a protein with NPs can determine the exposure of amino-acid residues normally buried in its core. For example, fibrinogen binding to poly(acrylic acid) polymer-coated gold nanoparticles

determines the exposition of a cryptic peptide that specifically interacts with macrophages Mac-1 receptors resulting in the activation of nuclear factor κB (NF- κB) signaling pathway and the release of inflammatory cytokines [40].

Functional aspects

One of the main problems concerning NPs injection into the bloodstream is their rapid clearance from the circulation by the cells of the mononuclear phagocytic system (MPS), also known as the reticuloendothelial system (RES), represented by monocytes and macrophages located in the liver (Kupffer cells) or in the spleen and specialized in the engulfment of foreign particles (viruses, bacteria, cellular debris or "non-biological" entities). Once internalized by phagocytes, NPs became ineffective as site-specific delivery devices (they cannot reach the target tissue/organ). Moreover, if they are non-biodegradable (resistant to enzymes and other oxidative reactive chemical factor normally produced to break down the phagocytized material) or with a molecular weight higher than renal threshold (only molecules of around 5,000 Da can be removed by renal system), they accumulate in the MPS organs leading to possible cytotoxic and inflammatory events [25,41]. In the majority of cases, phagocytes of the MPS cannot identify the nanoparticles themselves, but rather recognize specific proteins (the so called "opsonins") bound to the surface of the particles that promote phagocytic event (for example, recognizing a particular receptor expressed on cellular membrane). The most common opsonins are complement proteins such as C3, C4, C5, and immunoglobulins, which respectively bind complement receptors or Fc receptors present on macrophages [42]. Recently, several methods of camouflaging or masking nanoparticles from possible opsonins have been developed, in order to increase NPs blood circulation half life. As a general rule, NPs surface has been modified by adding chemical groups (such as long hydrophilic polymer chains or non-ionic surfactants) which can block the electrostatic and hydrophobic interactions at the nano bio-interface (indeed, a charged or hydrophobic surface is more prone to adsorb serum proteins) [41]. The most common modification is "PEGylation", which consists in the covalent linkage of poly ethylene glycol (PEG) chains on NPs surface [25]. PEG is an hydrophilic and neutral polymer of ethylene oxide (C_2H_4O) with different weight and length, depending on the number of the repeated units. Several studies have demonstrated that PEG addition not only reduces the amount of proteins adsorbed to NPs [43,44] but also particles uptake and its possible connected adverse effects, such as toxicity and inflammatory response [43-46]. Protein binding to

NPs is, however, a still debated question, because in addition to opsonins there are also molecules promoting prolonged circulation times in the blood ("dysopsonins", e.g. albumin [32,47]) or useful for distribution of the particles in organs otherwise inaccessible. For example, it has been found that NPs coated with ApoE or ApoB (apolipoproteins belonging to low density lipoproteins (LDL) complexes) can cross the blood brain barrier (BBB) through the binding to LDL receptors, that are specifically up-regulated on the surface of the endothelium forming BBB, and consequently can act as "Trojan Horses" for drugs destinated to the Central nervous System [48,49]. In conclusion, a systematic biochemical and functional study of plasma proteins adsorbing to NPs surface is required, with the final aim to target nanomaterials at a determined site by attaching a particular plasma protein *ex vivo* or, alternatively, by engineering nanoparticles preferentially binding specific molecules that direct them at the desired district.

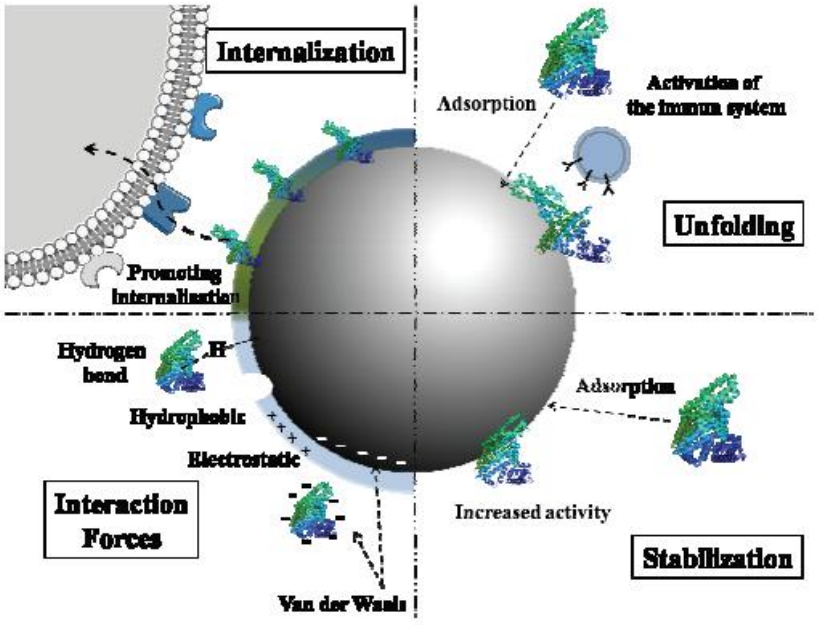

Figure 4: Effects of NPs on proteins, and the forces of interactions [181].

1.3 Silica Nanoparticles

1.3.1 Silicon dioxide

Silicon dioxide (SiO_2) is, after oxygen, the second most abundant compound present on Earth's crust, as a major component of rocks, sands and environmental dusts. SiO_2 derives from the condensation of silicic acid -$Si(OH)_4$- monomers through formation of siloxane bonds and water (Figure 5a). Usually, silicic acid polymerization occurs when its concentration exceeds $2*10^{-3}$ M [50]. This simple reaction can be repeated hundreds of times, forming a regular structure in the space where silicon is tetrahedrically coordinatinated with 4 oxygen atoms (Figure 5b).

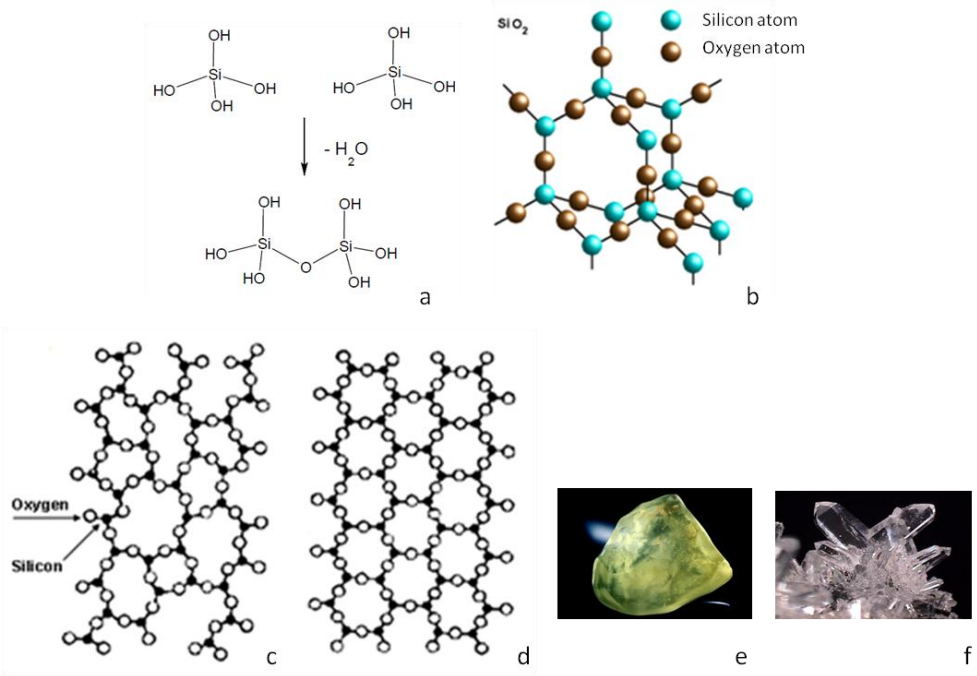

Figure 5: (a) Polymerization of silicic acid molecules through formation of siloxane bond and water [50]. (b) three-dimensional structure of silicon dioxide. (c) structure of amorphous silica, (d) structure of crystalline silica, (e) glass, an example of amorphous silica (f) quartz, an example of crystalline silica.

Silica can be present in amorphous form (glass, opal) or in crystalline form (quartz, cristobalite), depending on the disposition of atoms in the lattice. In amorphous silica, tetrahedral are randomly connected while in crystalline silica the arrangement of all the atoms is ordered in all dimensions [50]. This difference can be appreciate at microscopic level by X-ray diffraction experiments (Figure 5 c, d) and also at macroscopic level (Figure 5 e, f).

1.3.2 Silica nanoparticles applications

Thanks to its abundance and cheapness, silicon has been largely employed in several fields in the form of silica nanoparticles (SiO_2-NPs). A first application is at the industrial level, where SiO_2-NPs (e.g. the commercial available Ludox®) are used as additives in the production of toners, varnishes, anticorrosive coatings, cosmetics and food (for example, as clarifying agents for beverages or anticaking agents in powdered products) [24,50]. Another common employment is in the biomedical sector, where SiO_2-NPs have been proposed for drug delivery, DNA transfection, imaging and enzyme immobilization. In particular, SiO_2-NPs (and, in general, all ceramic nanoparticles) appear to be preferable than other types of NPs (organic polymers, liposomes and dendrimers) because of their rigidity and chemical stability, conferring a higher resistance to the denaturing effects of pH, solvent or temperature [8,45] and their transparency (that allows the conjugation with photoactivable compounds). Moreover, the presence of superficial silanol groups (Si-OH) confers an high hydrophilicity (by forming hydrogen bonds with the surrounding water molecules), that decreases to some extent the adsorption of plasma proteins (opsonins) on SiO_2-NPs surface, compared with other materials, and their consequent clearance by macrophages of RES, incrementing their circulation time in the blood [182].

SiO_2-NPs are generally synthesized following three principal methods (I, II, III, Figure 6). Stöber synthesis is based on the hydrolysis and condensation of tetraethylortosilicate (TEOS) in ethanol, in the presence of ammonia as catalyst [183]. NPs dimension depend on the amount of water and ammonia in the reaction. In the microemulsion protocol, SiO_2-NPs are produced by the hydrolysis of TEOS in the presence of ammonia (catalyst), a non-ionic surfactant and a microemulsion of water in octane [51]. In Prasad synthesis, vinyltriethoxysilane (VTES) units polymerize in the hydrophobic core of detergent micelles (e.g. Brij 35). This method has been employed to synthesize ORMOSIL-NPs (*organically modified silica nanoparticles*) that, thanks to the possibility of entrapping hydrophobic molecules in the lipophylic core of micellar aggregates, can be modified by the addition of several biomolecules (such as PEG, targeting agents or drugs) [45] improving the biocompatibility, selectivity and therapeutic efficacy or SiO_2-NPs for biomedical applications. Owing to these advantages provided by ORMOSIL-NPs (first of all, the much less adverse effects on health in comparison to amorphous and crystalline silica), they have become the primary SiO_2-NPs studied in the field of nanomedicine.

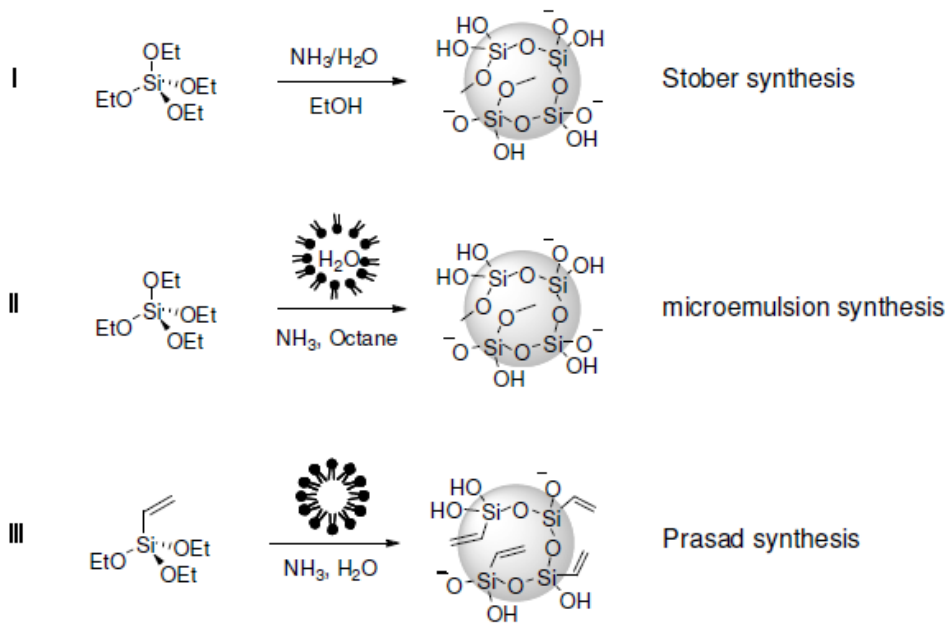

Figure 6: Synthesis methods of silica nanoparticles.

1.3.3 The toxicity of silica

Prolonged or chronic exposure to silica crystals induces silicosis, one of the oldest occupational diseases documented in particular in miners and ceramic workers [52-54]. Once inhaled, because of their micro-nanoscale dimension and fiber shape, silica crystals easily accumulate in small airways of the lungs, where mucocilial clearance is not functional and where they are ingested by resident macrophages (alveolar macrophages) [54]. As non-biodegradable material, phagocytized crystals stimulate the secretion of inflammatory cytokines and chemokines from alveolar macrophages and also alveolar epithelial cells [55] with an auto-sustained mechanism, indeed uptake of silica crystals can initiate apoptotic cell death with concomitant release of ingested material, which is re-engulfed by other macrophages inducing a new cycle of inflammation [56]. Some cytokines released by macrophages, such as interleukin-1 (IL-1), tumor necrosis factor α (TNF-α), platelet derived growth factor (PDGF), fibronectin and type-1 insulin like growth factor promote fibroblasts proliferation and collagen synthesis, leading the formation of fibrotic scars that replace pulmonary tissue damaged by excessive/prolonged inflammation and reactive oxygen species production [55,57]. As final result, lungs undergo a progressive failure and, in some cases, also pulmonary cancer can be developed. Due to this evidence, in 1997 the International Agency of Research on Cancer (IARC) has classified some crystalline silica polymorphs (quartz and cristobalite) in

group 1 (sufficient evidences for the carcinogenicity to experimental animals and to humans) [50].

Amorphous silica (probably because of its less fibrogenic nature) is not considered as toxic as crystalline (it was classified by IARC in group 3 – inadequate evidence for carcinogenicity), but several *in vitro* and *in vivo* studies have documented possible adverse effects occurring after amorphous silica exposure. Chang *et al*. [58] reported that amorphous silica causes a reduction of mitochondrial activity and plasma membrane permeabilization in human normal and tumor cells belonging to district most exposed to NPs (lungs, gastrointestinal system and skin), with a more pronounced toxicity on non-tumoral cells. Similar metabolic and membrane damages have been described in mouse keratinocytes [184], human endothelial cells [50,59], murine macrophages [60] and fibroblasts [61], and rat myocardial cells [62]. Interestingly, in comparative studies with nanoparticles of different sizes cellular toxicity was stronger upon treatment with small NPs. For instance in rat cardiomyocites LD50 of 21 nm NPs (0.32 mg/ml) was significantly lower than LD50 of 48 nm NPs (1.29 mg/ml) [62], in human endothelial cells LD50 of 15 nm NPs was 5 times lower than that of 60 nm NPs (50 $\mu g/cm^{-2}$ *vs* 250 $\mu g/cm^{-2}$) [50] and 30-48 nm NPs killed more effectively mouse keratinocytes than 118-535 nm NPs [184]. Confirming that increased cytotoxicity of smallest NPs depends on their higher surface area, Waters *et al*. have shown that the expression of cellular viability as a function of surface concentration (cm^2/ml) instead of mass concentration ($\mu g/ml$) results in the convergence of different size particles dose-response curves [63].

In addition to mitochondrial and membrane damage, also the ability of SiO_2-NPs to induce reactive oxygen species (ROS), reduced glutathione (GSH) decrease (index of anti-oxidant activity) and lipid peroxidation have been documented in human HepG2 cells [64,65], HUVEC cells [59], A549 cells [66] and L-02 cells [67], highlighting that amorphous silica can lead to oxidative stress (more pronounced in the presence of smaller particles). Since ROS cause DNA damage and this triggers apoptosis, several studies have investigated the pro-apoptotic potential of amorphous silica evaluating various markers of programmed cell death. In effect, phosphatidylserine exposure [64,65,67], caspase-3 activation [60,64], induction of pro-apoptotic proteins such as p53, pro-caspase 9 and Bax reduction of the anti apoptotic factor Bcl-2 [65] and DNA laddering [67] have been observed after cellular exposure to SiO_2-NPs.

Other studies investigating the different sensitivity of phagocytic and non-phagocytic cells to SiO_2-NPs found that, in general, the first ones are more affected by NPs. For example, Rabolli *et al.* documented that Ludox SM NPs killed murine macrophages J774 ~ 2.5 folds more effectively than murine fibroblasts 373 [68]; Mohamed *et al*. showed that different size SiO_2-NPs induced cytocidal effects in monocytic THP1 cells but not in alveolar epithelial A549 [69] and Herd *et al*. reported that silica nanomaterials of different geometries (worms, cylinders and spheres) caused functional damage in murine macrophages RAW 267.4 at lower doses (~ 80 μg/ml) than in A549 cells (> 200 μg/ml) [70]. A possible explanation of the major sensitivity to SiO_2-NPs of monocytes/macrophages compared to epithelial cells could be that phagocytes have an inherent capability in engulfing nanoconstructs, as reported by [69,70]. Also amorphous silica microparticles were shown to affect macrophages more than non-macrophages cell lines, although in this case both cellular types showed similar ability to internalize the particles [60].

The higher sensibility of macrophages to amorphous silica and the fact that, in lungs, alveolar macrophages engulf inhaled silica nanoparticles/nanofibers leading to the inflammatory disease silicosis (in the case of crystalline silica) have determined an increasing interest around the mechanism of SiO_2 induced inflammatory response. Crystalline silica is known to activate the NLRP3 inflammasome, a cytosolic multiprotein complex responsible of the production of IL-1β from its immature form through the caspase-1 mediated cleavage of pro-IL1β (see paragraph 1.5). Indeed, it has been demonstrated that both LPS primed murine and human monocytic-macrophagic cells secrete IL-1β after stimulation with silica crystals, and that the blockage or the deletion of NLRP3 proteins (such as caspase 1, ASC and Nalp3) reduce/abolish this process [53,54,71,72]. Further, Hornung *et al.* highlighted the role of crystals phagocytosis, lysosomal damage and lysosomal cathepsins activation in silica induced NALP3 activation, while the production of ROS was not found to be essential [54]. On the contrary, Cassel *et al.* showed that the inhibition of NADPH oxidase (source of cellular ROS) markedly abrogated silica induced IL-1β and caspase-1 activation [53].

Recently, evidences concerning the pro-inflammatory potential of amorphous SiO_2-NPs have been described in both *in vivo* and *in vitro* models. Park *et al*. reported an increase of inflammation related genes (IL-1β, TNF-α, IL-6 and iNOS) and pro-inflammatory

cytokines (IL-1β, TNF-α) in mice treated with SiO_2-NPs [52]. In other studies, SiO_2-NPs of different diameters were found to activate the NALP3 inflammasome in murine and human macrophages (respectively, RAW264.7 and THP-1) via mechanisms similar to crystals, such as endosomal rupture, lysosomal proteases activation and ROS production [73,74]. Moreover, amorphous silica was found to induce a pro-inflammatory activity (in particular, NF-kB activation and upregulation of IL-6/IL-8 gene) also in non-immune cells HUVECs [75]. All these results clearly indicate that, despite amorphous silica nanoparticles are widely used in cosmetics, food and medicinal products, they can have cytocidal and inflammatory effects potentially dangerous for health [74]. However, additional studies are necessary to better clarify death and inflammation mechanisms, and how they affect each other.

1.4 Immune system and inflammation

In addition to the mechanical barrier of skin, mammals present a complex and extremely effective immune system, in which two arms cooperate to assure a successful defense against pathogens: the innate and the adaptive immune systems. The first (whose major players are phagocytic cells and natural killer cells) provides a very rapid response (e.g. phagocytizing and killing a microorganism), but lacks in specificity and memory. The second (represented by B and T lymphocytes) is able to produce a response specific (and so more effective) for each pathogen and, after the first contact, can "remember" the undesired host and quickly react at the subsequent exposures. Innate and adaptive systems collaboration derives from their complementary functions (a rapid non-specific action *vs* a slower selective one), and from their ability to communicate and potentiate one each other, by a complex signaling of cytokines, chemokines, receptors and co-stimulatory molecules. Since crystalline and amorphous silica activate mechanisms characteristic of the innate immunity (uptake by phagocytes, ROS and pro-inflammatory cytokines production), the next section will be focused on this topic.

Generally, innate immune system can be activated by two types of signals, the so called PAMPs (pathogen associated molecular patterns) and DAMPs (damage associated molecular patterns). PAMPs are highly conserved microbial structures (essential for microbial survival) such as the cell wall components peptidoglycans and

lipopolysaccharide; DAMPs are molecules, normally present in the cell, released by injured or danger tissues as danger signal (e.g., ATP) [76]. Both PAMPs and DAMPs are recognized by germline-encoded pattern recognition receptors (PRRs), expressed by classical immune cells (e.g., myeloid cells as monocytes, macrophages, dendritic cells and neutrophils) and also by non immune cells (epithelial) [77,78]. PRRs can be classified into phagocytic PRRs (which directly bind the microorganisms and mediate their internalization), and sensor PRRs, responsible of the initiation of pro-inflammatory signaling pathways [79]. Four main categories of sensor PRRs, characterized by a specific ligand and cellular localization, have been identified:

1) Toll-like receptors (TLRs), located on the cell surface and lumen of endosomes and lysosomes and able to recognize a plethora of PAMPs and DAMPs
2) RIG-I-like receptors (RLRs), cytosolic and able to sense viral RNA
3) C-type lectin receptors (CLRs), associated to cellular membrane and specific for glycopeptides and polysaccharides
4) Nod-like receptors (NLRs), localized in the cytosol and activated by many DAMPs and PAMPs.

The most important PRRs for this work are TLRs (implicated in monocytes/macrophages LPS stimulation) and NLRs (involved in myeloid cells activation by silica). They will be described in the next sections.

1.4.1 TLR 4 activation by LPS

Bacterial endotoxin (lipopolysaccharide, LPS) constitutes the outer layer of the outer membrane of Gram-negative bacteria, and represents one of the most potent microbial initiators of inflammation, by activating myeloid cells to produce pro-inflammatory cytokines (such as IL-1β, TNF-α, IL-6 and IL-8) [80,81] It consists of three covalently linked regions (as represented in Figure 7):

- Lipid A: this is an hydrophobic domain (formed by six fatty acyl chains linked to two glucosamine residues) situated in the inner part of the membrane and responsible for toxicity
- Oligosaccharide core, situated in the centre of the molecule and consisting of 10 saccharidic residues

- O antigen: this hydrophilic domain (made up of many repeated units of a branched tetrasaccharide) is exposed in the outer side of the membrane and is variable between different bacteria, determining LPS antigenic specificity [81].

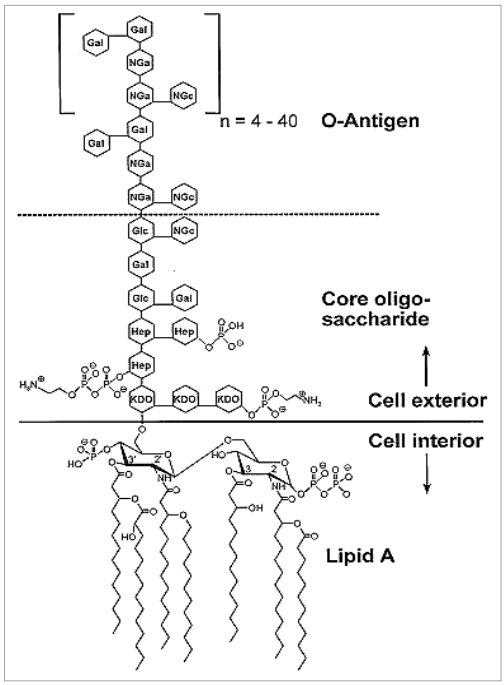

Figure 7: Structure of lypopolisaccharide

Host response to LPS begins with LBP (lipid binding protein) mediated transfer of endotoxin to CD14. LBP is a soluble serum glycoprotein, while CD14 is a glycoprotein either expressed on the surface of myelomonocytic cells as glycosylphosphatydilinositol anchored molecule (mCD14) or is present in the bloodstream as a soluble molecule (sCD14). A first pathway consists in LPS clearance, through its localization in high density lipoproteins particles (HDL) and subsequent excretion by the liver (Figure 8a). The second important pathway leads to inflammatory response, involving the ternary complex CD14-TLR4-MD2 (Figure 8b). mCD14 (in case of cells lacking this receptor, sCD14) concentrates LPS in proximity of the transmembrane protein TLR4 (Toll like receptor 4), made up of an extracellular leucine-rich-domain for ligand interaction, a transmembrane portion and an intracellular domain TIR (Toll IL-1 receptor), responsible of subsequent signal transduction. MD-2 (myeloid differentiation protein-2) is a small molecule associated to the external domain of TLR4, important for LPS recognition and regulation of TLR4 cellular distribution [80]. As demonstrated by Akashi *et al.*, CD14-

TLR4-MD2 cooperate to form a very stable complex with LPS before signal transduction step [82]. After LPS binding, the complex TLR4-MD2 dimerizes and activates two possible pathways: MyD88 dependent and MyD88 independent. MyD88 (myeloid differentiation factor 88) is an adaptor cytosolic protein that with its TIR domain interacts with TLR4 and with its death domain recruits members of IL-1 receptor associated kinases (IRAK), that activates mitogen activated protein kinases (MAPK) such as p38, ERK and JNK, leading the activation of the transcription factor AP-1 (activator protein 1). In parallel, IRAK can recruit IkBα kinase complex (IKK), that induces the phosphorylation, polyubiquitination and proteasome-mediated degradation of IkBα (an inhibitor of nuclear factor-κb (NF-κB)). Once NF-κB is liberated, it can migrate into the nucleus and, together with AP-1, activate the transcription of many genes for inflammatory cytokines. In MyD88 independent pathway, TLR4 recruits through TIR-TIR domains interactions two molecules (TRIF and TRAM) that activate IRF3 (INF regulatory factor 3), leading to the induction of INFα/β [81]. Interferons can act in a autocrine/paracrine way, binding their receptor and activating STAT1, a transcriptional activator of genes for iNOS and MCP-5 (monocytes chemoattractant protein 5). As the previous pathway, also MyD88 independent one activates NF-κB [81]

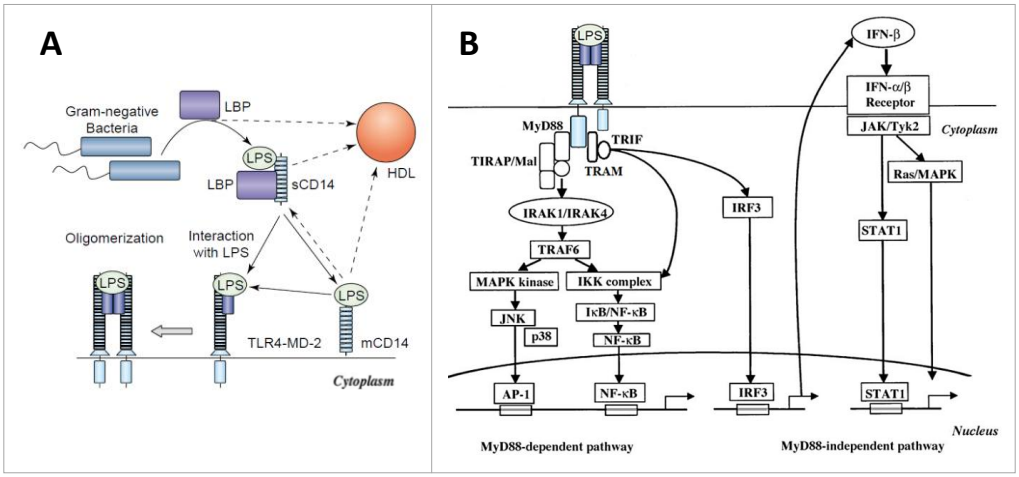

Figure 8: (a) LPS processing, signaling and clearance [81]. (b) LPS activation of MyD88 – dependent/independent pathway (modified from [80]).

1.4.2 NLRs and inflammasomes

Inflammasomes (whose name derives from the fusion of the word inflammation with the suffix "some", form Greek meaning body) are cytosolic molecular platforms involved in the production of pro-inflammatory cytokines (IL-1β, IL-18), through the recruitment and subsequent activation of inflammatory caspases (over all, caspase 1) [76]. They result from PAMP/DAMP induced assembly of NLRs to other inflammasome associated molecules (such as adaptors and effector molecules) [83].
NLRs, as mentioned before, are cytosolic receptors able to sense danger or pathogen associated signals. They present a tripartite architecture, consisting of:

- an N-terminal effector domain (different for each receptor), which mediates signal transduction to downstream targets.
- a central NACHT domain, conserved in all NLR members , able to bind nucleotides (ATP) and responsible of oligomerization. NATCH is commonly associated to an additional domain NAD (NATCH associated domain), and together they are called NBD (nucleotide-binding domains)
- a C-terminal domain LRR (leucine rich repeat), consisting of a 20-30 residues repeated motif enriched in the hydrophobic amino acid leucine, and responsible of ligand sensing (probably through amino acid hydrophobic interactions) [77,78]

On the basis of N-terminal domain, NLRs can be classified in 5 big families designed as NLRA (A as AD, acidic activation domain), NLRB (B as BIR, baculoviral inhibitory repeated domain), NLRC (C as CARD, caspase activation and recruitment domain), NLRP (P as PYD, pyrin domain) and NLRX (X because lacks omology to any known domain) [76,78,83] (Figure 9a). Interestingly, mammalian NLRs structure strongly resembles plant R-proteins, implicated in immune defense against bacteria, virus, fungi and other pathogens [76]. The main adaptor molecule involved during inflammasomes formation is ASC (apoptosis-associated speck-like protein containing a CARD), that mediates pro-caspase 1 recruitment through its PYD and CARD domains (Figure 9a). On the base of the molecular assembly of NLRs – Caspase 1 complex and on the different stimuli activating inflammasome pathway, at least 10 inflammasomes have been identified. The four more studied are NLRP1, NLRC4, AIM2 and NLRP3 (Figure 9b).

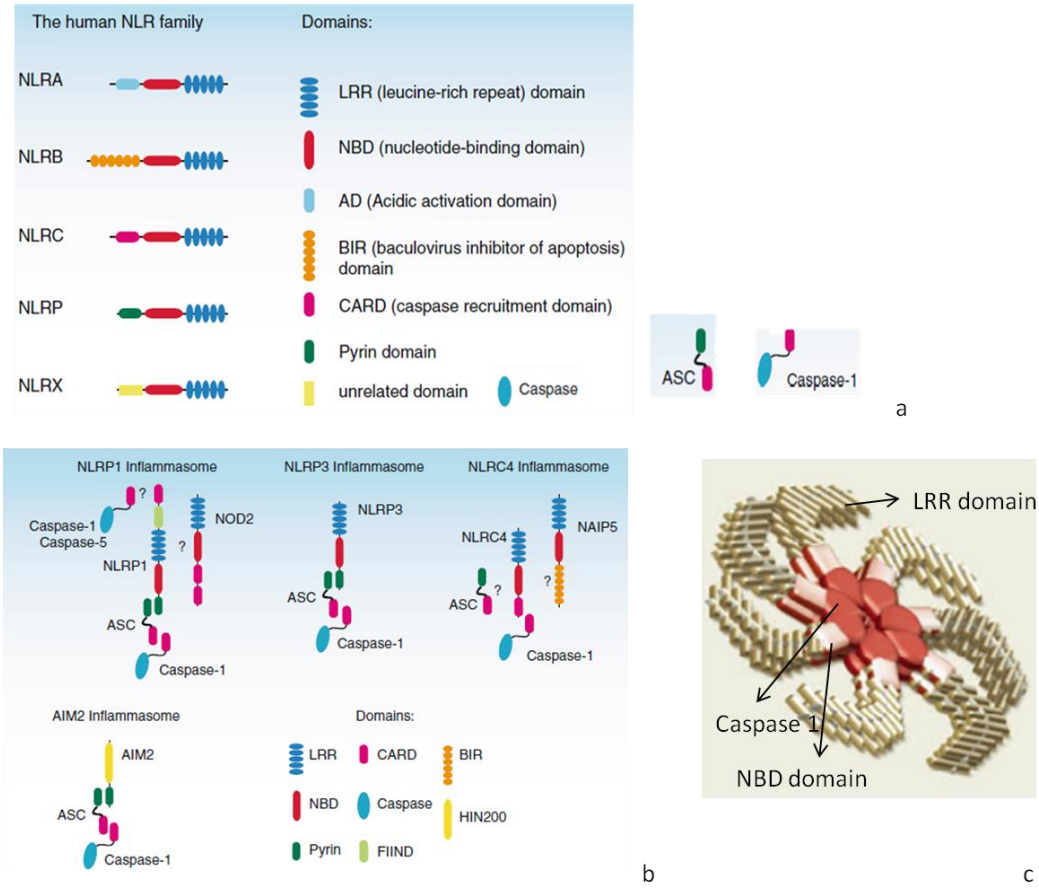

Figure 9: (a) members of human NLR family. (b) structure of the four main inflammasomes . Modified from [78] . (c) structural organization of the NALP3 inflammasome (modified from [76]).

NLRP1 was the first inflammasome described in 2002 by Martinon *et al*. [84]. In addition to the common LRR, NATCH and PYD domains, it presents a C-terminal extension consisting of a FIIND motif and a CARD. It can directly recruit pro-caspase 1 and pro-caspase 5 by CARD-CARD interaction, or even include ASC with an augmented activation [77,85]. NLRP1 is activated by *Bacillus Antracis* lethal toxin and cell wall component muramyl dipeptide (MDP) [78].

NLRC4 (also known as IPAF) is activated by gram negative bacteria possessing type III or IV secretion systems, such as *Salmonella typhimurium*, *Shigella flexneri*, *Pseudomonas Aeruginosa* [77]. With its N-terminal CARD, NRLC4 can directly recruit pro-caspase 1 without the need of an adaptor protein (even if ASC may stabilize or facilitate this process) [78].

AIM2 inflammasome is composed by AIM2, ASC and Caspase-1. It contains a PYD domain that interacts with ASC via PYD-PYD interactions, allowing the ASC CARD

domain to recruit pro-caspase 1 to the complex. AIM2 is activated by cytosolic double strand DNA from virus, bacteria or the host itself [77,78].

The NLRP3 (also known as NALP3 or cryopirin) is currently the most studied and characterized inflammasome, as sensor of many sterile/microbial and exogenous/endogenous stimuli. It was for the first time described in 2004 by Agostini *et al.*, as involved in the Muckle-Wells autoinflammatory disorder [86]. NALP3 inflammasome "monomer" consists of the NLRP3 scaffold, the adaptor protein ASC and the functional unit caspase 1. In the presence of activators signals (they will be presented in section 1.5), NLRP3 PYD domain interacts with ASC PYD domain, and ASC CARD domain recruit pro-caspase 1. Usually, seven monomers are assembled in a big complex of 2 μM diameter [85], (Figure 9c). Once pro-caspase 1 is recruited, in all the four inflammasomes listed above it is subjected to autoproteolitic activation, leading to a mature form able to cleave pro IL-1β into IL-1β and the consequent start of inflammatory response against a particular DAMP or PAMP.

1.4.3 IL-1β

IL-1β represents one of the most important mediators of inflammation following host stimulation with a PAMP or a DAMP, and is mainly produced by cells of the monocytic lineage (monocytes, macrophages, dendritic cells and polymorphonucleates) as inactive precursor of 31 kDa, subsequently cleaved by caspase 1 into the bioactive form of 17 kDa [87,88]. IL-1β is released extracellularly through a non-classical secretory pathway (in fact, it lacks the conventional hydrophobic signal sequence for the secretion via endoplasmic reticulum and Golgi apparatus), and then binds to its membrane receptors (IL-1R1, IL-1R2, IL-1R3) promoting pro-inflammatory activities (such as increasing the expression of adhesion molecules, vasodilatation and induction of chemokines for the recruitment of inflammatory cells at the injured site, or inducing other inflammatory cytokines as TNF-α and IL-6), and executing also regulatory functions of blood heat and appetite [89]. As mentioned before, IL-1β is not released via the traditional secretory pathway. To date, five different mechanisms have been suggested [88]. The first, proposed in 1990 by Rubartelli *et al.* [90], suggests that both pro IL-1β and caspase 1 are transported from the cytosol into secretory lysosomes, where pro IL-1β is processed to the mature form during their trafficking to the plasma membrane. After docking to the membrane, lysosomal content is released into the extracellular space in a Ca^{2+}- dependent

manner, while lysosomal membrane fuses with the plasma membrane. In a second model, IL-1β is released through the shedding of membrane derived microvesicles of dimension varying from 0.1 to 1 μM and characterized by phosphatidylserine exposure on the outer side of lipid bilayer. Also in this case, IL-1β processing occurs inside microvesicles, and shedding seems to be calcium dependent [91]. A third model proposes that IL-1β is released in a protected form by being packaged and secreted via small exosomes (30-100 nm diameter), accumulated into bigger multivesicular bodies (MVB) [92]. In a fourth model, pro IL-1β is cleaved to the mature form in the cytosol, and IL-1β is released by direct passage through the plasma membrane via a plasma membrane transporter (possible candidates for this role are ABC transporters) [93]. Alternatively (fifth model), IL-1β can be passively released as a consequence of cellular lysis or can reach extracellular space by passing through membrane pores (e.g. the ones formed during pyroptosis) [88,94].

1.4.4 Caspase-1

Caspases are cysteine proteases that hydrolyze peptide bonds on the carboxyl side of an aspartate residue. At present, 11 human caspases have been identified [95] and classified in apoptotic caspases (initiator caspases 2, 8, 9, 10 and effector caspases 3, 6, 7) and inflammatory caspases (pro-inflammatory caspase 1, 4, 5 and anti-inflammatory caspase 12) [76]. Briefly, catalytic mechanism (schematized in Figure 10a) involves the deprotonation of the sulfydhryl Cys 285 (caspase 1 numbering) by the imidazole ring of His 237, producing a thiolate nucleophile that attack the carbonyl carbon of the scissile bond forming a tetrahedral intermediate, which is stabilized by hydrogen bonding to the amide nitrogen of Gly 238. After the detachment of the C-terminal portion of peptidic bond, an oxidrylic group (derived from an H_2O molecule deprotonated by H 237) attacks the carbonylic carbon of peptide (bound to S of Cys 285), allowing the release of N-terminal portion of peptide and the free enzyme. Due to their catalytic function, C 285, H 237 and G 238 are conserved in all human caspases [95]. Another characteristic in common between all caspases is that they are synthesized as inactive precursors (zymogens) and, only when it is strictly necessary, they become active through an autoproteolitic process. In this way, a widespread and uncontrolled activation/ proteolitic action (dangerous for the cell) is avoided.

The first identified caspase was caspase 1, described in 1989 by Kostura *et al*. as a "processing activity" present only in cytosolic extracts of human monocytes and THP.1 cells, "capable of cleaving precursor IL-1β to authentic mature IL-1β" [96]. For this characteristic, it was also called ICE (interleukin 1 converting enzyme). In the subsequent years, the enzyme was purified, cloned and its structure determined by X-ray diffraction [97,98]. In immune cells, caspase 1 is constitutively expressed as an inactive homodimeric precursor of 90 kDa (each subunit has a molecular weight of 45 kDa (p45)). In the presence of an activation stimulus, an autoproteolitic process occurs, resulting in two 20 kDa fragments (p20) and two 10 kDa fragments (p10) that intimately associate and form mature caspase 1 [97] (Figure 10b).

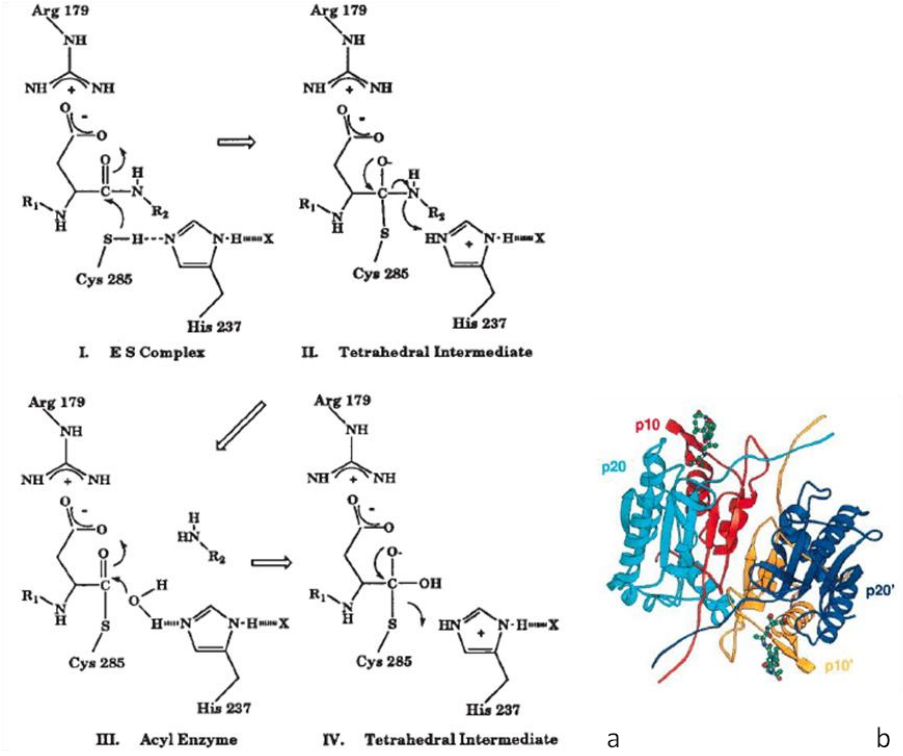

Figure 10: (a) Caspase 1 catalytic mechanism [97]. (b) Caspase 1 structure.

In addition to its original function (the processing of proIL-1β to IL-1β), caspase 1 is implicated also in the maturation of other members of the IL1 family, such as IL-18 (a pro-inflammatory cytokine constitutively expressed in human PBMCs and implicated in the activation of NK cells and induction of interferon γ (INFγ)), IL1F7 (an anti-inflammatory cytokine that negatively regulates the expression of inflammatory molecules), and IL-33 (promoter of Th2 response, regulator at nuclear level of the gene transcription of IL-4, IL-5, IL-13 and, on the contrary of IL-18 and IL1F7, inactivated by

caspase 1 proteolytic process) [78,89]. Moreover, caspase 1 appears to be the key determinant of pyroptosis, a particular cell death type that affects macrophages infected by pathogens (see paragraph 1.4.5).

1.4.5 Pyroptosis

Pyroptosis is defined as "Caspase-1 dependent programmed cell death" [99], and was first described in macrophages infected by *Shigella flexneri* as a cell suicide induced by an invasive bacterial pathogen [100]. Subsequent studies (in most cases performed in macrophages subjected to a microbial infection) have revealed that this is a new type of cell death, although it has characteristics in common with necrosis and apoptosis (the two classic cell deaths). During apoptosis (an high regulated cellular suicide aimed at removing damaged individual components to preserve the safety of an organism or a cellular population), the so called apoptotic caspases are activated, resulting in chromosomal DNA cleavage in fragments of approximately 180 bp [101], nuclear and cytoplasmic condensation, cell shrinking (pyknosis) and formation of "apoptotic bodies" (membrane-bound cellular compartments containing cellular residues and destined to be engulfed by resident phagocytes) [102-104]. In addition, apoptotic cells retain an intact plasma membrane and no inflammatory events occur. Necrosis, a passive accidental cell death resulting from environmental perturbations (e.g. chemical or thermal damage), is characterized by dilatation and dismantling of cellular organelles, membrane damage with consequent water entrance, cytoplasmic swelling and final cellular lysis. Contrary to apoptosis, chromatin condensation and degradation is not observed, while a strong inflammatory process is initiated. At a microscopic level, the major features of pyroptotic cells are chromatin condensation, DNA cleavage (but, differently from apoptosis, the classical oligonucleosomal DNA fragmentation pattern is not observed) and cytoplasmic swelling with large spherical protrusions of the membrane [99,104] (Figure 11). A peculiar characteristic is represented by 1.1-2.4 nm diameter membrane pores throughout cellular ionic gradient is dissipated, producing an increased osmotic pressure, water influx and consequent swelling and lysis (with the release of inflammatory intracellular contents) [104] (Figure 11). Pathogens-infected or toxin treated cells in the presence of osmoprotectants with molecular diameter > 2.4 nm (glycine or PEG) are protected from cellular lysis, as demonstrated in [101,105]. At a molecular level, pyroptotic cell death is not characterized by the activation of apoptotic caspases (over all, caspase 3) [99,106], but it strongly depends on caspase 1, as largely reported in literature. Indeed, it has been

demonstrated that caspase 1 inhibitor YVAD significantly reduced macrophages death induced by *Salmonella typhimurium* [101,106] or *Shigella* [107], and the same result was obtained in caspase 1 deficient mice after macrophages infection with *Francisella tularensis* [108]. Moreover, inhibition or deletion of caspase 1 abolished pyroptosis-associated IL-1β and IL-18 production and DNA fragmentation [105], suggesting a possible role of ICE even in nucleic acid degradation (that, as said before, in pyroptosis are not dependent on caspase 3 classical pathway). Recently, several studies have documented caspase-1 importance in regulating cell death in systems different from pathogens-infected cells, such as macrophages treated with carbon black nanoparticles [109] and in models of cardiovascular-cerebral diseases [102].

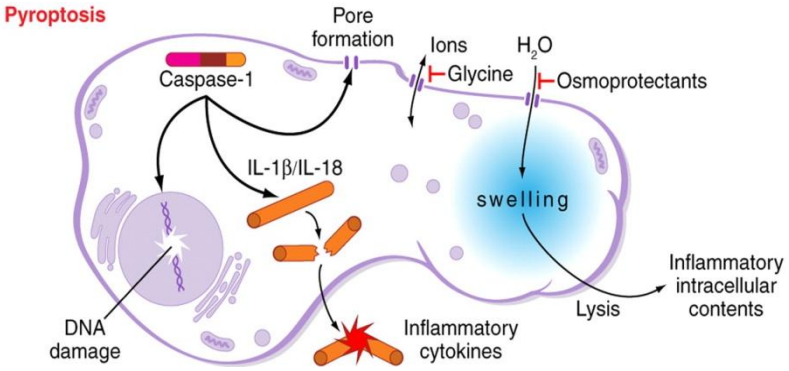

Figure 11: the typical pathway of pyroptosis [105].

1.5 NLRP3 inflammasome

1.5.1 Stimuli and models for NLRP3 inflammasome activation

NLRP3 activates in the presence of several infection/danger signals. At present, the better characterized are:

- monosodium urate (MSU) crystals, derived from precipitation of uric acid in the joints of the hyperuricemic patients and responsible of gout
- silica and asbestos particles, that cause pneumonitis and the progressive pulmonary fibrotic diseases asbestosis and silicosis [53,56,71]
- alum and chitosan (used as adiuvants for vaccines) [110]
- extracellular β amyloid aggregates, accumulated in senile plaques during the development of Alzheimer disease [111]

- a large variety of bacteria and their toxins, that form membrane pore in the infected cells
- high concentration of extracellular ATP (sensed as danger signal) [112].

Given the structural dissimilarity of the NLRP3-activating stimuli, it is unlikely that NLRP3 directly interacts with all of them. However, it is plausible that different stimuli can promote the release, modification or recognition of a common ligand, which can interact with the inflammasome [113]. Several mechanisms leading to NLRP3 have been proposed. The three widely supported in the literature concern (1) K^+ efflux through the $P2X_7$ ATP gated ion channel, (2) lysosomal damage, (3) generation of reactive oxygen species (ROS).

K^+ efflux and the role of $P2X_7$ receptor

Under basal conditions, the normal intracellular K^+ concentration is about 150 mM, while the extracellular concentration is typically 5 mM. This ionic gradient is maintained by the sodium-potassium pump (also known as Na^+/K^+-ATPase). It has been demonstrated that K^+/H^+ ionophore nigericin (a bacterial pore forming toxin from *Streptomyces hygroscopicus*) activates caspase 1 processing and formation of mature IL-1β in LPS-primed macrophages [114,115]. Moreover, classical NLRP3 activators (ATP, nigericin, MSU, silica crystals) lose their functionality in the presence of extracellular medium containing an high potassium concentration (130 mM) [71,114,116]. Both these evidences indicate that for NLRP3 (and also for NLRP1-NLRC4 and AIM2) [78] activation a potassium efflux is required. At least two potential mechanisms may explain how cytosolic K^+ levels might regulate inflammasome activation. The first is that the basal concentration of cytoplasmic K^+ could block the recruitment of caspase-1 to ASC (by inhibiting the interaction between their CARD domains) and consequently avoid inflammasome oligomerization [114,116]. This is also supported by other studies showing that caspase-1 activation in THP-1 extracts is repressed by high ionic strength [117]. A second mechanism purposes that K^+ efflux activates phospholipases C (PLC) and Ca^{2+} -independent phospholipase A_2 ($iPLA_2$). Activated PLC promote an increment of Ca^{2+} intracellular concentration, and the consequent activation of Ca^{2+} -dependent phospholipase A_2 ($cPLA_2$) that might generate a lipidic messenger recognized by LRR domain and inducer of inflammasome oligomerization. On the other hand, activation of $iPLA_2$ could generate lipid second messengers inducing the assembly of scaffolding

molecules and promoting pro-IL1β recruitment by caspase-1 [114,118]. In addition to ionophore nigericin (that directly exchanges K^+ for H^+ across membrane), K^+ intracellular loss can be indirectly determined by the binding of ATP to the receptor $P2X_7$. Under basal conditions, intracellular ATP derived from glicolysis and oxidative phosphorylation is present at concentrations of 3-5 mM [119], while outside the cell its concentration is negligible. Following cellular lysis or signaling mechanisms, ATP is released respectively in a passive and active manner and can bind purinergic receptors in an autocrine or paracrine way determining a specific cellular response (depending on cellular type and class of bound receptor). In the case of NLRP3 activation, secreted ATP binds to $P2X_7$ receptor, a cation selective channel constituted by two transmembrane hydrophobic domains separated by a bulky extracellular region and with N- and C-terminal residue on the cytoplasmic side of the membrane [120,121]. ATP binding determines on one hand K^+ efflux (and consequently NALP3 activation, as described above) and Ca^{2+} influx (activating $cPLA_2$ involved in IL-1β maturation); on the other the formation of a pannexin-1 hemichannel allowing the entrance of microbial molecules (such as MDP) into the cytosol and the direct interaction with NLRP3 components [122,123].

Lysosomal damage

The model of NLRP3 activation through lysosomal rupture has been proposed for large particulate activators, such as alum, silica and amyloid-β. Once phagocytized by monocytes/macrophages, these particulates are inefficiently cleared and accumulate into lysosomes, leading to a phagosomal destabilization and subsequent leakage [78,85,113,124]. The mechanisms throughout lysosomal rupture can occur are still unknown, however, it can be assumed that particles directly damage lysosomal membrane [125] or that induced ROS trigger membrane destabilization through lipid oxidation [74]. After lysosomal disruption, a plethora of proteolitic enzymes normally confined in these compartments are reversed into the cytoplasm, where on the one hand they can degrade cellular structures, on the other hand they may induce the cleavage of a yet-unidentified substrate, which in turn leads to NLRP3 activation [78]. Particularly, the protease cathepsin B has been found to be important in particulates mediated inflammasome activation. Indeed, several studies have demonstrated that the inhibition as well as deficiency of cathepsin B leads to greatly reduced caspase 1 processing and IL-

1β secretion, while stimuli acting from the cell surface (e.g. ATP) are not affected [56,73,74,111]. However, it seems likely that also other lysosomal proteases are involved in this process, since cathepsin B deficient macrophages still display NLRP3 activation when stimulated by phagosomal activators at very high concentrations [78].

Generation of reactive oxygen species

It has been reported that almost all NLRP3 activators trigger the generation of ROS [124], that derive from the activity of NADPH oxidases family (NOX) (e.g., the membrane bound NOX2 present in phagocytes), or from other cellular sources such as mitochondria or xanthine oxidase [78]. In addition, ROS inhibition by N-acetyl-L-cysteine (NAC) and (2R,4R)-4-aminopyrrolidine-2,4,-dicarboxylate (APDC) can reduce IL-1β secretion induced by crystals [71] and MSU [116], and blockage or knock down of NADPH oxidase results in a diminished IL-1 β production [53,71], suggesting that reactive oxygen species play a role in NLRP3 inflammasome activation. A possible mechanism explaining cryopirin triggering by ROS has been proposed by Thsopp and colleagues in 2010 [126]. Briefly, they found that, under basal conditions, thioredoxin-interacting protein (TXNIP) is constitutively bound and inhibits the oxidoreductase thioredoxin (TRX), while after cellular ROS concentration increases the complex TRX-TXNIP dissociates and TXNIP binds to LRRs of NLRP, inducing inflammasome activation.
However, it has to be kept in mind that in some cases the deletion or inhibition of ROS producing machinery did not affect macrophages response to NLRP3 activators [56,124], or that cathepsin B blockage and lysosomal acidic pH neutralization did not impair ATP induced inflammation [56]. This suggests that the best model for NLRP3 activation is an integration of the three proposed mechanisms, in some circumstances substituting and in others potentiating each other (Figure 12).

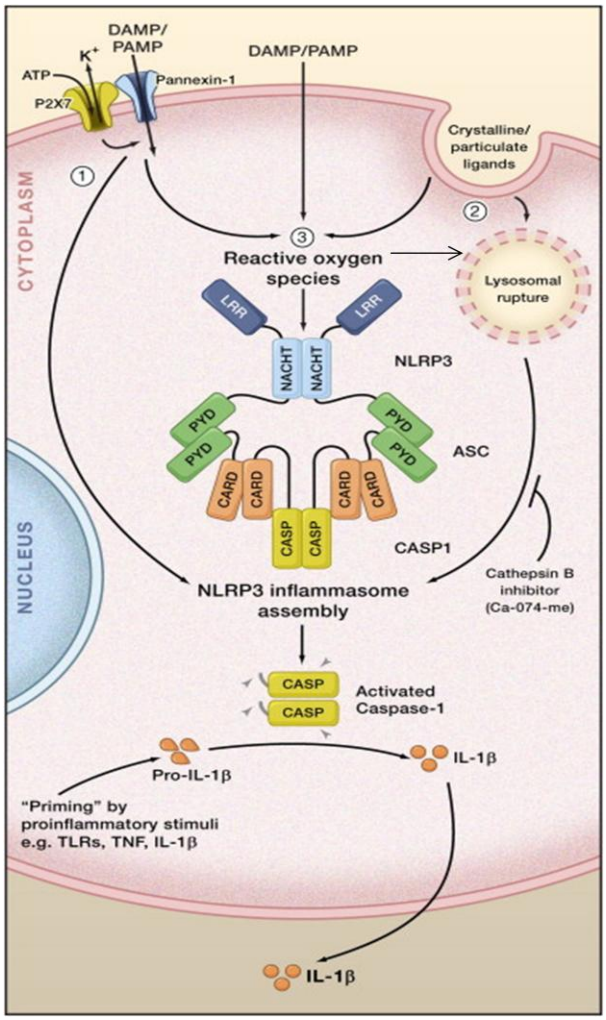

Figure 12: the three major models for NLRP3 inflammasome activation:

(1) ATP-mediated K^+ efflux
(2) Lysosomal rupture
(3) Reactive oxygen species generation

[77].

2. Methods

2.1 Nanoparticles

LUDOX® TM40 colloidal silica nanoparticles (SiO_2-NPs) (40% wt. suspension in H_2O) were purchased from Sigma Aldrich. Dynamic light scattering (DLS) measurements (Malvern Zetasizer Nano S instrument) provided an average diameter of 25±2 nm (number weighted) in phosphate-buffered saline [PBS], pH 7.4, while transmission electron microscopy (TEM) analysis (FeiTecnai 12, 100 kV) yielded a 24±2 nm diameter in good agreement with the DLS size. The zeta-potential value (same conditions as DLS analysis) was -15.6 mV.

FITC-labeled Stöber nanoparticles were prepared in the laboratory of Professor Fabrizio Mancin (Dipartimento di Scienze Chimiche, Università di Padova) following Stöber method [183]. DLS measurements provided an average diameter of 32±3 nm (number weighted) in phosphate-buffered saline pH 7.4, while TEM analysis yielded a 30±3 nm diameter in good agreement with the DLS size. The zeta-potential value (same conditions as DLS analysis) was -18.3 mV. All NPs suspensions were endotoxin free (<0.05 Endotoxin units/ml [1 EU = 100 pg] as measured with *Limulus* test (Sigma Aldrich)).

All physicochemical characterizations of nanoparticles were performed in the laboratory of Prof. Fabrizio Mancin, at a temperature value of 37°C to reproduce the conditions of biological assays.

2.2 Cells

2.2.1 Monocytes isolation from Buffy Coat

Human monocytes were obtained from Buffy Coat (the fraction of non coagulated blood enriched in leukocytes and platelets), gently provided by Centro Trasfusionale of the Hospital of Padua (ULSS16). Whole blood (generally 40 ml) was divided in 2 Falcon, washed with phosphate saline buffer (PBS) without Ca^{2+} and Mg^{2+} to a final volume of 50 ml and centrifuged at 1100 rpm for 10 minutes at room temperature (RT), without accelerator and brake. Supernatant (containing residual serum) was removed, and cellular pellet was resuspended in 25 ml of PBS and stratified on 15 ml of Ficoll-Paque PLUS (Amersham Biosciences). After 30 minutes centrifugation at RT, 2000 rpm without

accelerator and brake, lympho-monocytes were recovered and washed with 50 ml of PBS by centrifuging at 1000 rpm for 10 minutes at RT (with accelerator and brake). Then, cellular pellet was resuspended in 30 ml of "A solution" (containing RPMI-1640 (Gibco) supplemented with 10% (v/v) fetal calf serum (FCS) (Euroclone) plus 100 U/ml penicillin - 100 µg/ml streptomycin (Gibco) and Hepes 4 mM (Sigma Aldrich), 285 mOs), and stratified on "C solution", containing 50.3% of "A solution" and 49,7% of "B solution" (92.5% Percoll (Amersham Biosciences) diluted in PBS 10X, 285 mOs). After 30 minutes centrifugation at RT at 1500 rpm without acceleration and brake, monocytes were recovered, washed with 50 ml PBS, resuspended in RPMI 2% FCS, seeded in 24 wells plates (Falcon) at 2 x 10^6 cells/well (500 µl) or in 96-wells plates (Falcon) at 2 x 10^5 cells/well (200 µl) (depending on the experiment), and incubated for 1 h at 37°C for adhesion step. Adherent monocytes were extensively washed with medium to remove non-adherent contaminating lymphocytes and subsequently treated with stimuli.

2.2.2 Macrophages differentiation

Monocytes adherent to 24 wells plates were incubated with 500 µl of RPMI supplemented with 20% FCS and macrophage colony-stimulating factor (M-CSF) 100 ng/ml (Immunological Sciences), and differentiated to macrophages for 7 days at 37°C. At day 4 or 5, half medium was removed and replaced with new.

2.2.3 Lymphocytes isolation from Buffy Coat

Whole blood was incubated for 20 minutes at RT with 50 µl/ml of RosetteSep® Human T Cell Enrichment Cocktail (StemCell Technologies). Then, it was diluted with an equal volume of PBS + 2% FCS, stratified on Ficoll-Paque PLUS and centrifuged for 30 minutes at 2000 rpm at RT (no accelerator and brake). After centrifugation, lymphocytes were recovered, washed with 25 ml PBS + 2% FCS, resuspended in complete medium (RPMI supplemented with 10% FCS and antibiotics) and seeded onto 96 wells plates at 2 x 10^5 cells/well in 75 µl.

2.2.4 HeLa cells

Human stable epithelial cell line HeLa was maintained in DMEM (Gibco) supplemented with 10% FCS and antibiotics (complete medium). At the moment of splitting (every 2-3 days), cells adhered to flask were washed with PBS and detached with trypsin-EDTA (Gibco) for 3-5 minutes at 37°C. Then, complete medium was added to neutralize trypsin

and about 2/3 of cellular suspension were removed and replaced with new complete medium. The day before experiments, HeLa were detached and seeded onto 24 well plates at 1 x 10^5 cells/well in 500 µl or onto 96 wells plates at 5 x 10^3 cells/well in 200 µl.

2.3 Cellular viability assays

2.3.1 Propidium iodide – Annexin V viability assay

Monocytes, macrophages, lymphocytes and HeLa cells seeded onto 24 wells plates were incubated for different times in the presence of different stimuli, depending on the experiment. At the end of incubation, cells were recovered (monocytes and macrophages by gentle scraping; HeLa by trypsinization) and, after centrifuging for 7 minutes at 1600 rpm at RT, culture medium was collected for ELISA assays while cellular pellets were washed with 1 ml of PBS. Then, cells were resuspended in 300 µl of cold FACS buffer (PBS containing 1% FCS and 0.1% sodium azide) and, just before cytofluorimetric analysis, stained with 15 µg/ml propidium iodide (PI) (Sigma Aldrich).

In apoptosis experiments, cells were treated for 16-18 h with Ludox TM40-NPs at different concentrations in complete medium or with Actinomycin D 1 µg/ml (positive control for apoptosis) [127]. Then, cells were recovered by centrifugation for 5' at 200 x *g*, washed, resuspended in 50 µl of Incubation Buffer and stained with 1 µl of Annexin V for 15' at RT in the dark. Incubation Buffer and Annexin V were provided by Annexin-V-FLUOS Staining Kit (Roche). Finally 250 µl of Incubation Buffer were added, cells were stained with PI as above and acquired for 30 seconds at flow cytometer (BD FACSCanto II). Data analysis of the gated cellular populations was performed with FACSDiva software (Becton Dickinson).

2.3.2 MTS cytotoxicity assay

Monocytes, lymphocytes, HeLa (seeded on 96 wells plates) and macrophages (seeded on 24 wells plate) were incubated with different stimuli for different times, depending on the experiment. Treatment with H_2O was used as positive control. At the end of incubation, cellular culture medium was collected and stored for other assays, while cells were incubated in the dark at 37°C for 0.5-18 h (depending on cell type) with 110 µl (monocytes, lymphocytes and HeLa) or 200 µl (macrophages) of CellTiter 96® AQueous One Solution Reagent (Promega), diluted 1:11 in serum free medium. After colour

development, plates were centrifuged for 5 minutes at 1500 rpm at RT (to precipitate any component responsible of aspecific scattering phenomena, such as NPs at high concentrations), and 80 µl of supernatant were collected and immediately red at 492 nm, using a Biotrak II Reader spectrophotometer. Cellular viability was expressed as % of absorbance value compared to untreated cells (assumed as 100% viable).

2.3.3 LDH cytotoxicity assay

LDH assay was performed on the same samples prepared for MTS assay, using CytoTox 96® Non-Radioactive Cytotoxicity Assay (Promega). Cells incubated for 45 minutes at 37°C with Lysis Solution diluted 1:10 in serum free medium were used as positive control (assumed lysed at 100%). 50 µl of cellular supernatants (collected just before MTS assay) were incubated with 50 µl of reconstituted Substrate Mix for 30-60 minutes at RT in the dark. After colour development, reaction was stopped adding 50 µl of Stop Solution and samples absorbance was red at 492 nm with Biotrak II Reader spectrophotometer. Cellular lysis was expressed as % of absorbance value compared to 100% lysed cells (positive control).

2.3.4 Caspase 3 assay

Monocytes (3 x 10^6 /well), lymphocytes (3 x 10^6 /well), macrophages (2 x 10^6 /well) and HeLa (250 x 10^3 /well) seeded onto 24 wells plates were incubated for 18 h with Ludox TM40 NPs diluted in medium + 10% FCS at different concentrations (0-50-100-300-500 µg/ml). Actinomycin D 1 µg/ml was used as positive control for apoptosis. At the end of incubation, cells were washed with PBS and resuspended in lysis buffer (10 mM Tris-HCl pH 7.5, 0.2 M NaCl, 0.5% Triton X-100, 1 mM dithiothreitol (DTT) at 170 x 10^6 cells/ml for monocytes and lymphocytes, 40 x 10^6 cells/ml for macrophages and 2.5 x 10^6 cells/ml for HeLa. Cells were vortexed for 50", then NaCl was added at a final concentration of 200 mM to induce osmotic shock and cells were re-vortexed for 15" to complete lysis. After centrifugation at 13000 rpm, 4°C for 10' to separate the particulate fraction (membrane, organelles) from soluble fraction (proteins), supernatants were collected and protein concentration was determined by *DC* Protein Assay (Biorad), according to manufacturer's instruction. Caspase 3 activity was evaluated using a colorimetric assay system (CaspACE^{TM}, Promega), based on the cleavage of Ac-DEVD-pNA by caspase 3 and the consequent release of the chromophore p-nitroaniline (pNA), detectable by a spectrophotometer at 405 nm. Briefly, 100 µg of protein were incubated in a 96 wells

plate at 37°C over night in the dark with Caspase Assay Buffer, DMSO 2%, DTT 10 mM and DEVD-pNA 200 µM. After colour development, absorbance was red at 405 nm.

2.4 Hemolysis assay

Fresh buffy coat was washed 3 times with PBS to remove residual serum and resuspended in the initial volume of phosphate buffer. Then blood was mixed at 1:1 (v/v) ratio with Ludox TM40 NPs at increasing concentrations (0-12.5-25-50-100-300-500 µg/ml) diluted in 150 mM NaCl (saline solution) with or without FCS 10% at two different pH (5.2-7). In other experiments, blood was incubated with 150 mM NaCl alone or supplemented with 35 µg/ml HDL or 5 mg/ml human serum albumin (HSA). Saline solution and distilled water were used respectively as negative and positive control. Samples were incubated for 1, 4, or 18 h at 37°C and then centrifuged at 1500 rpm for 5'. Supernatants were collected and absorbance values of released hemoglobin (indicative of red blood cells lysis) were determinated at 450 nm with a microplate reader spectrophotometer. The percentage hemolysis was calculated as ((sample absorbance-negative control absorbance)/(positive control absorbance-negative control absorbance)) x100.

2.5 Cytofluorimetric analysis

Monocytes, macrophages and HeLa cells seeded onto 24 wells plates were rapidly washed with PBS and incubated for 1, 5 and 18 h with increasing doses of FITC labeled Stöber-NPs, in the presence of different serum concentrations (0-2-10% v/v). At the end of incubation, monocytes and macrophages were detached from plate by gentle scraping, HeLa cells by trypsinization. Then, cells were centrifuged for 7' at 1600 rpm, washed with 1 ml of PBS and finally resuspended in 300 µl of cold FACS Buffer supplemented with 10 mM NH_4Cl to neutralize acidic compartments. Samples were acquired for 30 seconds at flow cytometer (BD FACSCanto II). Data analysis of the gated cellular populations was performed with FACSDiva software (Becton Dickinson).

In fluorescence quenching experiments, the relative contributions to total cell MFI by fluorescein labeled Stöber SiO_2-NPs on the cell surface (MFI^{out}) and inside cells (MFI^{in}) were estimated by Trypan Blue (TB, Sigma Aldrich) quenching effect obtained by flow-cytometry in the presence of 10 mM NH_4Cl. TB concentration of 3 mg/ml was used since it quenched the fluorescence of FITC-labeled anti EGF-R on A431 cells after binding at 0°C to 7% of the value with no TB (not shown). Assuming that $MFI^{out} + MFI^{in} = MFI$ and

that MFI_{TB}^{out} + MFI_{TB}^{in} = MFI_{TB} intracellular percentage of NPs ($\%NPs^{in}$) can be calculated with the derived equation: $\%NPs^{in}$= [(MFI_{TB}/MFI) – *fe*]x[100/(*fi*-*fe*)] (a); were *fe* and *fi* corresponded to the correction factor in the presence of TB to be multiplied with MFI^{out} and MFI^{in} in case of fully surface bound and fully internalizes NPs, respectively. SiO_2-NPs were bound to cells at 0°C, a condition which does not allow cell endocytosis, for two hours at different doses (25-100 µg/ml) and quenching by TB was then analyzed producing a *fe* value of 0.4 ± 0.04 (n=8 ± SE), corresponding to a ~ 60% decrease of cell fluorescence. Alternatively, monocytes and macrophages were incubated for two hours with NPs at 37°C and chased for 24 hours in complete medium, allowing the estimation of a *fi* value of 0.84 ± 0.06 (n=4 ± SE), corresponding to ~ 16% decrease of cell fluorescence. Equation (a) assumed then the following form in our experiments: $\%NPs^{in}$= (MFI_{TB}/MFI – 0.4)x(100/0.44).

2.6 Confocal microscopy analysis

Monocytes, macrophages and HeLa cells seeded on cover glasses in 24 wells plates were incubated for 18 h at 37°C in the dark with FITC labeled Stöber-NPs at different concentrations (0-25-50-100-300-500 µg/ml), diluted in medium + 10% FCS. 30 minutes before pictures acquisition, cellular lysosomes were stained adding the lysosomotropic agent *LysoTracker*® Red (Invitrogen) at a final concentration of 75 nM.
In other experiments, cells were washed with PBS to remove serum excess and then incubated for 1 h at 37°C with Stöber-NPs, in the presence of different amounts of serum (0-0.5-2-10% v/v). Unfixed cells were rinsed with PBS and directly analyzed under a confocal microscopy (SP2 Leica). Representative pictures were collected as Tiff files and processed with standard imaging programs.

2.7 Inhibition experiments

In some experiments, monocytes and macrophages were pre-incubated for 1 h with ammonium chloride (NH_4Cl) 10 mM (Sigma Aldrich), Bafilomycin AI (BafAI) 12.5 nM (Sigma Aldrich) or Ac-YVAD-CMK 100-200 µM (Cayman Chemical), and subsequently incubated for 4 or 18 h with increasing doses of Ludox TM40 NPs, in the absence or in the presence of 10% FCS. In other experiments, cells were treated with TM40 NPs for 4 or 18 h at 37°C in RPMI 10% FCS in the presence of oATP 100 µM (Sigma Aldrich). At the end of incubation, samples were analyzed for cellular mortality by PI, MTS, LDH

assays (see paragraph 2.3), and IL-1β and TNF-α production was evaluated by ELISA assays (see paragraph 2.8).

2.8 ELISA assays

In this work ELISA assays were performed to quantify the three main pro-inflammatory cytokines (IL-1β, TNF-α and IL-6) released by monocytes and macrophages in culture medium after stimulation. Supernatants tested derive from samples used for cytofluorimetric analysis.

2.8.1 IL-β

IL-1β ELISA kit was provided by Bender MedSystems. Briefly, the day before the assay a Nunc MaxiSorp flat-bottom 96 well plate was coated with 50 µl of Capture antibody (diluted 1:100 in PBS) for 16-18 h at 4°C. After coating, unbound antibody was removed by 4 washes with 200 µl of Wash Buffer (PBS + 0.05% Tween), using a Biotrak II plate washer (Amersham Biosciences), and subsequently wells were blocked with 200 µl of PBS + 5% Bovine serum albumin (BSA) for 2 h at RT. Afterwards, wells were washed and 50 µl of supernatants or standards (consisting of IL-1β at known concentrations [1000-500-250-125-62.5-31.25-15-6-0 pg/ml] diluted in the same medium of samples) were added for 3 h, in the presence of 25 µl of biotinylated detection antibody (diluted 1:50 in PBS + 1% BSA). After plate wash, 50 µl of HRP-Streptavidin (diluted 1:6666 in PBS +1% BSA + 0.1% Tween) were added for 30' and, following wash, 100 µl of the substrate solution TMB (3,3',5,5'-Tetramethylbenzidine, KPL) were added until blue colour development. Samples absorbance was read at 405 nm with Biotrak II Reader spectrophotometer.

2.8.2 TNF-α and IL-6

TNF-α and IL-6 ELISA kits were provided by Peprotech. The day before assay, Nunc MaxiSorp flat-bottom 96 well plates were coated with 50 µl of Capture antibody (diluted at a final concentration of 1 µg/ml in PBS) for 16-18 h at RT. After washes as described above, plates were blocked with 200 µl of PBS + 1% BSA for 2 h at RT. Then plates were washed and 50 µl of supernatants or standards (TNF-α and IL-6 at known concentrations [4000-2000-1000-500-250-125-0 pg/ml] diluted in the same medium of samples) were added for 2 h at RT. After washes, detection antibody (50 µl, diluted in

PBS + 0.1% BSA + 0.05% Tween at 0.25 µg/ml for IL-6 and 0.5 µg/ml for TNF-α) was incubated for 1 h, washed and finally 50 µl of HRP-Avidin (diluted 1:2000 in PBS + 0.1% BSA + 0.05% Tween) were added for 30'. Plates were washed again, 100 µl of TMB were added and, after colour development, samples absorbance was read at 405 nm.

2.9 Intracellular and extracellular ATP determination

Monocytes and macrophages (2 x 10^6 cells/well) seeded onto 24 wells plates were incubated for 4 or 18 h with Ludox TM40 NPs at increasing doses (diluted complete medium), in the presence or in the absence of lypopolisaccharide (LPS) 1 ng/ml as co-stimulus. To reduce the activity of ecto-ATPases (membrane associated enzymes responsible of ATP degradation), ecto-ATPases inhibitor ARL 67156 (6-N,N-Diethyl-β-γ-dibromomethylene-D-adenosine-5′-triphosphate, Sigma Aldrich) was added at a final concentration of 200 µM. At the end of incubation, cellular medium was collected and centrifuged at 1600 rpm for 7' to eliminate residual cellular component, while cells were lysed as described in paragraph 2.11, with the addition of 1 mM sodium orthovanadate (Na_3VO_4), in order to inhibit ATP dephosphorylation by ATPases or phosphatases. ATP concentration in extracellular medium or cellular lysate was determined using an ATP Determination Kit (Invitrogen), based on the oxidation of luciferin, in the presence of ATP, to oxyluciferin with the concomitant production of photons (detectable, for example, by a luminometer). First, a working solution (kept at 4°C in the dark) was prepared just before measures. It contained dH_2O, reaction buffer (consisting of 25 mM Tricine Buffer pH 7.8, 5 mM $MgSO_4$, 100 µM EDTA and 100 µM NaN_3), 0.5 mM D-luciferin, 1 mM DTT and 1.25 µg/ml firefly luciferase. Standard solution was prepared by diluting ATP in dH_2O at known concentrations (serial dilutions from 1 µM to 0.12 nM). At the moment of the measure, 90 µl of working solution were rapidly added to 10 µl of samples/standards in special plastic tubes (Sarstedt), and emitted light was detected by a TD-20/20 luminometer (Turner Designs) set on these parameters:

- delay: 3 seconds
- integrate time: 12 second
- replicates: 1

2.10 Single proteins influence on SiO_2-NPs toxicity/association

Monocytes (2 x 10^6 cells/well) seeded onto 24 wells plates were briefly washed with PBS to remove serum excess and subsequently incubated for 18 h at 37°C with Ludox TM40 or fluorescent Stöber-NPs at different concentrations, in the presence of serum free RPMI-1640 supplemented with IgG 140 µg/ml (Sigma Aldrich), HRG 3 µg/ml (purified from human plasma as described in paragraph 2.19), HSA 1.2 mg/ml (Sigma Aldrich), ApoAI 24 µg/ml (Calbiochem) or HDL 50 µg/ml (Calbiochem). Proteins were used at a concentration correspondent to 2% human plasma. At the end of incubation, cellular viability (PI negative cells) and NPs cellular association were evaluated by cytofluorimetric analysis.

2.11 Cellular lysis

Monocytes and macrophages (2 x 10^6 cells/well) seeded onto 24 wells plates were incubated at 37°C for 18 h with different doses of Ludox TM40 NPs with or without LPS 1 ng/ml in complete medium, or for 4 h in RPMI-1640 supplemented with antibiotics and 1% Nutridoma SP (Roche). At the end of incubation, supernatants were collected for ELISA assays or for precipitation procedure, while cells were washed with 1 ml ice cold PBS and immediately lysed for 30' on ice in lysis buffer (50 mM Tris, pH 7.4, 150 mM NaCl, 2 mM EDTA, 2 mM EGTA,10% glycerol, 1% Triton X-100, 40 mM glycerophosphate, 50 mM sodium fluoride, 200 mM sodium vanadate and protease inhibitor mixture (Roche) [128]. Cells from 2 wells (4 x 10^6) were lysed in 120 µl buffer. Afterwards, samples were centrifuged for 10' at 13000 rpm at 4°C, soluble fraction (supernatant) was collected and stained with Loading Sample Buffer (LSB) (50 mM Tris HCl pH 6.8, 0.8% β-mercaptoethanol, 2% SDS, 0.06% bromophenol blue and 6% glycerol) for electrophoresis and western blot analysis.

2.12 Cellular supernatants precipitation

Supernatants of cells stimulated in RPMI-1640 + 1% Nutridoma were precipitated with the following procedure. After supernatants brief centrifugation to eliminate any cellular residue, Trichloroacetic acid (TCA) was added at a final concentration of 10% (v/v) for 1 h at RT. Then, samples were centrifuged at 13000 rpm for 15' at 4°C, pellet of proteins was washed from TCA with 1 ml ice cold acetone and centrifuged as above. Precipitated proteins were solubilized in 42 µl of LSB, supplemented with protease inhibitors cocktail

(Roche). In case of yellow coloration development (indicative of TCA residues), 0.5 µl of Tris 2M were added to adjust pH.

2.13 SDS-PAGE (Sodium Dodecyl Sulphate – Polyacrylamide Gel Electrophoresis)

Samples solubilized in LSB were heated at 95°C for 5', spun down and loaded (15 µl) into a Polyacrylamide gel. 5 µl of ColorBurst™ Electrophoresis Marker (Sigma Aldrich) were loaded in each gel as reference. Resolving gel, stacking gel and running buffer composition is indicated in Table 2.

Resolving gel	**Stacking gel**	**Running Buffer**
Tris-HCl 0.39 M pH 8.8	Tris-HCl 0.125 M pH 6.8	Tris-HCl 25 mM pH 8.3
Acrylamide solution 12%	Acrylamide solution 4%	Glycine 192 mM
SDS 0.1%	SDS 0.1%	SDS 0.1%
APS 0.1%	APS 0.05%	-
TEMED 0.1%	TEMED 0.35%	-

Table 2: Composition of buffers for electrophoresis

Electrophoresis was run for 60' – 90' at 25 mA /gel and 100 V. At the end, gels were recovered, prepared for Western Blot or directly stained by Colloidal Coomassie or Silver Staining procedure, depending on the experiment.

2.14 Western Blot

PVDF (polyvinylidene difluoride) membranes (Biorad) were activated for 30'' in methanol, rinsed 3 times in water and equilibrated together with gels, sponges and paper towels (Whatman) in cold Transfer Buffer (Tris-HCl 25 mM pH 8.3, Glycine 192 mM, Methanol 10%). Then, proteins were transferred from gel to membrane at 4°C for 60' - 90' at 200 mA – 80 V, under stirring. Once the transfer was completed, membranes were blocked for 1 h at RT with 5% non fat milk powder solubilized in TBS (Tris Buffered Saline) + 0.1% Tween, and subsequently incubated for 18 h at 4°C with primary antibody (diluted in 3% non fat milk solubilized in TBS 0.1% Tween). Then, membranes were

washed 3 times for 15' with TBS 0.1% Tween, incubated for 1 h at RT with horseradish peroxidase (HRP) conjugated secondary antibody (diluted in 3% milk + TBS + 0.1% Tween), washed again 4 times and developed with enhanced chemo-luminescence reaction (ECL) as follows. Briefly, each membrane was incubated for 1' in the dark with a solution containing Tris-HCl 100 mM pH 8.5, H_20_2 0.05%, Luminol 1.25 mM and p-Coumaric acid 0.2 mM, and exposed for 10'' – 5' to a photographic plate (Fujifilm Super RX). Plates were developed with Hyperprocessor developer (Amersham Biosciences). Signal quantification was performed using Image J.
In Table 3 a list of all primary and secondary antibodies used in this work is reported.

Primary antibodies			
	Company	**Species**	**Dilution factor**
anti human Albumin	Calbiochem	Rabbit	1 : 2000
Anti human ApoAI	Calbiochem	Goat	1 : 2000
Anti human ApoE	Millipore	Goat	1 : 2000
Anti human Actin	Sigma Aldrich	Mouse	1 : 10000
Anti human Caspase 1	Millipore	Rabbit	1 : 500
Anti human HRG	Abnova	Mouse	1 : 2000
Anti human IL-1β	Cell Signaling	Rabbit	1 : 1000
Anti human IgG2	Millipore	Mouse	1 : 1000
Secondary antibodies			
	Company	**Species**	**Dilution factor**
Anti-goat	Calbiochem	Rabbit	1 : 2500
Anti-mouse	Calbiochem	Goat	1 : 2500
Anti-rabbit	Bio-Rad	Goat	1 : 3000

Table 3: list of primary and secondary antibodies

2.15 Silver Staining

Silver staining procedure was carried out at RT. First, gels were fixed for 30' in 50% methanol 10% acetic acid, incubated for 15' in 5% methanol 1% acetic acid , washed 3 times for 5' with water and incubated for 90'' in thiosulfate solution (200 µg/ml $Na_2S_2O_3$

pentahydrate), in order to sensitize proteins to following treatment. Then, gels were washed 3 times for 30'' with water and incubated in the dark for 30' with 2 g/l silver nitrate ($AgNO_3$), which binds aminoacid side chains. Gels were developed for 5-15' with a solution containing 60 µg/ml sodium carbonate (Na_2CO_3), 4 µg/ml $Na_2S_2O_3$ pentahydrate and 0.0175% formaldehyde, through the reduction of Ag^+ ions to metallic silver (Ag^0) and the consequent formation of a brown precipitate in correspondence of proteic bands. Reaction was stopped with a 6% acetic acid solution. Bands quantification was performed using Image J.

2.16 Colloidal Coomassie G-250 Staining

Coomassie staining was carried out at RT. First, gels were fixed for 18 h in 50% methanol 2% phosphoric acid (H_3PO_4), rinsed 3 times for 30' minutes with water and incubated for 1 h in a solution containing 34% methanol, 2% phosphoric acid and 17% ammonium sulfate $(NH_4)_2SO_4$. Staining step was performed for 3 day in 34% methanol, 2% phosphoric acid, 17% ammonium sulfate and 0.066% Coomassie G-250, and it was followed by destaining in water for other 3 days. Coomassie stained proteins were excised from the gel and subsequently identified by mass spectrometry, in collaboration with Dr Patrizia Polverino De Laureto laboratory.

2.17 In-Gel Digestion, MS/MS protein identification and database research

After Coomassie staining, bands of interest were excised from the gel, crumbled in 1x1 mm cubes into a low binding proteins tube (Eppendorf), washed with 150 µl of water for 5' and shrinked for 15' at RT in 200 µl acetonitrile. Then gel particles were spun down, liquid was removed and gel pieces were dried in a vacuum centrifuge. To reduce disulphide bonds, gel bands were incubated at 56°C for 30' with 200 µl of 10 mM dithiothreitol /0.1 M NH_4HCO_3, and subsequently spun down to better remove liquid, shrinked with acetonitrile as above and dried in a vacuum centrifuge. Reduced disulphide bonds were then alkylated for 20' at RT in the dark with 150 µl of 55 mM iodoacetamide/0.1 M NH_4HCO_3. Then, iodoacetamide solution was removed, gel pieces were washed for 15' with 200 µl of 0.1 M NH_4HCO_3 and, after liquid removing, they were shrunk with acetonitrile and dried. In order to completely destain gel pieces, they were incubated for 15' with 0.1 M NH_4HCO_3 and, at the end, an equal volume of

acetonitrile was added for additional 20' minutes (vortexing every 5'). At this point liquid was removed, gel pieces were shrinked and totally dried. This step was repeated until samples were completely destained. To digest proteins in smaller peptides, gel pieces were rehydrated by covering with the digestion buffer containing 50 mM NH_4HCO_3 and 12.5 ng/µl of trypsin, incubated for 45' at 4°C and subsequently kept over night at 37°C. At the end of incubation, gel particles were spun down and the supernatant was collected for an eventual MALDI analysis. Then, 15 µl of 25 mM NH_4HCO_3 were added to gel pieces at 37°C for 15' with shaking, and additional 50 µl of acetonitrile were added for 15' at 37°C under stirring. After spinning, supernatant was collected, gel pieces were incubated with 50 µl of 5% formic acid for 15' at 37°C with shaking, additional 50 µl of acetonitrile were added for others 15' at 37°C with shaking and finally gel pieces were spun down and supernatant was collected and put together with the one collected just before. At this point, supernatants were dried in a vacuum centrifuge and reconstituted in 20 µl of 5% acetonitrile 0.1% formic acid. For electrospray MS analysis, the peptides were eluted in 50% acetonitrile containing 0.2% formic acid. Data were collected on a Q-Tof AGILENT 6520 mass spectrometer (capillary voltage: 3,000–3,200 V; cone voltage: 45 V; scan time: 1 s; interscan: 0.1 s). Spectra were analyzed using Micromass MassLynx V4.1 software. The MASCOT program (Matrix Science, www.matrix-science.com) was used to search for all MS/MS spectra against the Swiss-Prot and NCBI databases. The following parameters were used in the MASCOT search: trypsin specificity: maximum; number of missed cleavages: 1; fixed modification: carbamidomethyl (Cys); variable modifications: oxidation (Met); peptide mass tolerance: 61.0 Da; fragment mass tolerance: 60.5 Da; protein mass: unrestricted; mass values: monoisotopic.

2.18 Nanoparticles incubation with human plasma or fetal calf serum

Venous blood was taken from healthy volunteers and immediately treated with sodium citrate (at a final concentration of 0.38% v/v) as anticoagulant. Platelet poor plasma (typically 50% of blood volume) was obtained after a centrifugation for 10' at 3000 rpm at RT without accelerator and brake. Fetal calf serum was the same used for cellular cultures. Human plasma (HP) or bovine serum (FCS) were diluted at different concentrations in PBS pH 7.4 + EDTA 1 mM, and incubated for different times (in most experiments, 15') with various amounts of Ludox TM40 NPs at 37°C with shaking, in a final volume of 1 ml. dH_2O was used instead of NPs as control. At the end of incubation,

the mixture was transferred in polycarbonate tubes (Beckman Coulter), which were completely filled with PBS 1 mM EDTA before ultracentrifugation. Nanoparticles were recovered by ultracentrifuging for 1 h at 100000 g at 4°C, using a XL-70 Ultracentrifuge (Beckman). Afterwards, supernatants were collected, NPs pellet was washed twice with PBS EDTA 1 mM filling the tubes (after each washing NPs were ultracentrifuged) and finally dissolved in 150 µl of non reducing loading sample buffer plus protease inhibitors cocktail. After heating at 95°C for 5', equal volumes (4 µl – 19 µl) or equal amounts (3.3 µg) of solubilized NPs were loaded into a 12% polyacrylamide gel (see paragraph 2.11).

In pH dependence experiments, FCS was diluted at a final concentration of 10% v/v in PBS + sodium citrate 5 mM pH 5 or pH 7.2 (depending on the sample) and, after ultracentrifugation, NPs pellet was washed with the buffer at the same pH of the sample.

2.19 Histidine rich glycoprotein purification

HRG was purified from fresh or thawed human plasma (centrifuged at 12000 rpm for 20' at 4°C to remove any aggregate), using a fast protein liquid chromatography (FPLC) system (Pharmacia), in collaboration with Prof. Luigi Bubacco laboratory. Briefly, 6 ml of water-swollen cation exchange resin Phosphocellulose (P-11, Whatman) were equilibrated at 4°C for 18-20 h with 10 volumes (1 volume = 6 ml) of Loading buffer (0.5 M NaCl, 10 mM sodium phosphate, 1 mM EDTA, pH 6.8) supplemented with protease inhibitors. Plasma was diluted 1:2 with Loading Buffer + protease inhibitors, filtered through a 0.22 µM filter and loaded on the equilibrated column. Unbound proteins were removed by extensive washing (20-25 volumes) with Wash Buffer (0.8 M NaCl, 10 mM sodium phosphate, 1 mM EDTA, pH 6.8) plus protease inhibitors, and HRG was eluted by a progressive saline gradient (from 0.8 M to 2 M NaCl, 12 fractions of 1 ml were collected) followed by 4 volumes (12 fractions of 2 ml) of Elution buffer (2 M NaCl, 10 mM sodium phosphate, 1 mM EDTA, pH 6.8), without protease inhibitors. The presence of HRG in collected fractions was evaluated by SDS-PAGE under reducing conditions, followed by silver staining and Western Blot analysis. HRG positive fractions were dialyzed for 20 h at 4°C against 1000 ml PBS, quantified by Bradford assay according to manufacturer's instruction, frozen in liquid nitrogen and stored at -80°C.

2.20 IgG removal from HRG

Immunoglobulins were removed from HRG fractions by the binding to Protein A Sepharose CL-4B resin (GE Healthcare). 100 µl of powdered resin were hydrated with 500 µl of ice cold PBS at 4°C for 30'; then 1 ml of PBS was added and resuspended resin was divided in aliquots of 120 µl. After a wash with 1 ml of HRG Elution buffer, resin was incubated with 250 µl of HRG-containing fraction at 4°C for 8 h under shaking. At the end, resin was spun down, supernatant was collected and, after 2 washes with 1 ml of Elution buffer, pelleted resin was resuspended in 50 µl of reducing LSB 1X. Immunoglobulin removal was analyzed by SDS-PAGE and subsequent silver staining.

3. Results

3.1 SiO_2-NPs cytotoxicity

Cytotoxicity of amorphous silica nanoparticles is largely documented in literature, both in *in vitro* [52] and *in vivo* models [58,61,62,64,66]. In some articles a better ability to induce cytocidal effects in phagocytic cells compared to non phagocytic ones is described, suggesting that nanoparticles endocytosis is important in determining adverse effects [60,68,69]. The majority of studies, however, are conducted on immortalized cells lines (murine or human), so the interaction, and its consequences, between nanoparticles introduced in the body and cellular types they come in contact with are not well represented. With the aim to document a "more physiological" condition, we decided to test amorphous silica nanoparticles toxicity on primary cells, directly purified from buffy coat. We chose two types of phagocytic cells (human monocytes and monocytes-derived human macrophages) and two types of non phagocytic cells (human lymphocytes and human epithelial cell line HeLa, used as control). We performed a systematic approach evaluating different parameters related to cytotoxicity, in order to understand something more about the mechanism. Experiments were conducted treating cells for 4 h or 20 h with increasing doses of Ludox TM40 or Stöber NPs, diluted in medium + 10% FCS (complete medium).

3.1.1 Nanoparticles-induced membrane permeabilization

To check if SiO_2-NPs induce change in the permeability of the cell plasma membrane, we used propidium iodide (PI) and lactate dehydrogenase (LDH) assays. The first method is based on a dye, propidium iodide, unable to permeate cellular membrane. Damaged cells can be stained because they present membrane pores that allow PI (a small molecule, MW 670 Da) to enter, bind to DNA and increase its fluorescence (detectable, for example, at flow cytometer at 670 nm after excitation at 488 nm). The second method measures extracellular levels of LDH, a big homotetrameric enzyme (MW 145 kDa) normally present in the cytosol to catalyze the NADH dependent reduction of pyruvate to lactate (lactic fermentation). In case of cellular lysis, LDH is released in extracellular medium and can be detected with a colorimetric assay.

3.1.2 Nanoparticles-induced mitochondrial damage

Mitochondria are organelles indispensable for vitality of cells, providing the first energy source (ATP) through a complex series of reactions (oxidative phosphorylation). To measure mitochondrial activity (indicative of cellular viability) we used MTS assay, based on the reduction of a tetrazolium salt to colored formazan by mitochondrial dehydrogenases, present in metabolically active cells.

3.1.3 Nanoparticles-induced intracellular ATP decrease

Intracellular ATP level is determined by the balance between its synthesis (through glicolysis and oxidative phosphorylation), its degradation to liberate energy and its release by passive (e.g., as consequence of cellular lysis) and active (e.g., in signaling processes) mechanisms. Even if this parameter is not used as a classic indicator of cytotoxicity, we investigated if it was affected by SiO_2-NPs treatment in inflammatory cells (monocytes and macrophages), considering its importance in inflammasome activation mechanism.

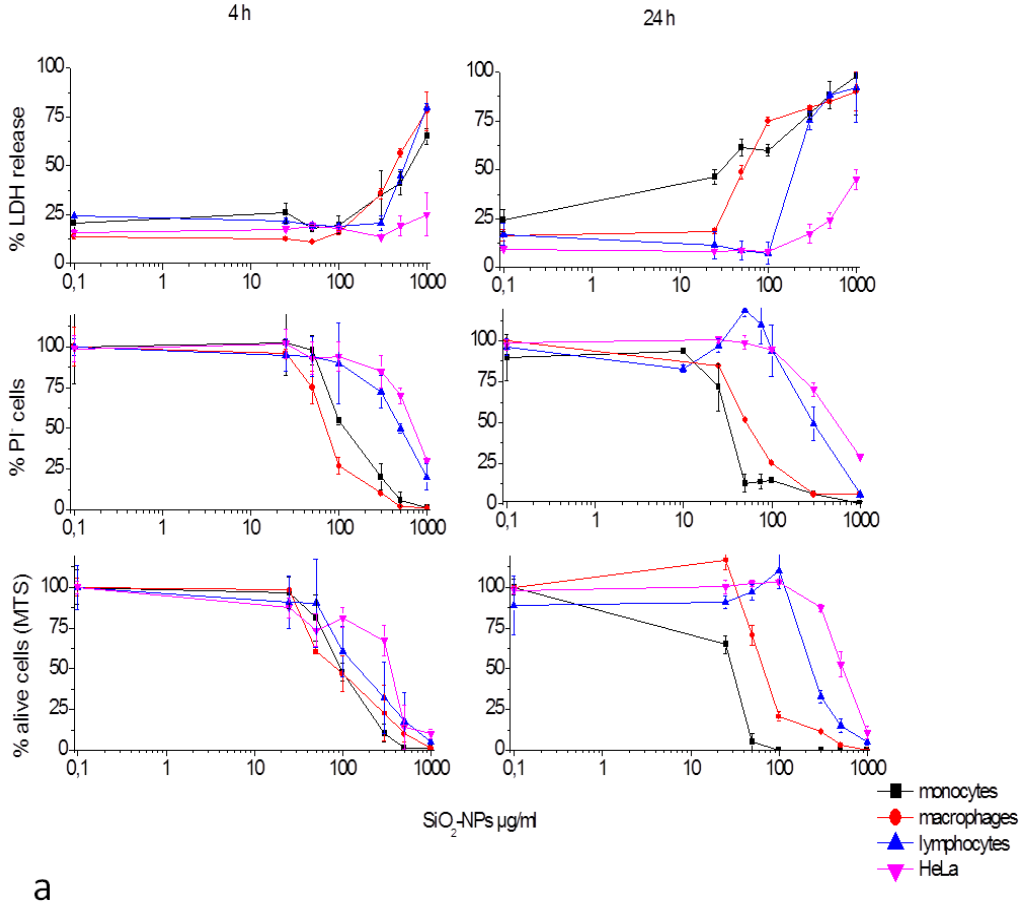

a

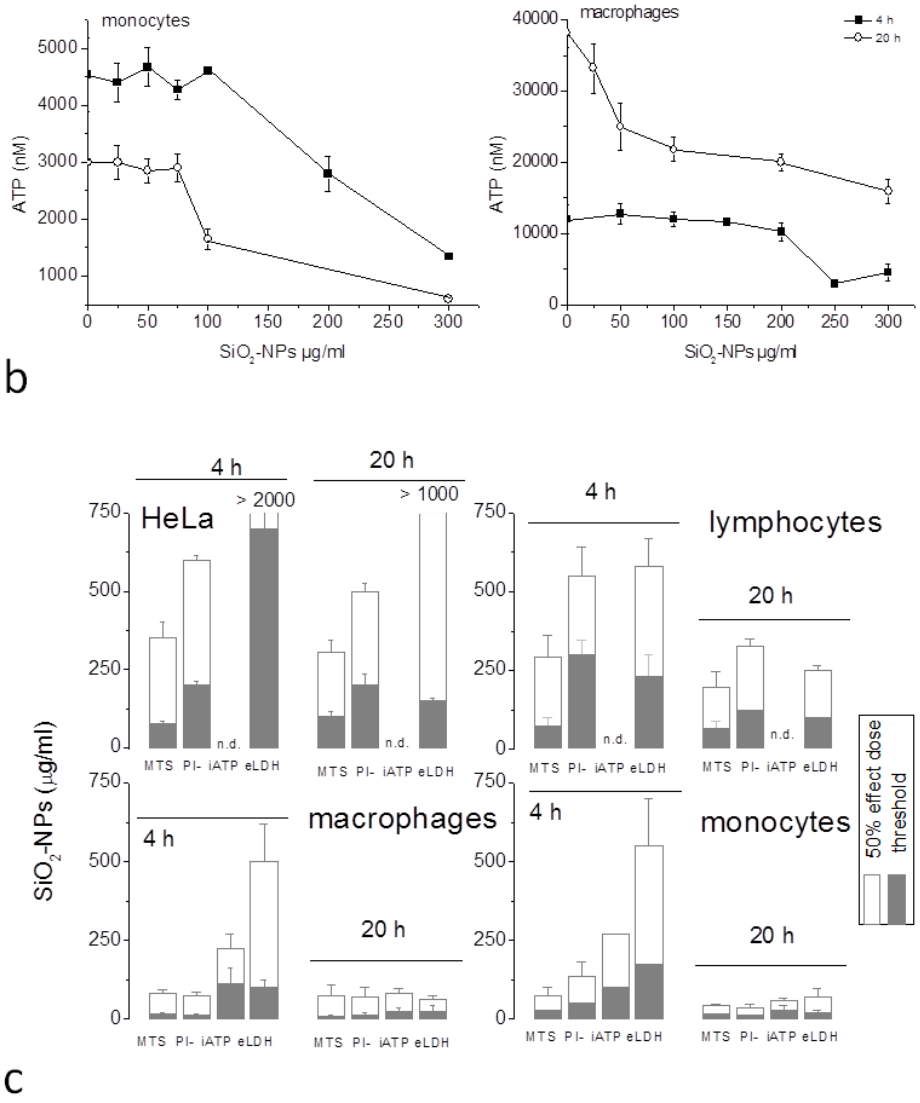

Figure 13: SiO_2-NPs cytotoxic effects on human monocytes, macrophages, lymphocytes and HeLa cells. (a) Time/dose-response analysis of Ludox TM40 NPs induced cellular lysis (% LDH release), membrane permeabilization (% PI^- cells) and mitochondrial damage (MTS), in the presence of complete medium. (b) Intracellular ATP content of monocytes and macrophages treated for 4 and 20 h with increasing doses of Ludox TM40 NPs, in the presence of complete medium. (c) Ludox TM40 cytotoxicity threshold and LD50 after 4 and 20 h cellular treatment. Data are the mean of three independent experiments run in duplicate.

As can be observed from LDH, PI and MTS mortality curves (Figure 13a), SiO_2-NPs cytotoxicity is time dependent and occurs above a threshold concentration, higher for lymphocytes and HeLa in comparison to monocytes and macrophages in all the assays performed. Even LD50 values (representing nanoparticles doses that induce 50% of cellular mortality compared to untreated cells) are ~ 10 fold higher for non phagocytic cells than phagocytic cells (as represented in Figure 13c). These results suggest that

phagocytes are more sensitive than non phagocytes to SiO_2 NPs effects, and are in agreement with data reported in the literature and obtained with cellular immortalized lines. An interesting observation is that cytotoxic NPs doses revealed by propidium iodide and MTS assays are quite similar and significatively lower than the ones revealed by LDH assay, especially after a short time treatment (4 h). This could be due to a first cellular damage involving mitochondrial failure and membrane semi-permeabilization, followed by the complete cellular lysis and the consequent release of lactate dehydrogenase (an enzyme otherwise retained in intracellular environment for its big dimensions). At 20 h this effect is less evident because of the stronger toxicity of NPs, significantly compromising also membrane integrity.

We also found that SiO_2-NPs induce a decrease of intracellular ATP level (Figure 13b) in both monocytes and macrophages, in a time-dose dependent way. This is in accord with a result obtained by Yang *et al.* [129], where ATP depletion was documented in human mesothelial cells after treatment with asbestos (an other inflammasome activator). Surprisingly, threshold and EC50 determined for ATP release are 2-5 fold higher than for mitochondrial activity, suggesting that mitochondrial dysfunction could be compensated by glicolytic pathway and that the event determining intracellular ATP fall is cell disruption (hypothesis supported by the similar threshold and LD50 values between iATP assay and LDH assay).

3.1.4 Necrosis or apoptosis?

Membrane permeabilization and mitochondrial damage are events typical of necrotic death. Necrosis is a “passive” cell death resulting from environmental perturbations (e.g. heat shock and UV irradiation) accomplished with an uncontrolled release of inflammatory mediators [102]. On the other hand, necrosis can also be considered the sum of postmortem cellular changes that cells undergo following their death, regardless the real mechanism of death [130]. An other common type of cellular death is apoptosis, defined as a programmed cellular suicide with the aim to remove undesired individual components (for example affected by genetic mutations or chromosomic aberrations), preserving the safety of the entire cellular population or organism [102,131]. Apoptosis occurs under a strong genetic and environmental control, and is not associated to any inflammatory event [132].

Nano-SiO_2 induced apoptosis is reported in human hepatoma HepG2 cells [64], normal human hepatic cell line L-02 [67], human umbilical vein endothelial cells HUVEC [59] and in several studies performed on murine macrophages [133,134]. To assess if our cellular models undergo apoptotic death after silica nanoparticles treatment, we measured two peculiar markers of apoptosis: phosphatidylserine extracellular exposure and caspase-3 activation.

Phosphatidylserine is a membrane phospholipid normally present in the cytosolic face of the plasmalemma. In apoptotic cells, it is traslocated in the outer side of the membrane, here it contributes to the well controlled death process serving as *eat-me* signal for macrophages [135]. Surface exposed phosphatidylserine can be detected with fluorescent labeled Annexin V, a protein able to bind phosphatidylserine in the presence of calcium. [135,136]. Double staining with propidium iodide and Annexin V allowed to distinguish, at flow cytometer, necrotic cells (Annexin V + and PI +) and apoptotic cells (Annexin V + and PI -).

Caspase 3 is cysteine protease belonging to the effector caspases of apoptosis and responsible of the cleavage of caspase-activated DNase inhibitor, resulting in typical nuclear fragmentation [102]. The activation of caspase-3 from its inactive pro-form can be assessed by a colorimetric assay.

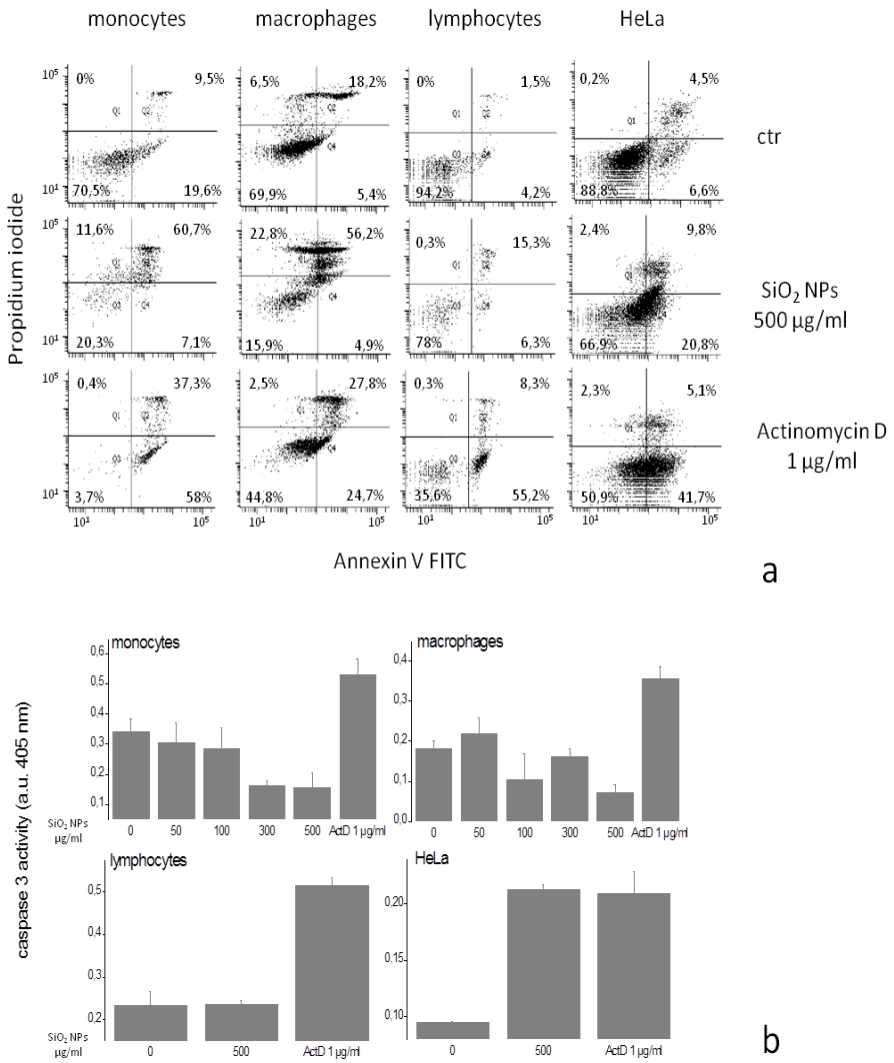

Figure 14: Evaluation of SiO_2-NPs induced apoptosis in human monocytes, macrophages, lymphocytes and HeLa cells. (a) cytofluorimetric analysis of phosphatidylserine exposure and plasma membrane permeabilization of cells treated with medium (negative control), ActD 1 µg/ml (positive control for apoptosis) and Ludox TM40 NPs. Representative dot plots with percent of viable (bottom left quadrant), early apoptotic (bottom right quadrant), late apoptotic (top right quadrant) and necrotic (top left quadrant) cells are shown. (b) analysis of caspase 3 activation through a colorimetric assay. A.u. : Absorbance units. Data are from one of three representative experiments.

After 18 h incubation with Actinomycin D (ActD) (a positive control for apoptosis), all cells show an apoptotic phenotype (PS exposure and caspase 3 activation) compared to the control. On the contrary, SiO_2-NPs treatment induce apoptosis only in HeLa cells, as revealed by both assays, suggesting a different death mechanism between endothelial cells and leukocytes.

3.2 SiO_2-NPs cellular association and localization

Cellular response to nanoparticles derives, in the majority of cases, from their physical interaction. To characterize SiO_2-NPs association with our cellular models, I performed experiments using cytofluorimetry and confocal microscopy, respectively, to quantify the amount of NPs interacting with cells and to determine their cellular localization, by incubating monocytes, macrophages, lymphocytes and HeLa with the fluorescein (FITC) conjugated Stöber NPs. It is possible to use Stöber NPs as a fluorescent (and so detectable) variant of Ludox TM40 NPs because they have very similar physic-chemical properties and they kill at the same manner our cellular models, with an higher toxicity for phagocytic cells.

3.2.1 Cytofluorimetric analysis

Cells incubated for 18 h with different doses of fluorescent Stöber NPs were analyzed for NPs-cellular association at flow cytometer, keeping the same FITC setting to compare different cellular types (that naturally have different autofluorescences) (Figure 15).

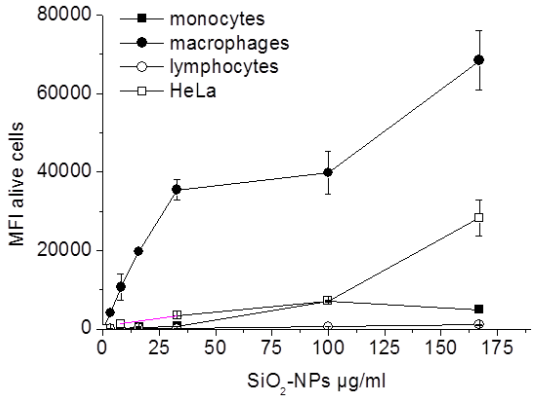

Figure 15: Dose dependent Stöber NPs association to monocytes, macrophages, lymphocytes and HeLa cells after 18 h cellular treatment in complete medium. Data are from one of four representative experiments. MFI: mean fluorescence intensity

Macrophages resulted to be the cells that interact more efficiently with SiO_2-NPs, having the highest association rate and reaching values of medium fluorescence intensity (MFI, indicative of NPs-cells interaction) 10-20 times higher than other cells. Lymphocytes, small non-phagocytic cells, poorly associated to SiO_2-NPs, while monocytes and HeLa cells appeared to be intermediate between macrophages and lymphocytes (HeLa present a higher MFI at higher NPs concentration tested). This result could reflect the innate ability

of macrophages (called "professional phagocytes") to engulf undesired objects (cellular debris, viruses, particulates) compared to other cells. Phagocytic cells are known to internalize different types of particles into endosomes or phagosomes, that can be fused with acidic compartments (lysosomes) forming a phagolysosome, where for example antigens are processed by hydrolytic enzymes. We investigated if lysosomal internalization was conserved also for SiO_2-NPs by incubating cells for 4 h and 18 h with the non fluorescent variant of SiO_2-NPs (Ludox TM40) and monitoring at flow cytometer the signal associated to the fluorescent lysosomotropic probe Lysotracker Green, a flourophore linked to a weak base permeant to lysosomal membrane and retained into the acidic compartment after protonation (Figure 16).

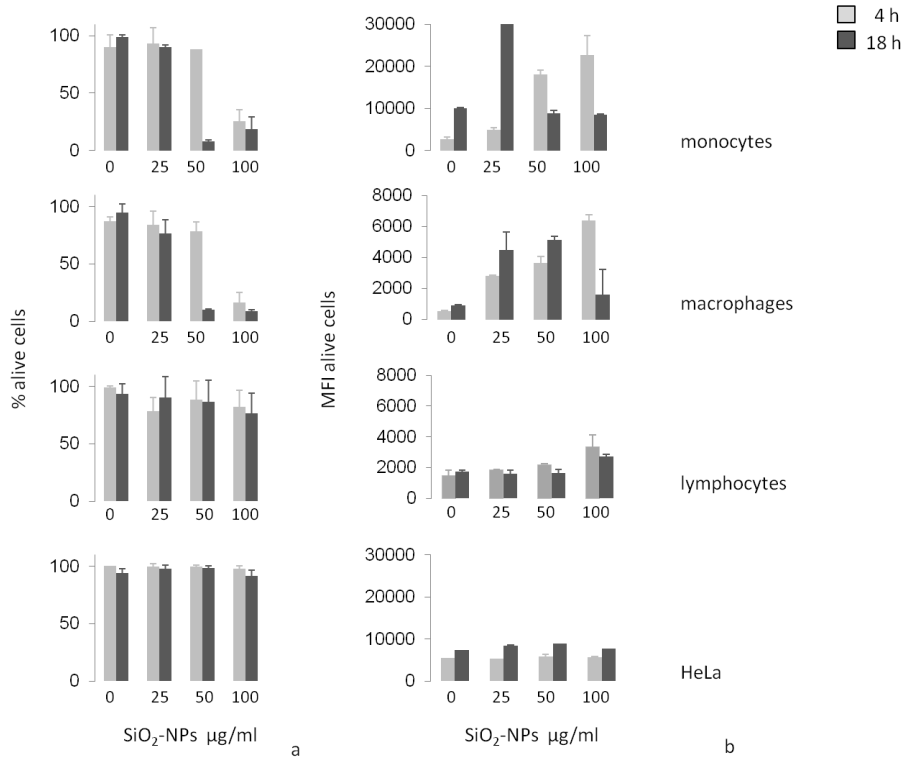

Figure 16: Induction of acidic intracellular compartments in monocytes, macrophages, lymphocytes and HeLa cells by Ludox TM40 NPs. After indicated times, cellular viability (a) and Lysotracker fluorescence intensity associated to alive cells (b) were quantified by cytofluorimetric analysis and expressed as a percentage of control samples (no NPs) and as mean fluorescence intensity (MFI), respectively. Data are the means from three experiments run in duplicate.

After 4 h treatment, the fluorescence associated to Lysotracker clearly increased with the increment of SiO_2-NPs doses in monocytes and macrophages, indicating a hypothetical accumulation of particles in new forming phagolysosomes. After a prolonged treatment (18 h), Lysotracker signal increased in the correspondence of non toxic SiO_2-NPs doses

(as a possible consequence of lysosomal engulfment), while in cytotoxicity conditions (high NPs doses) it was subjected to a fall in both cells. This phenomenon could be attributed to Lysotracker fluorescence dissipation in the presence of cytotoxicity, and is probably consequent to lysosomal destabilization/loss of integrity induced by SiO_2-NPs. Our hypothesis is supported by confocal microscopy experiments reported in recent papers [56,60,134], where a transition from a punctuate pattern of lysosomal loading agents (FITC dextran, acridine orange) to a diffuse cytoplasmic signal (indicative of lysosomal leakage) has been observed after silica treatment. In non phagocytic cells, Lysotracker associated signal remained unchanged (HeLa) or poorly increased (lymphocytes) at any time with the augment of SiO_2-NPs doses, suggesting a negligible formation of new endo-lysosomes consequent to the low amount of phagocytized NPs.

An indirect method to predict SiO_2-NPs localization in our cellular models was to roughly estimate the pH around NPs in cells, assuming that pH values ~ 4.5-5 were representative of acidic compartments. Our experimental approach consisted in the cytofluorimetric measure of the fluorescence associated to FITC-Stöber NPs in the absence or in the presence of NH_4Cl 10 mM (added just before FACS acquisition) as acidic compartments neutralizing agent (for more details, see paragraph 3.3.6). Since FITC fluorescence increases with the increment of pH (as known from the literature [137] and confirmed by our spectrofluorimetric measures reported in Figure 17a), we speculated that the fluorescence of particles inside acidic vesicles would increase after NH_4Cl neutralization, whereas fluorescent signal of particles located in a neutral environment (e.g., cytoplasm) would remain unchanged. The analysis of the ratio of MFI signals obtained from the same sample - or + NH_4Cl allowed a pH value prediction (Figure 17b).

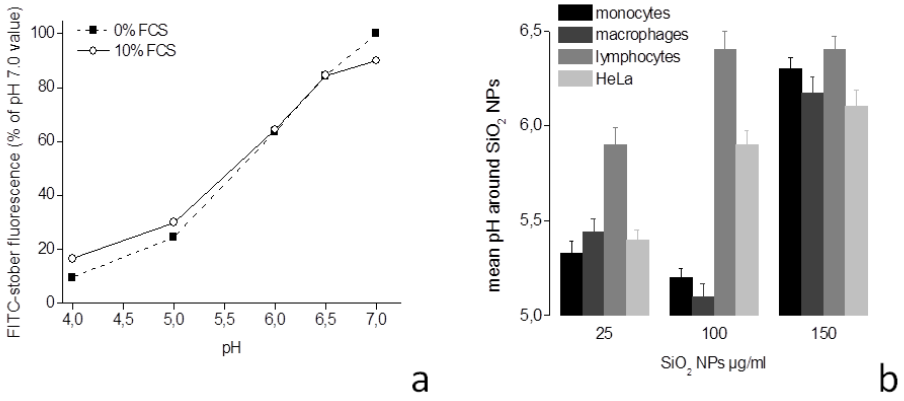

Figure 17: (a) Fluorescein labeled Stöber SiO_2-NPs were incubated at 37°C in serum free medium (0% FCS) or medium plus 10% FCS at different pH values (4-7), and fluorescence maximal intensity was measured with a spectrofluorimeter and expressed as a percentage of the pH 7.0 value. (b) Indicated cells were incubated with the indicated doses of Stöber SiO_2-NPs and the ratio of mean fluorescence intensity in the same alive cells samples before and after neutralization of intracellular acidic endosomal compartments by NH_4Cl 10 mM was evaluated at flow cytometer. The mean pH around cell associated NPs was inferred from the titration curve exemplified in panel (a).

At low doses (25 μg/ml) SiO_2-NPs were in acidic compartments (estimated pH ~ 5.4) in monocytes, macrophages and HeLa, while in lymphocytes they were in a weakly acidic/nearly neutral environment. Upon increasing the NPs dose to 100 μg/ml, the two phagocytic cells maintained the ability to localize NPs in acidic compartments (estimated pH ~ 5.2) while HeLa started to behave similarly to lymphocytes (with a approximate pH ~ 6 around NPs), indicating a less efficient phagocytosis in comparison to phagocytes. In the presence of SiO_2-NPs cytotoxicity (150 μg/ml) the pH surrounding NPs in monocytes and macrophages shifted to more neutral values (> 6), as a possible consequence of lysosomal rupture and dissipation of the H^+ gradient normally maintained in these vesicles. This result is in agreement with the fall of Lysotracker signal under mortality conditions presented above.

3.2.2 Confocal microscopy analysis

To provide more information on SiO_2-NPs uptake by the different cellular models, I assessed their cellular localization by confocal microscopy (lymphocytes were not considered because they did not interact significantly with NPs and, as cells in suspension, they are more difficult to prepare for this type of analysis). Monocytes, macrophages and HeLa were incubated for 18 h with fluorescent Stöber NPs, and

subjected to a lysosomal staining with the fluorescent lysosomotropic probe Lysotracker Red, in order to study the possible co-localization with nanoparticles accumulated in lysosomes (Figure 18).

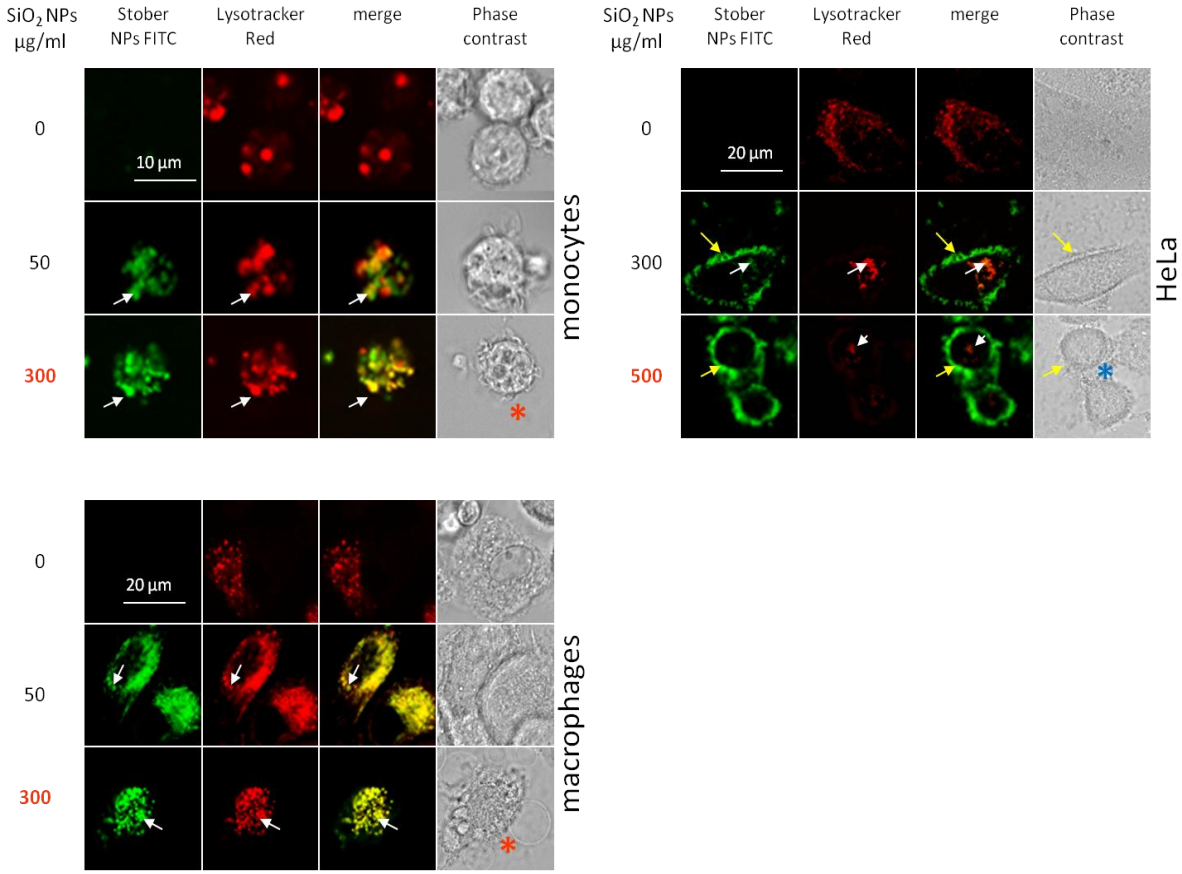

Figure 18: SiO_2-NPs localization in monocytes, macrophages and HeLa. Indicated cells were incubated for 18 h with medium (control) or two doses of Stöber SiO_2-NPs (black: non toxic dose; red: toxic dose). Acidic compartments were stained with the lysosomal probe Lysotracker red. White arrows indicate Lysotracker positive acidic intracellular vesicles; yellow arrows indicate plasma membrane; red asterisks show cytoplasm vacuolization and membrane swelling; blue asterisk indicates small contracted cells.

As expected, in professional phagocytes (macrophages) the signal associated to FITC labeled SiO_2-NP (green) completely overlapped with the one of lysosomes (red), suggesting a very efficient phagocytosis. In monocytes this phenomenon was less evident but could be detected too, while in HeLa NPs associated signal was mostly located on the plasma membrane, indicating that epithelial cells poorly include NPs in intracellular endosomal compartments but, at the same time, are able to establish a superficial interaction (confirming significant MFI values obtained at flow cytometer). In addition, phase contrast pictures were indicative of the different type of cellular death induced by

toxic doses of SiO_2-NPs (indicated in red), providing observations in agree with cytotoxicity data presented in the previous paragraph. Indeed, treated monocytes and macrophages presented big cytosolic vacuoles and membrane bleps (red asterisks), representative of necrosis, compared to untreated cells; HeLa after NPs exposure became smaller and contracted (blue asterisk), as characteristic of apoptotic cells.

3.3 Inflammasome activation by SiO_2-NPs

Several studies document the pro-inflammatory potential of crystalline nanoparticles, responsible of the development of silicosis in many workers daily exposed to this material. Recently, also amorphous silica was found to promote inflammatory genes transcription and correspondent cytokines production (IL-1β, TNF-α) in mouse and rat models, even if in a less strong way than quartz [52,73]. However, most of these studies were conducted by priming cells with LPS (to induce IL-1β transcription) and subsequently adding silica as second stimulus for NALP3 activation, while the ability of SiO_2 to induce an inflammatory response *per se* is poorly documented. To elucidate this aspect, we tested Ludox TM40 NPs on our two models of inflammatory cells (circulating monocytes and monocytes derived macrophages), focusing on different features of inflammasome activation.

3.3.1 Nanoparticles-induced inflammatory response

After treatment of monocytes and macrophages with Ludox TM40 NPs for 4 and 18 h, the levels of the three main inflammatory cytokines (IL-1β, TNF-α and IL-6) released in culture medium were measured (Figure 19).

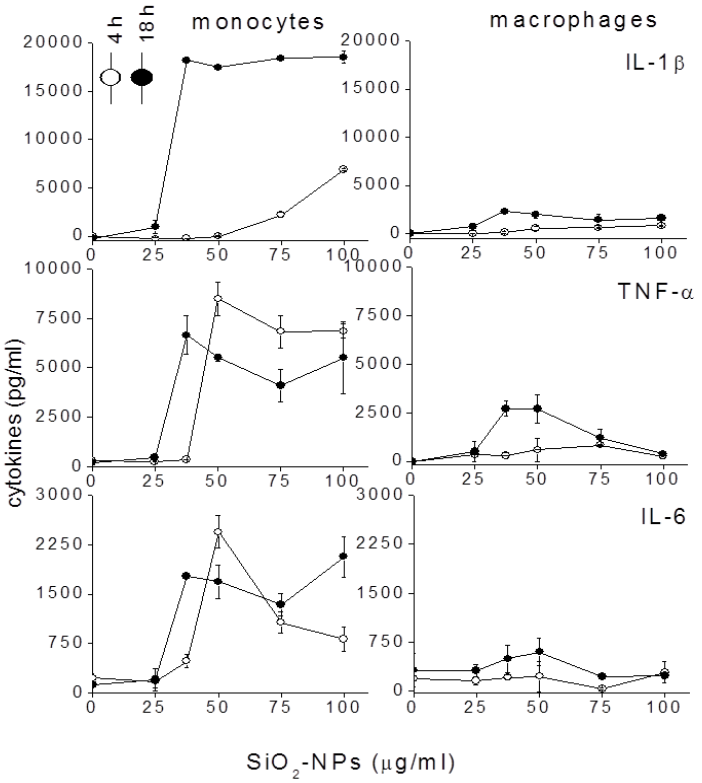

Figure 19: Dose-time dependent inflammatory response induced by SiO_2-NPs in monocytes and macrophages. Cells were incubated for 4 and 18 h with increasing doses of Ludox TM40 SiO_2-NPs, and the levels of IL-1β, TNF-α and IL-6 released in the medium were measured by ELISA assays. Data are from one representative experiment out of five.

A first evidence is that both monocytes and macrophages, if treated with SiO_2-NPs, produce and release inflammatory mediators (IL-1β, TNF-α and IL-6) in a dose-time dependent way. Indeed, all the three cytokines show a "triphasic" trend, with a null/minimal production at low NPs concentration, a central peak (where NPs exert their inflammatory action) and a final fall at highest NPs doses, probably caused by the reduced number of cells still metabolically active because of the strong and very rapid toxicity. The time dependence of the phenomenon is evident because after 4 h treatment the first "NPs inflammatory dose" is 75 μg ml (IL1-β) and 50 μg/ml (TNF-α and IL-6) for monocytes and 50 μg/ml (IL-1β and TNF-α, IL-6 is not detectable) for macrophages, while it results anticipated after 18 h treatment to 37.5 μg/ml for the three cytokines in both cells. Also the absolute quantity of cytokine released is influenced by the time of NPs exposure, with a general increasing tendency, indicating a progressive accumulation of cytokines in the medium. An interesting exception is represented by monocytes

produced TNF-α and IL-6, whose amount does not change between 4 and 18 h. A possible explanation could be that, differently from IL-1β that is produced by a three steps mechanism (gene transcription-protein translation-post traductional maturation) requiring a longer time, TNF-α and IL-6 are synthesized as already mature proteins (so they need less time to be produced) and after 4 h have reached the maximum concentration in the medium. This effect is not observable in macrophages, probably because as less efficient cells in producing inflammatory mediators (compared to monocytes) they synthesize all the three cytokines in a longer time. Comparing the amount of cytokines released by the two cellular types, it is evident that monocytes produce a higher quantity of cytokines (~ 10 folds for IL-1β and ~ 2/5 folds for TNF-α and IL-6). The minor reactivity of macrophages is not attributable to a higher resistance to NPs (in fact SiO_2 toxicity in similar in the two cellular types), but to a reduced ability in producing inflammatory mediators. In both cellular models the main inflammatory cytokine induced by SiO_2-NP is IL-1β, followed by TNF-α and lastly IL-6 (that in macrophages is just detectable because of its very low quantity), confirming that the main effect of silica is on the activation of inflammasome.

3.3.2 SiO_2 NPs – LPS synergism

In the majority of studies reported in literature, cellular treatment with LPS (a TLR4 agonist) is performed to "prime" cells before silica treatment [53,56,73,74]. In other words, LPS is used just as "first stimulus" for inflammasome activation to induce pro IL-1β synthesis, while silica is added as "second stimulus" able to activate inflammasome and promote IL-1β maturation and release. Even if in this way the ability of silica to activate NLRP3 has been demonstrated, the real contribution of the two stimuli is not completely clear because they "work" together and, on the other hand, very little is known on the synergism between LPS and silica [138,139]. In 2011 our group demonstrated that Formyl-methionine-leucil phenylalanine (f-MLP, a model of formylated tripeptide) synergized with ORMOSIL NPs in IL-1β, TNF- α, IL-6 and IL-8 production in monocytes and neutrophils [46]. I have studied the possible synergistic effect between LPS and amorphous SiO_2-NPs by incubating monocytes and macrophages for 18 h in complete medium with Ludox TM40 NPs at different doses, with or without LPS at different concentrations.

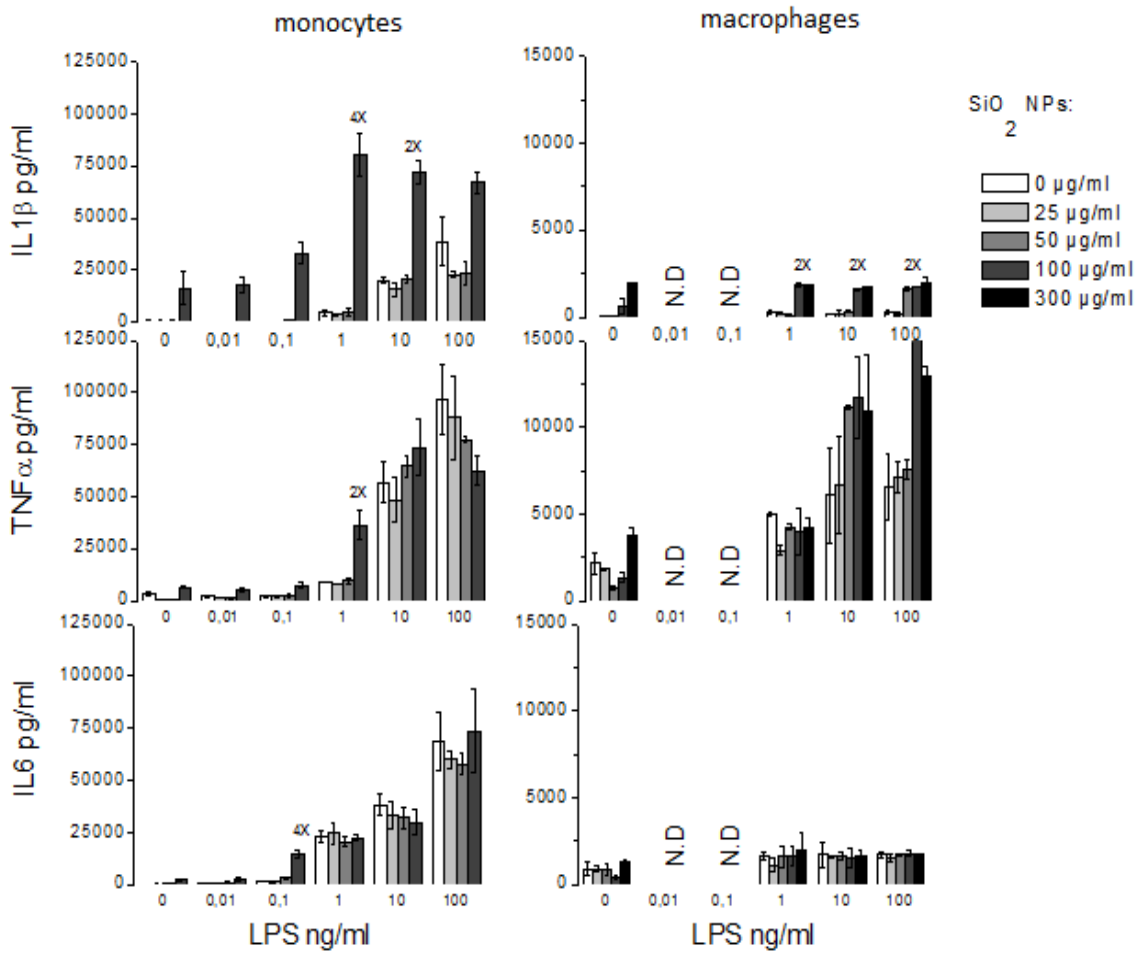

Figure 20: Evaluation of the synergism between LPS and SiO_2-NPs in the induction of inflammatory response. Indicated cells were incubated for 18 h with the indicated doses of LPS and Ludox TM40 SiO_2-NPs at different concentrations, and the levels of IL-1β, TNF-α and IL-6 released in the medium were measured by ELISA assays. Data are from one representative experiment out of four. N.D.: not determined.

Synergism between two stimuli can be observed when the effect of their combination is major than the addition of their single effects. As expected, SiO_2-NPs induced inflammatory cytokines above a threshold concentration in monocytes and, in lower amount, in macrophages, confirming our previous result that silica can promote inflammatory response *per se* (Figure 20). As seen before, IL-1β was the most represented cytokine, followed by TNF-α and, in a very small quantity, IL-6 (in macrophages almost null). After co-stimulation with LPS we obtained different results, depending on NPs and LPS concentration. In monocytes, LPS 1 ng/ml and 10 ng/ml enhanced IL-1β production after treatment with 100 µg/ml NPs respectively 4 and 2 times; TNF-α was increased 2 times after treatment with LPS 1 ng/ml + NPs 100 µg/ml, while IL-6 was increased 4 times after stimulation with LPS 0.1 ng/ml + NPs 100 µg/ml.

It's important to consider that high doses of LPS (100 ng/ml for IL-1β, 10/100 ng/ml for TNF-α and 1/10/100 ng/ml for IL-6 did not induce any synergism because LPS effect was maximum *per se*. In macrophages (less reactive to endotoxin), only a doubling in the production of IL-1β was visible after co-stimulation with LPS 1/10/100 ng/ml + NPs 100 μg/ml, while TNF-α and IL-6 production were not synergized (the first because of the high effect of LPS "per-se", the second because of the very weak cytokine production). To be sure that eventual synergistic effects were not determined by an increased toxicity or cellular association of NPs in the presence of the co-stimulus, I performed control experiments monitoring cellular viability and NPs association with or without LPS. In Figure 21 is shown that LPS 1 ng/ml does not influence these two parameters in monocytes. Macrophages provided the same results, but data are not shown. In conclusion, we demonstrated that endotoxin enhances SiO_2-NPs induced inflammatory response, with the highest effect for IL-1β in monocytes. To better understand the mechanism of this synergism, we performed other experiments using LPS at a final concentration of 1 ng/ml (as dose providing the most effective effect). We concentrated our attention on IL-1β, which is the main cytokine produced after inflammasome activation.

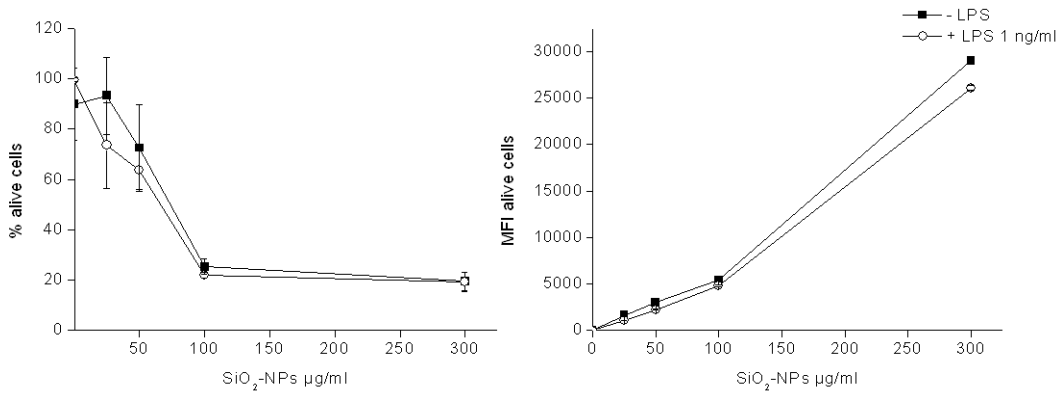

Figure 21: Effect of LPS co-stimulation on SiO_2-NPs cellular toxicity and association. Monocytes were incubated for 18 h with Stöber SiO_2-NPs, in the presence or in the absence of LPS 1 ng/ml. Cellular viability and NPs cellular association were measured at flow cytometer. Data are the means of two experiments.

3.3.3 Caspase 1 and IL-1β activation

As described in paragraphs 1.4.3 and 1.4.4, mature IL-1β (17 kDa) derives from pro IL-1β (31 kDa) after a processing operated by the active form of caspase 1 (the

heterotetramer p10 p20), which, in turn, derives from the autocleavage of pro-caspase (p45) to the mature form. We analyzed the dynamic of caspase 1 and IL-1β induction and activation in the presence of SiO_2-NPs and LPS alone or together. This type of analysis is not easy because intracellular signal seen in western blot derives from a combination of multiple events (immature protein form is a balance between its production and processing; mature protein form between its formation and extracellular release). However, some macroscopic evidences can be observed.

After 18 h cellular stimulation in complete medium, SiO_2-NPs induced pro IL-1β (with a transcriptional and traductional steps) in monocytes and, at lower levels, in macrophages. Also LPS 1 ng/ml (as a classic inflammatory molecule) induced proIL-1β and, if combinated with NPs, the resulting level of pro-IL1β was the sum of the two stimuli alone (Figure 22a). At high NPs doses (100-300 μg/ml ± LPS for monocytes / 100-300 μg/ml + LPS for macrophages) pro-IL1β decreased and IL1-β was correspondently released in the medium, as detected by ELISA assay. In monocytes, residues of the processed form of the cytokine were still visible inside cells in samples treated with 100-300 μg/ml + LPS, while in the other cases cytokine amount was so low that was not detectable by western blot (but ELISA confirmed that it was produced and released in extracellular medium) (Figure 22 a-c).

Caspase 1 resulted already present in its pro-form both in control samples of monocytes and macrophages, while a small amount of activated p20 was visible in macrophages. After treatment with NPs (with or without LPS), p45 appeared to be induced in monocytes, and at 300 μg/ml (a very toxic dose) a significant decrement was detectable (probably because of cellular lysis and consequent release of intracellular content). However, western blot did not provide any information on caspase 1 activation, because the mature form p20 was not visible (Figure 22b). On the contrary, macrophages showed some evidences of caspase 1 activation. In fact, p45 levels remained almost constant after NPs, LPS and NPs+LPS treatment, while p20 subunit increased (at NPs 25-50 μg/ml and NPs 25-50-100 μg/ml + LPS), suggesting (as one can expect) that both silica and endotoxin can activate caspase 1 processing. As for monocytes, high NPs doses (300 μg/ml) determined a decrease of intracellular proteins (in this case p45 and p20) through cellular lysis (Figure 22b).

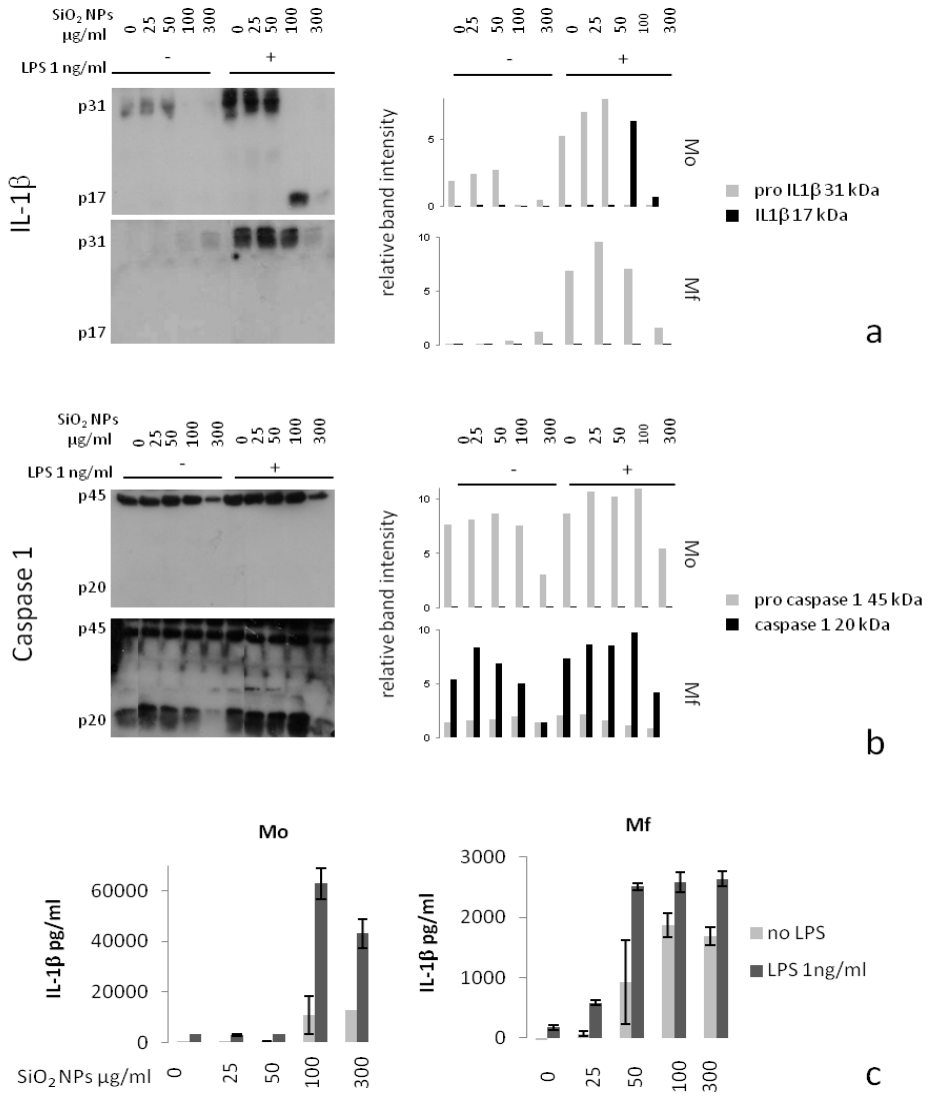

Figure 22: Western blot analysis of pro IL-1β and caspase 1 processing by LPS and SiO_2 NPs treatment in monocytes and macrophages. (a, b) indicated cells (Mo: monocytes; Mf: macrophages) were treated for 18 h in complete medium with increasing doses of Ludox TM40 NPs, with or without LPS 1 ng/ml. Intracellular pro IL-1β (p31), mature IL-1β (p17) (panel a), pro caspase 1 (p45) and caspase 1 (p20) (panel b) were detected by Western blot analysis. Histograms on the right represent the blot signal quantification. (c) IL-1β levels (measured by ELISA assay) present in the extracellular medium of the same samples analyzed in (a, b)

Furthermore, I have performed additional experiments to detect caspase 1 and IL-1β not only inside the cells but also in extracellular medium. It's known that, after inflammasome activation, caspase 1 could be released extracellularly in a form of inflammasome inhibition [140]. Moreover, both proteins can be liberated as a consequence of cellular lysis. In these experiments, cells were incubated with SiO_2-NPs and LPS in a serum free medium to avoid, after supernatants precipitation, a huge amount

of albumin and other abundant serum proteins that could interfere with electrophoretic separation. To compensate the lack of serum, a low concentrated mixture of proteins (Nutridoma) was added to medium. Cellular treatments were performed for a short time (4 h) and with low doses of SiO_2-NPs, to avoid too high toxicity. As shown in Figure 23c, these conditions allowed us to obtain a synergism between NPs and LPS, reproducing the effect seen after treatments in complete medium for a longer time.

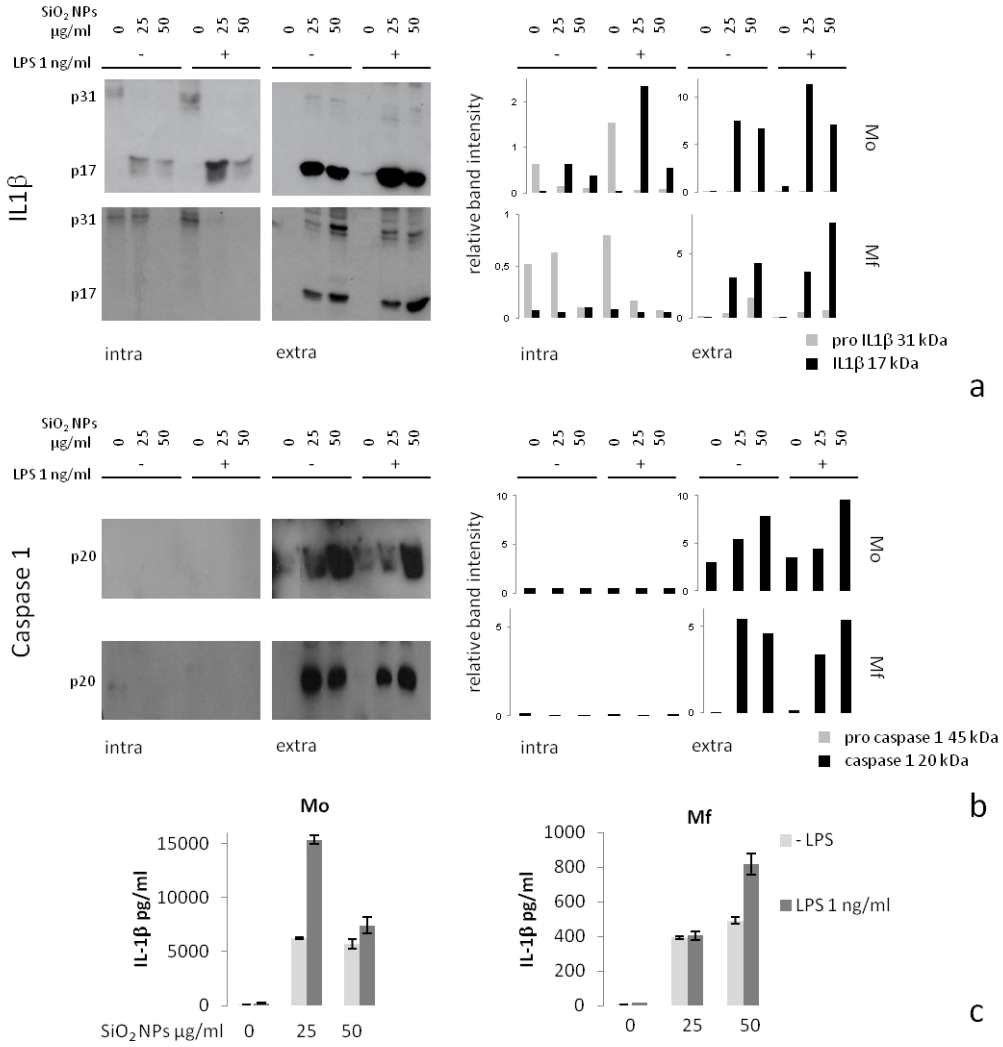

Figure 23: Western blot analysis of pro IL-1β and caspase 1 processing by LPS and SiO_2 -NPs treatment in monocytes and macrophages. (a, b) indicated cells (Mo: monocytes; Mf: macrophages) were treated for 4 h in serum free medium supplemented with Nutridoma with increasing doses of Ludox TM40 NPs, with or without LPS 1 ng/ml. Intracellular (intra) and extracellular (extra) pro IL-1β (p31), mature IL-1β (p17) (panel a), pro caspase 1 (p45) and caspase 1 (p20) (panel b) were detected by Western blot analysis. Histograms on the right represent the blot signal quantification. (c) IL-1β levels (measured by ELISA assay) present in the extracellular medium of the same samples analyzed in (a, b).

In both monocytes and macrophages, intracellular pro-IL1β was induced by LPS, while a small increment after NPs treatment was visible only in macrophages. What appeared clear was that NPs (in the presence and absence of co-stimulus) determined the cleavage of IL-1β precursor (31 kDa) into its mature form (17 kDa) in both cells, and the majority of IL-1β was released in extracellular medium, through active mechanisms and also by cellular lysis (confirmed by extracellular presence of aspecific bands in silica treated samples) (Figure 23a). As in complete medium, monocytes produced higher amount of cytokine than macrophages (Figure 23c).

Looking at caspase 1 blots (Figure 23b), the fact that p20 subunit was not present inside cells and appeared in extracellular medium in correspondence of SiO_2-NPs treatment clearly indicated that it was activated by silica (confirming what is reported in literature). Our additional result was that LPS did not synergize with SiO_2-NPs in caspase 1 activation, suggesting that the enhanced IL-1β production after co-stimulation was not related to a caspase 1 "hyperactivation" but to other factors (e.g., LPS induced pro IL-1β transcription).

3.3.4 The role of ATP

As described in paragraph 1.5.1., extracellular ATP strongly activates NLRP3 inflammasome, by binding to its receptor P_2X7, opening the ion gated channel and promoting K^+ efflux and the consequent oligomerization of NLRP3. In monocytes, this mechanism is responsible for endotoxin induced IL-1β secretion, so that blockage of P_2X7 with oATP (an inhibitor) abolishes IL-1β production [141]. As amorphous silica is able to activate NLRP3, I have investigated the role of ATP and P_2X7 receptor in inflammasome assembly.

Studying cytotoxicity mechanism of SiO_2-NPs, we have found that they induce a decrease of intracellular ATP (Figure 13b). Following the hypothesis that ATP could be in part released outside the cell, I have measured (in the same experiment) intracellular and extracellular ATP after silica stimulation, focusing on the time dependence of the phenomenon (I have stimulated cells for 4 and 18 h) and on LPS possible influence.

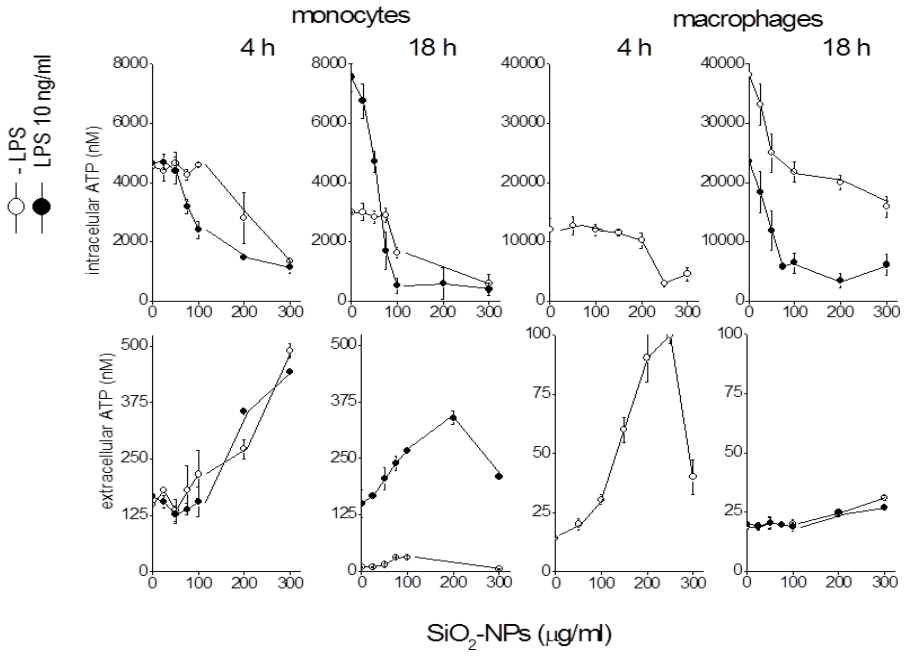

Figure 24: Evaluation of intracellular and extracellular ATP concentration after monocytes and macrophages treatment with SiO_2-NPs, in the presence or in the absence of LPS. Indicated cells were treated for 4 h and 18 h with increasing doses of Ludox TM40 SiO_2-NPs with or without LPS 10 ng/ml. Intracellular and extracellular ATP levels were measured by a chemoluminescence assay in cellular lysate and in culture medium, respectively. Data are the mean of four experiments.

After 4 h and 18 h treatment with SiO_2-NPs, intracellular ATP decreased in monocytes and macrophages in a time dependent way (ATP fall was higher after a long time stimulation) (Figure 24, upper panels). LPS appeared to accelerate and increment ATP release in monocytes, while in macrophages the presence of endotoxin did not influence significantly the curve of ATP release. Macrophages presented a higher intracellular ATP concentration, because they are bigger than monocytes and contain an elevated number of organelles (in this case, mitochondria that are the main source of intracellular ATP).

In general, SiO_2-NPs treatment induced an increment of ATP concentration in extracellular medium in all the conditions, suggesting that, through cellular lysis or active mechanisms, the nucleotide is released outside the cells (Figure 24, lower panels). An important observation is that extracellular ATP concentration (following extrusion) remained in the order of nanomolar, not corresponding with the decrease registered inside the cells (which reached the order of millimolar). This can be due to extracellular degradation of the nucleotide by ecto-ATPases (despite the presence of ATPases inhibitor ARL), or to a decrease of intracellular ATP partially caused by a mitochondrial

dysfunction. In a more detailed analysis of data, ATP release in monocytes after 4 h treatment with SiO_2-NPs clearly increased in a dose dependent way, and was not influenced by the presence of endotoxin. Also after 18 h treatment extracellular ATP augmented (the release was anticipated if compared to 4 h because of longer incubation), but in this case LPS *per se* induced a significant ATP extrusion (150 nM vs 10 nM of untreated cells) and, moreover, synergized with NPs in nucleotide release. At 300 µg/ml, plus or minus LPS, ATP level decreased because of the strong NPs cytotoxicity. LPS own effect is in accord with date present in literature [128,141], while the enhanced ATP release induced by silica and endotoxin co-stimulation could participate to the synergism in IL-1β production, acting as an enhanced second stimulus for inflammasome activation. Curiously, LPS role was visible only after 18 h stimulation, indicating that its action in promoting ATP externalization requires time. In macrophages, SiO_2-NPs induced ATP release in a dose dependent way and, differently from monocytes, LPS did not induce any additional extrusion of the nucleotide. This latter result is in accord with literature [128], where it is reported that macrophages, contrary to monocytes, cannot release endogenous ATP. In addition, it can partially justify the low synergism in IL-1β production after co-stimulation, in the sense that macrophages have a weaker second stimulus for inflammasome activation after NPs + LPS treatment.

Once demonstrated that SiO_2-NPs determine ATP release in extracellular medium in both monocytes and macrophages (probably through cellular lysis, but an active mechanism cannot be excluded), I have investigate if it could play a role in cytotoxicity and inflammatory response induced by SiO_2-NPs. Usually, extracellular ATP binds to its membrane receptor P_2X7 in an autocrine or paracrine way (respectively, when receptor is on the same cell that has released ATP or on a different cell), and triggers a series of pathways (first of all, NLRP3 assembly and activation to produce mature IL-1β). A way to study if the binding between ATP and P_2X7 is important in determining a particular cellular response to a certain stimulus is to block the receptor and check if any changes occur. This approach has been largely used in literature in studies concerning NLRP3 activation, and through these experiments the importance of ATP binding to its receptor has been demonstrated for NLRP3 activation by several PAMPs or DAMPs, such as LPS, muramyl dipeptide (MDP), monosodium urate (MSU) [128,141]. The inhibitor mostly employed is 2'-3' dialdehyde derivative of ATP [142], commonly known as oxidized ATP (oATP). As suggested by its name, it presents two aldehyde groups on ribose C_2 and

C_3, lacking the C_2-C_3 link present in ribose (Figure 25). As a structural analogue of ATP, it can bind P_2X7 receptors, and because of its higher affinity than ATP to P_2X7, it is used as irreversible inhibitor.

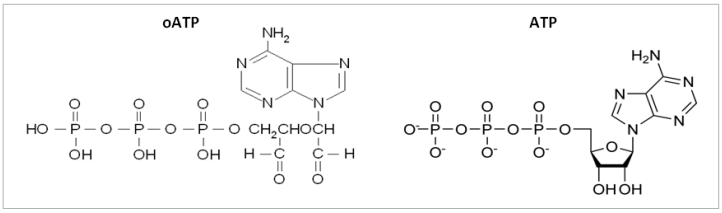

Figure 25: Chemical structure of oATP and ATP

Concerning ATP role in inducing cellular response to silica, Iyer *et al.* [185] reported that P_2X7R-deficient murine macrophages do not present any difference in IL-1β production in comparison with wt macrophages, suggesting that this pathway is not involved. Since this is an isolated study, I have decided to perform a systematic study, comparing cytotoxicity (MTS, LDH, PI assays) and inflammatory response (IL-1β) of SiO_2-NPs in monocytes and macrophages in the presence or in the absence of oATP. Experiments were performed for 4 and 18 h, while LPS possible influence was considered only for monocytes.

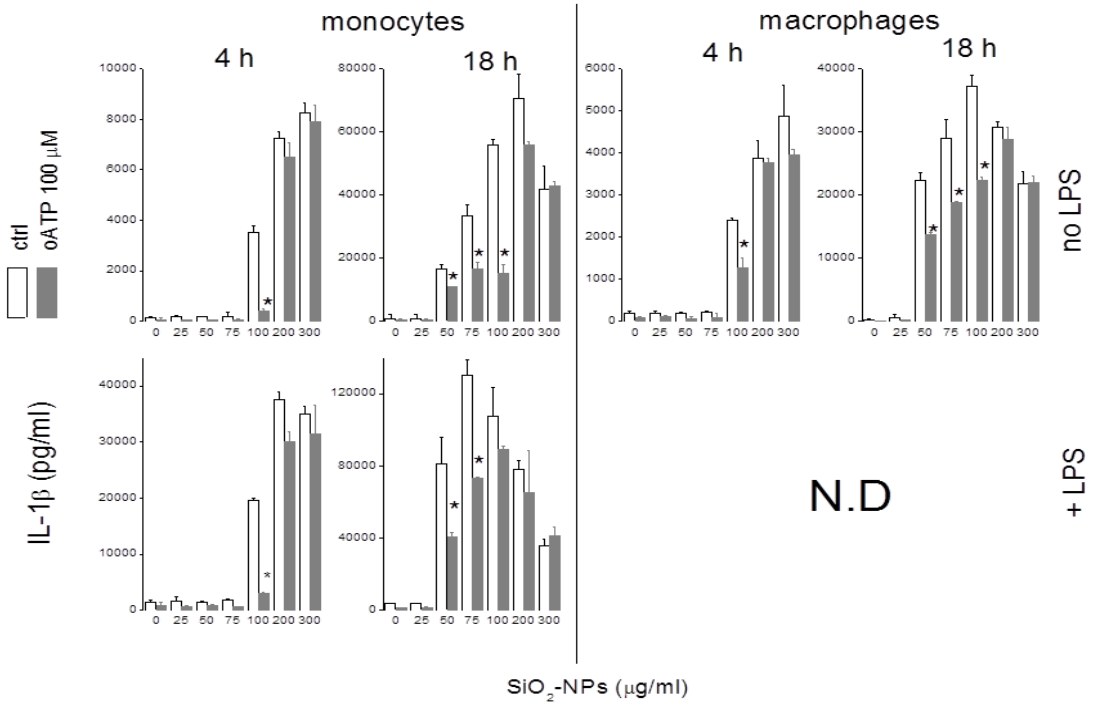

Figure 26: Effect of ATP receptor blockage on SiO_2-NPs induction of IL-1β in monocytes and macrophages. Indicated cells were incubated for 4 h or 18 h with increasing doses of Ludox TM40 NPs ± LPS, in the presence or in the absence of the ATP receptor inhibitor oATP 100 μM. IL-1β levels released in the medium were measured by ELISA assay. Data are the means of four experiments. Significance of differences with respect to ctrl (no oATP) are indicated by * ($p<0.05$). N.D: not determined.

As shown in Figure 26, in both monocytes and macrophages SiO_2-NPs induced a release of IL-1β above a threshold concentration. Such threshold diminished over time, confirming our previous data of the time dependence of the phenomenon. In the presence of oATP 100 μM, IL-1β production was significantly inhibited after 4 h (at 100 μg/ml NPs, ~ 85% inhibition in monocytes and ~ 50% inhibition in macrophages) and after 20 h (at 50-75-100 μg/ml NPs, ~ 50% inhibition in monocytes and ~ 40% in macrophages). Also IL-1β levels resulting from NPs + LPS co-stimulation decreased of ~ 90% after 4 h (at 100 μg/ml) and ~ 50% after 20 h (at 50-75 μg/ml) in monocytes. This result strongly suggests that the binding of ATP to its receptor contributes to NLRP3 activation (and the consequent IL-1β maturation) induced by amorphous silica NPs, acting as a second signal similarly to other PAMPs and DAMPs. At high doses of SiO_2-NPs (200-300 μg/ml) oATP was ineffective in IL-1β inhibition, probably because the strong NPs toxicity synergized with oATP intrinsic toxicity, masking the effect seen at lower doses of NPs.

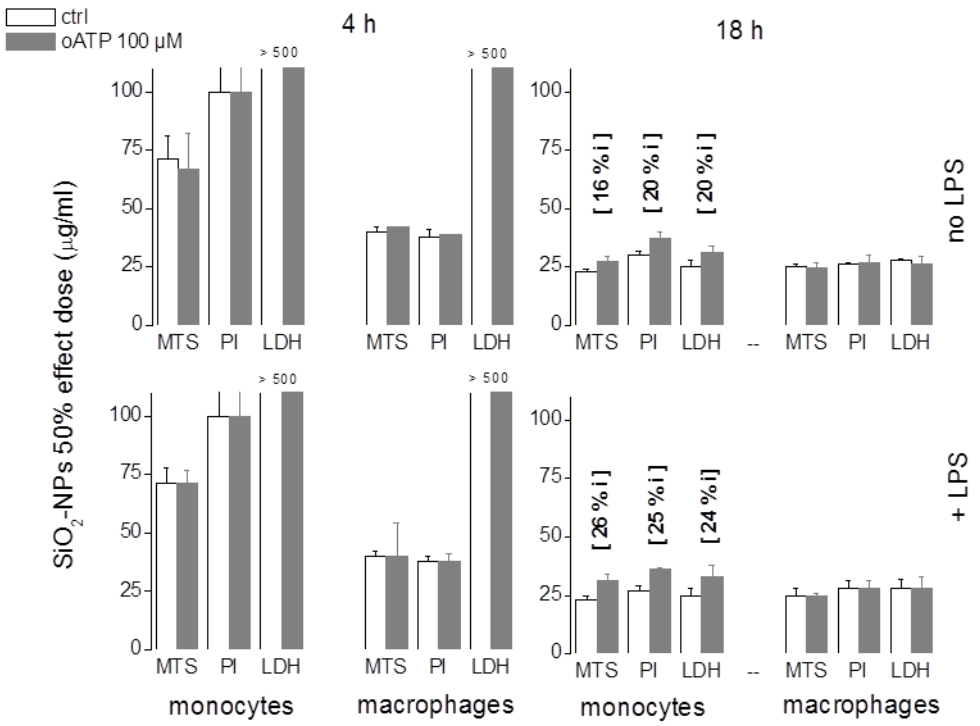

Figure 27: Effect of ATP receptor blockage on SiO_2-NPs cytotoxicity in monocytes and macrophages. Indicated cells were incubated for 4 h or 18 h with increasing doses of Ludox TM40 NPs ± LPS, in the presence or in the absence of the ATP receptor inhibitor oATP 100 µM. NPs cytotoxicity was evaluated as mitochondrial damage (MTS), membrane permeabilization (PI) and cellular lysis (LDH). i: inhibition.

In Figure 27 the effect of P_2X7 blockage on SiO_2-NPs cytotoxicity (evaluated by MTS, PI and LDH assays) is reported. After 4 h treatment, LD50 remained unchanged both in monocytes and macrophages in all the three assays. After 20 h treatment, in macrophages no changes were visible, while in monocytes SiO_2 NPs LD50 showed a small increment of ~ 20% with the three assays, in the presence either in the absence of LPS. This results suggest that, differently from IL-1β production, NPs induced cellular death does not depend (or minimally depends in the case of 20 h monocytes stimulation) on the pathway involving ATP binding to its receptor. In the next part of the thesis other possible mechanisms of cytotoxicity and inflammation will be considered.

3.3.5 The role of caspase 1

As reported in the literature for crystalline silica [53,56,71] and as confirmed by our experiments for amorphous silica (see paragraph 3.3.3), during NLRP3 activation the cysteine protease caspase-1 is subjected to autoprocessing, from its inactive precursor (p45) to the active form (p20 p10). Mature caspase 1 cleaves pro IL-1β in IL-1β.

Moreover, it has been reported by Reisetter *et al*. [109] that carbon black NPs induce in murine macrophages a cellular death requiring caspase-1 (the so called "pyroptosis", already documented for macrophages infected by several types of pathogens). In order to investigate the role of caspase 1 in SiO_2-NPs induced cellular death and inflammatory cytokines production, I have stimulated monocytes and macrophages for 4 and 18 h with SiO_2-NPs, in the presence or in the absence of the caspase 1 inhibitor Ac-YVAD-CMK (N-Ac-Tyr-Val-Ala-Asp chlorometyl ketone) (Figure 28). YVAD is a synthetic tetra peptide whose aminoacidic sequence resembles the ones recognized by caspase 1 (YVHD in pro IL-1β and AVQD in pro caspase 1). Thanks to this similarity, the peptide can bind caspase 1 active site and inhibit irreversibly caspase 1 autoproteolysis (and consequently, catalytic activity).

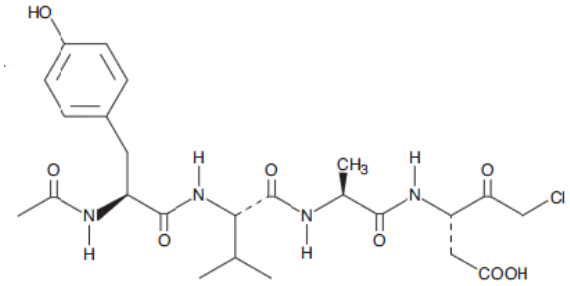

Figure 28: Chemical structure of caspase 1 inhibitor YVAD

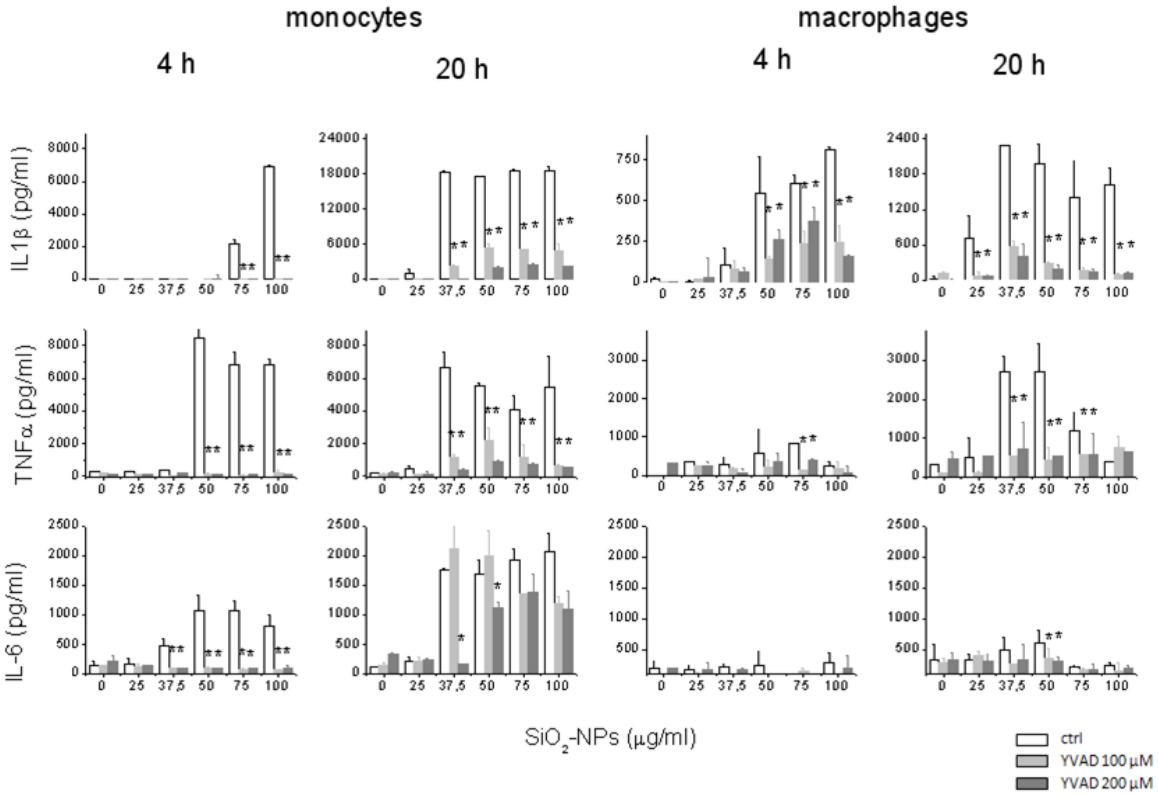

Figure 29: Effect of caspase 1 inhibition on SiO_2-NPs-induced inflammatory response in monocytes and macrophages. After pre-incubation for 1h with medium (ctrl) or caspase 1 inhibitor YVAD (100 or 200 µM), indicated cells were treated for 4 h or 20 h with increasing doses of Ludox TM40 NPs. IL-1β, TNF-α and IL-6 levels released in the medium were measured by ELISA assay. Data are from one of three representative experiments. Significance of differences with respect to ctrl (no YVAD) are indicated by * ($p<0.05$).

Figure 29 shows the effects of caspase 1 inhibition on cytokines (IL-1β, TNF-α and IL-6) induced by SiO_2-NPs. In monocytes, after 4 h stimulation with SiO_2-NPs, YVAD completely abolished IL-1β, TNF-α and IL-6 production at both concentrations used (100-200 µM), whereas after 18 h cytokines were less inhibited (even if their levels were still significantly reduced in comparison to controls) and 200 µM YVAD resulted more effective than 100 µM YVAD. This latter effect probably depends on the activation, over time, of major number of caspase 1 molecules, that to be successfully inhibited would need an higher concentration of YVAD. In a more detailed analysis, IL-1β decrease was ~70% (100 µM YVAD) and ~ 90% (200 µM YVAD); TNF-α decrease was ~60% (100 µM YVAD) and ~ 85% (200 µM YVAD); IL-6 decrement was visible only at 200 µM YVAD (~ 95% at SIO_2-NPs 37.5 µg/ml and ~ 35% at SiO_2-NPs 50 µg/ml).

In macrophages, after 4 h stimulation with SiO_2-NPs, IL-1β was reduced of ~ 50% at both YVAD concentrations, TNF-α decreased ~ 80% (100 μM YVAD) and ~ 50% (200 μM YVAD) at 75 μg/ml SiO_2-NPs (the only responsive dose) while, as seen in before, IL-6 was not produced and any YVAD effect could be detected. After 18 h stimulation, cytokines inhibition by YVAD appeared stronger (~ 80-90% for IL-1β and ~ 80% for TNF-α) and, surprising, there was no difference between the two YVAD concentrations used. Summarizing, a first observation is that inflammatory cytokines production (after SiO_2-NPs treatment) depends on caspase 1 activity in both cellular models, but in macrophages this phenomenon seems to be less important in such way, because at the two times cytokines decrease is minor than in monocytes and the increment of YVAD concentration does not increase its inhibitory effect (contrary to monocytes). The second relevant observation concerns the type of cytokine that is inhibited. To check if YVAD interferes *per se* with the mechanism of IL-1β, TNF-α and IL-6 production or if inhibition was due to an other mechanism, we performed control experiments stimulating monocytes and macrophages with LPS 1 ng/ml for 20 h with or without caspase 1 inhibitor. As expected, IL-1β levels decreased of 90% in both cells (according to YVAD action mechanism), while TNF- α and IL-6 decrement was lower (TNF- α: ~ 13% for monocytes and ~ 35% for macrophages; IL-6: 5% for monocytes and macrophages), and in agreement with data present in literature [143,144]. Interestingly, TNF- α and IL-6 produced after silica treatment were significantly more inhibited by YVAD than after LPS stimulation, suggesting that YVAD intrinsic effect is not sufficient for this inhibition, and an additional mechanism is probably involved. On the contrary, SiO_2-NPs induced IL-1β decrement is compatible with the one obtained after LPS treatment.

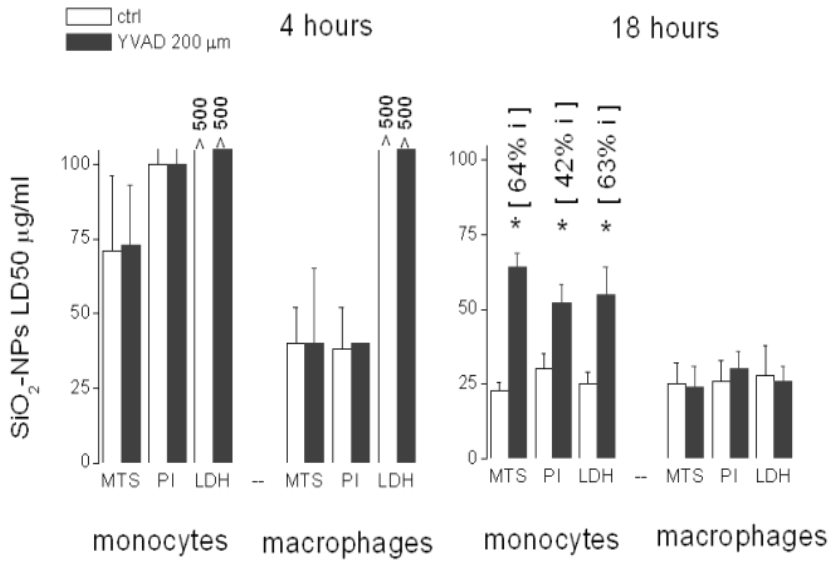

Figure 30: Effect of caspase 1 inhibition on SiO_2-NPs cytotoxicity in monocytes and macrophages. After pre-incubation for 1h with medium (ctrl) or caspase 1 inhibitor YVAD (200 µM), indicated cells were treated for 4h or 18h with increasing doses of Ludox TM40 NPs, and cytotoxicity was evaluated as mitochondrial damage (MTS), membrane permeabilization (PI) and cellular lysis (LDH). Histograms represent LD50 values. Data are the means of three experiments. Significance of differences with respect to ctrl (no YVAD) are indicated by * ($p<0.05$). i: inhibition.

In order to evaluate if SiO_2-NPs induce pyroptosis (a caspase 1 dependent cellular death), I have checked cellular viability (using MTS, PI and LDH assays) after silica treatment for 4 h and 18 h, in the presence or in the absence of YVAD. As reported in Figure 30, SiO_2-NPs LD50 was not influenced by caspase 1 inhibition in 4 h treated monocytes and in 4-18 h treated macrophages in all the three assays performed. On the contrary, in 18 h treated monocytes LD50 increased in the presence of YVAD, respectively from 23 to 64 µg/ml for MTS (64% inhibition of cytotoxicity), from 30 to 52 µg/ml for PI (42% inhibition of cytotoxicity) and from 25 to 55 µg/ml for LDH (62% inhibition of cytotoxicity), suggesting that, in such way, cellular death depends on caspase 1 activity. A possible explanation of the time – dependence of the process (viability increase is visible at 20 h but not at 4 h) could be the following. In macrophages, SiO_2-NPs induced cellular death appears as a rapid process, indeed silica LD50 at 4 h (~ 40 µg/ml, with the exception of LDH assay) is very similar to LD50 at 20 h (~ 25 µg/ml with the three assays), indicating that SiO_2-NPs exert in a short time their toxic effect. In monocytes the situation is different, because at 4 h LD50 is 71 µg/ml (MTS), 100 µg/ml (PI) and > 500 µg/ml (LDH), while at 20 h it decreases at 23 µg/ml (MTS), 30 µg/ml (PI) and 25 µg/ml (LDH), indicating a slower death process, depending, for example, on a more complex

mechanism that requires time to occur. Our results indicate that this unknown mechanism of cell death could be pyroptosis, in fact, it is detectable only in cells dying over time (monocytes) and after a long incubation with SiO_2-NPs (20 h). It is plausible that death occurring after short time treatment depends on a different, easier and more direct mechanism, similarly to macrophages (in fact, caspase 1 inhibition does not have any protective effect).

3.3.6 The role of lysosomes acidification

In paragraph 3.2.2 we have demonstrated that both monocytes and macrophages internalize SiO_2-NPs into acidic endo-lysosomes (fluorescence associated to NPs overlapped with fluorescence associated to the lysosomotropic agent Lysotracker). A possible mechanism of silica toxicity proposed in literature involves silica induced lysosomal destabilization and subsequent rupture ("lysosomal leakage"), with the consequent intracellular release of proteases and hydrolases normally contained in these organelles [56]. Once in the cytosol, such enzymes contribute to inflammasome activation (acting as "danger signal") and to cellular destruction. Recently, it has been shown that acidic lysosomal pH neutralization significantly reduces IL-1β production and, in few cases, cellular death consequent to amorphous/crystalline silica [56,73,74,134] and carbon nanotubes treatment [145]. To investigate if acidic pH may play a role in determining SiO_2-NPs adverse effects, we incubated monocytes and macrophages with SiO_2-NPs for 4 h and 18 h, with or without 1 h pre-treatment with 10 mM ammonium chloride (NH_4Cl) and 12.5 nM Bafilomycin AI (BafAI), and we checked if any modulation of cytotoxic and inflammatory activities occurred.

NH_4Cl is a salt whose dissociation in solution produces HCl and NH_3, a weak base that, thanks to its neutral charge, rapidly diffuses across plasma and lysosomal membranes. In lysosomes, NH_3 is protonated by H^+ to NH_4^+, subtracting protons to the acidic environment. Moreover, the membrane is much less permeable to the protonated species, leading NH_4^+ intralysosomal accumulation, osmotic water influx and lysosomal swelling, providing room for more NH_3 in an auto-powering process [146]. As a consequence, intralysosomal pH increase from 4.5 to 6.2 after NH_4Cl 10 mM perfusion [146,147].

Bafilomycin AI is a macrolide antibiotic produced by the bacteria *Streptomyces Griseus*, consisting of 16-membered lactone ring (Figure 31a) and able to inhibit Vacuolar-type H+-ATPase (V-ATPase) at nanomolar concentrations [148]. V-ATPases are proton

pumps situated on the membrane of several intracellular compartments (vacuoles, lysosomes, endosomes) responsible of the maintenance of acidic pH through the introduction of H^+ from the cytoplasm into the organelles lumen, using the energy released by ATP hydrolysis. They consist of a cytoplasmic portion V_1 (ATP-hydrolytic domain) and a membrane sector V_o (proton-translocation domain) (Figure 31b). V_1 contains three alternating copies of subunits A and B assembled in a ring, which participate to ATP binding and hydrolysis, a central stalk composed of single copies of subunits D and E and a peripheral stalk made of subunits C, E, G and H. Central and peripheral stalk connect V_1 to V_0 domain, that is composed of a ring of six proteolipid subunits (c^I, c^{II}, c^{III}, present in double copy), a subunit *a* (containing two H^+ hemi-channels) and other subunits (*d, e*) [149][150]. V-ATPases pump protons into the lumen through a rotary mechanism, with a stechiometry of $2H^+$/1ATP [149]. Briefly, protons are first engaged at the cytoplasmic side of the hemi-channel in subunit *a* and protonate specific Glu residues on each *c* subunit of the c-ring. ATP bound at the interface of A and B subunits in V_1 is hydrolyzed, and this drives the rotation of the c-ring, followed by protons displacement from the proteolipid subunits into the luminal hemi-channel of subunit *a* and the subsequent release into the lumen of the compartment. During this process, helical swiveling (rotation of the helices relative to one other) in c-ring and subunit *a* is important. Bafilomycin AI inhibition of V-ATPases occurs through the binding to the subunit *c* of V_0, by preventing helical swiveling [150].

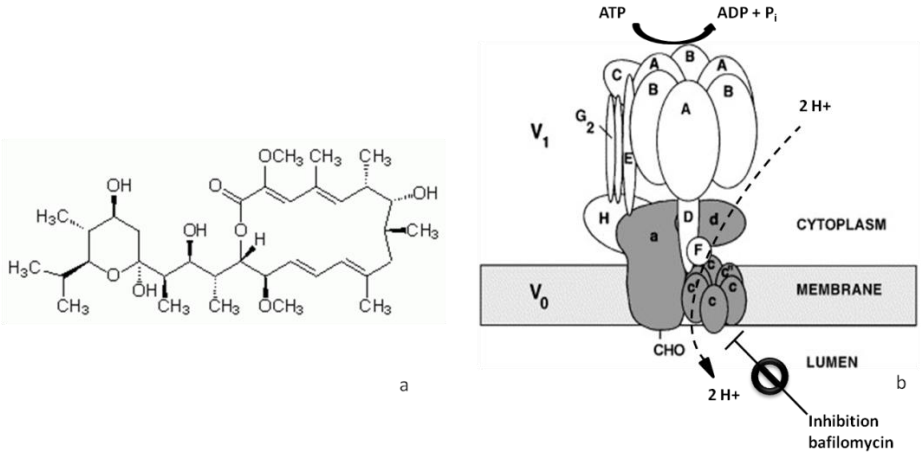

Figure 31: (a) chemical structure of Bafilomycin AI. (b) V-ATPase structural model (modified from [151]).

The eventual interference of NH_4Cl and BafAI with SiO_2-NPs cellular association was evaluated in preliminary experiments, by incubating monocytes and macrophages for 4

and 18 h with fluorescent Stöber NPs, with or without the two neutralizing agents. As represented in Figure 32, any significant change was detected at 50-100 µg/ml NPs after 4 h and at 25 µg/ml NPs after 20 h (the doses considered in cytotoxicity experiments).

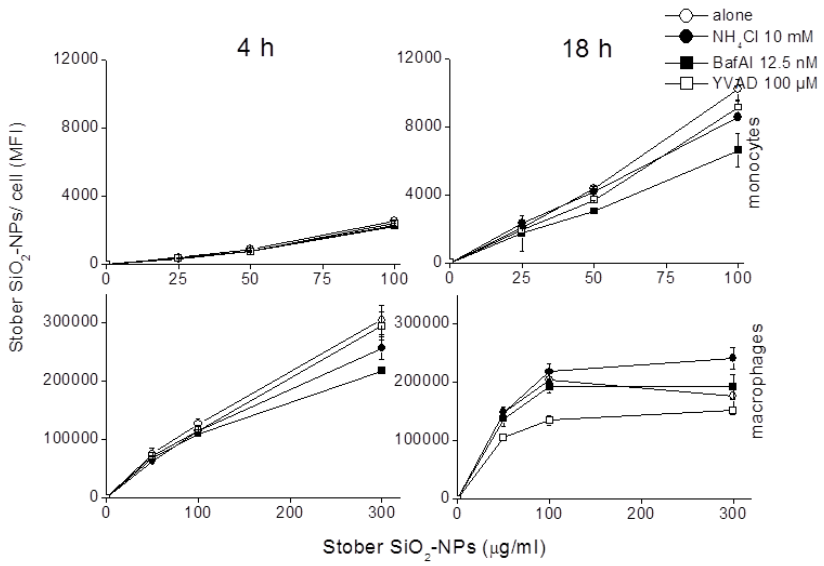

Figure 32: effect NH_4Cl, BafAI and YVAD on SiO_2-NPs cellular association. Indicated cells were pre-incubated for 1 h with medium alone or supplemented with NH_4Cl 10 mM, BafAI 12.5 nM or YVAD 100 µM, and then treated for 4 h and 18 h with Stöber SiO_2-NPs at increasing concentrations. NPs cellular association was measured at flow cytometer.

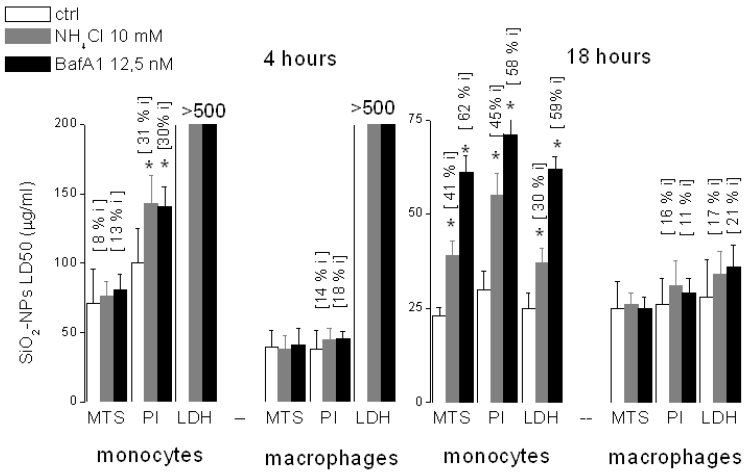

Figure 33: Effect of acidic compartments neutralization SiO_2-NPs cytotoxicity in monocytes and macrophages. After pre-incubation for 1h with medium (ctrl), NH_4Cl 10 mM or BafAI 12.5 nM, indicated cells were treated for 4h or 18h with increasing doses of Ludox TM40 NPs, and cytotoxicity was evaluated as mitochondrial damage (MTS), membrane permeabilization (PI) and cellular lysis (LDH). i: inhibition. Data are the means of three experiments. Significance of differences with respect to ctrl (no NH_4Cl and BafAI) are indicated by * ($p<0.05$). i: inhibition.

After 4 h treatment, SiO_2-NPs cytotoxicity was inhibited ~ 10% (MTS) and 30% (PI) in monocytes after lysosomal pH neutralization, whereas in macrophages this phenomenon appeared less evident (~ 16% with PI assay) (Figure 33). After 20 h treatment, in monocytes NH_4Cl induced a SiO_2-NPs LD50 augment from 26 μg/ml to 43 μg/ml (38% inhibition of cytotoxicity, considering the three assays), and BafAI incremented SiO_2-NPs LD50 from 26 μg/ml to 64 μg/ml (~ 60% inhibition of cytotoxicity), while in macrophages a medium inhibition of only 16% was detectable in samples treated with both neutralizing agents. Our result suggests that in monocytes SiO_2-NPs toxicity is influenced by lysosomal pH (alkaline pH protects from cellular death), and this effect is more pronounced after 18 h treatment. BafAI appeared more effective because it directly blocks the H^+-ATPase pump (the source of protons accumulated in lysosomes), while NH_4Cl acts with an indirect mechanism. On the contrary, SiO_2-NPs toxicity was less influenced by acidic pH in macrophages at both 4 h and 18 h, indicating that a different death mechanism is involved.

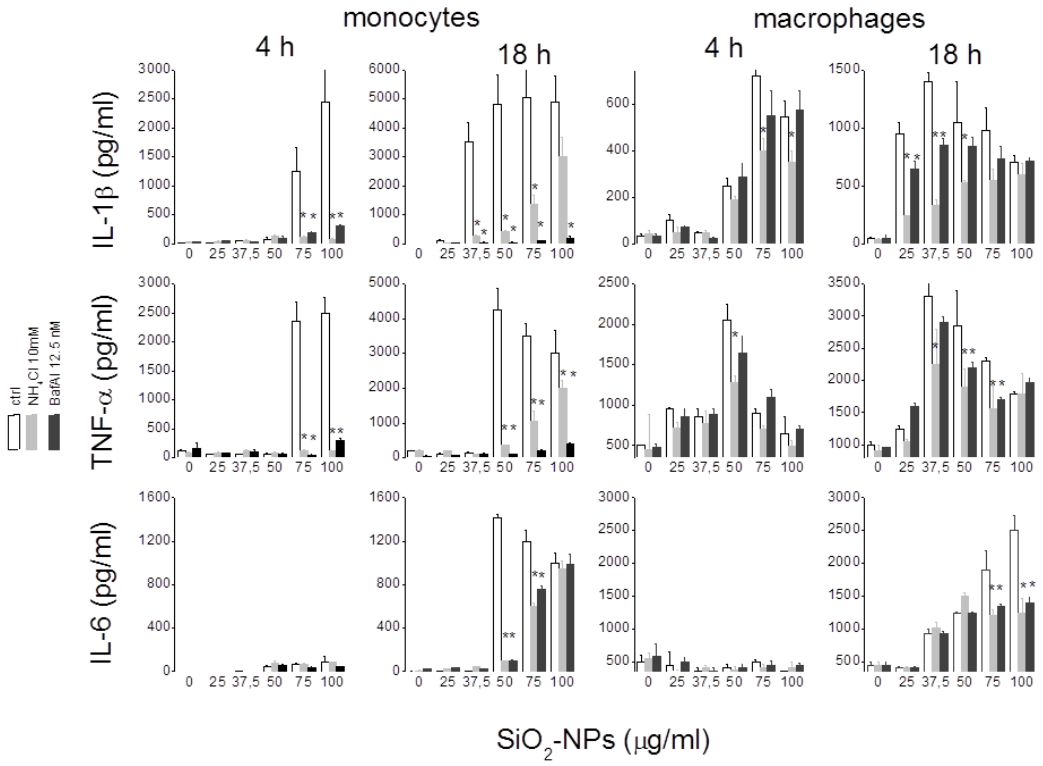

Figure 34: Effect of acidic compartments neutralization on SiO_2-NPs induction of inflammatory response in monocytes and macrophages. After pre-incubation for 1h with medium (ctrl), NH_4Cl 10 mM or BafAI 12.5 nM, indicated cells were treated for 4h or 18h with increasing doses of Ludox TM40 NPs, and IL-1β, TNF-α and IL-6 levels were measured in cellular medium by ELISA assay. Data are from one representative experiment out of four. Significance of differences with respect to ctrl (no NH_4Cl and BafAI) are indicated by * ($p<0.05$).

To check if acidic compartments neutralization interfered *per se* with inflammatory cytokines production, control experiments were carried out by stimulating cells with LPS 1 ng/ml as control. IL-1β levels were decreased of ~ 20% by NH_4Cl and 10% by BafAI in monocytes, while ~ 30% decrement was observed in macrophages for both agents. TNF-α and IL-6 were similarly reduced (~ 13% by NH_4Cl and 10% by BafAI in monocytes, and ~ 13% by NH_4Cl and 22% by BafAI in macrophages). Our result is in accord with the weak IL-1β, TNF-α and IL-6 inhibition after NH_4Cl treatment (< 40%) documented by Jang *et al.* [152].

In monocytes incubated for 4 h with SiO_2-NPs, IL-1β and TNF-α were strongly inhibited by NH_4Cl and BafAI (~ 90%) (for IL-6 any effect was detectable due to its negligible levels) (Figure 34). After 18 h, IL-1β and TNF-α inhibition by NH_4Cl was strong at low SiO_2-NP doses (at 37.5 and 50 μg/ml, > 80%) and weaker at higher doses (~ 30-40% at

100 µg/ml), whereas BafAI at all NPs doses reduced of ~ 90% cytokines level. Also IL-6 was decreased of 90% at 50 µg/ml NPs and ~ of 40% at 75 µg/ml NPs. SiO_2-NPs induced cytokines were less affected by acidic compartments neutralization in macrophages, indeed their levels were considerably less decreased than in monocytes (20-50% inhibition at 4 and 18 h).

In the two cellular types, inflammatory response reduction by NH_4Cl and BafAI was consistent with the correspondent decrease of sensitivity to SiO_2-NPs, in accord to the hypothesis that inflammatory event occurs as a consequence of a cytotoxic event. In fact monocytes (more protected against SiO_2-NPs by the presence of acidic compartments neutralization) presented a stronger inhibition of IL-1β, TNF-α and IL-6 production than macrophages, where neutralization did not lead to a significant cellular viability recovery. However, the fact that in both cells inflammatory response appeared to be more influenced than cellular mortality by NH_4Cl and BafAI, and this trend cannot be justified only by an interference on cytokines production mechanism, suggests that an unknown additional mechanism could be involved.

3.4 The effect of serum on SiO_2-NPs activity

Nanoparticles injected into the bloodstream (the most common way to reach a tissue for drug delivery, gene therapy or imaging) are rapidly coated by a series of plasma proteins, that influence and modulate NPs interaction with cells at different levels (toxicity, phagocytosis, induction of inflammation/coagulation). Since plasma (for *in vivo* models) or serum (for *in vitro* models) play a determinant role in NPs activity, I have investigated if and how serum amount modulates SiO_2-NPs effects described in paragraphs 3.1, 3.2 and 3.3.

3.4.1 DLS measurements

DLS measurements provided information about SiO_2-NPs aggregation state in the presence of different amounts of serum, useful for a better understanding and interpretation of results obtained from biological assays. To this aim, all DLS protocols were carried out at 37°C. Figure 35a shows that SiO_2-NPs diameter increased from ~ 35 nm of monodispersed form (0% FCS) to large aggregates (d =100-200 nm) in the

presence of low amounts of FCS (0.5-2%), decreasing to smaller nanoparticulated structures (40 < d < 80 nm) at 10-40% FCS. Measurements performed keeping serum concentration constant (10%) and varying NPs doses (0-500 μg/ml) confirmed the formation of large NPs-serum proteins agglomerates (d = 400-600 nm) at NPs concentrations > 200 μg/ml (Figure 35b). Both serum and NPs dependence experiments suggested that in conditions of serum deficiency (serum/NPs ratios (%(v/v) : mg/ml) below 100) nanostructures resulting from NPs interaction with serum proteins have size significatively larger than in the presence of serum excess, as schematized in Figure 35c.

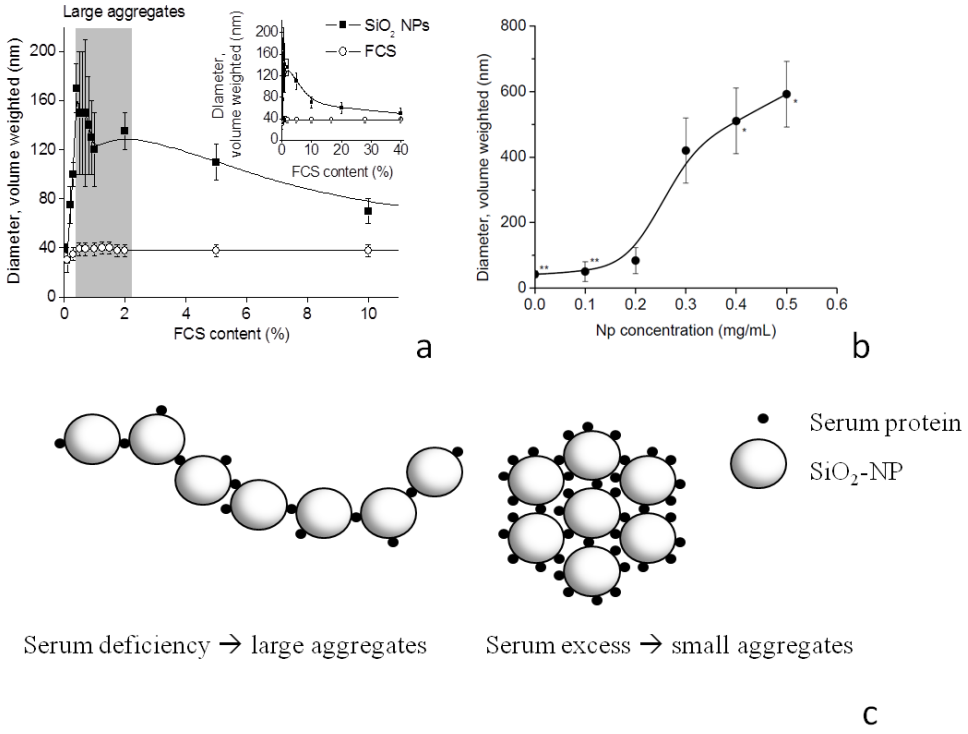

Figure 35: Dynamic light scattering measurements of SiO_2-NPs in the presence of fetal calf serum. (a) Stöber NPs were incubated for 10' at 37°C with increasing doses of FCS (0-40% v/v) in the presence of PBS, and volume-weighted distribution analyses were performed. Top right panel: 0-40% FCS range. Main panel: zoom on 0-10% FCS range, in gray large aggregates. (b) Stöber NPs at increasing concentrations (0-0.5 mg/ml) were incubated for 10' at 37°C with 10% FCS in the presence of PBS, and volume weighted distribution analyses were performed. * A second, minor, population of 80 ± 30 nm size is detected; ** A second population with 7 ± 2 nm size, owing to serum proteins is detected. (c) a schematic example of possible SiO_2 NPs-serum proteins aggregates in FCS deficiency and FCS excess condition.

3.4.2 Cytotoxicity

Figure 36 represents the LD50s obtained after 18 h incubation of monocytes, macrophages, lymphocytes and HeLa with SiO_2-NPs, diluted in media containing increasing serum concentrations (0-40% v/v). The macroscopic general trend in all cell types is an increase of LD50 with the increment of serum amount, indicating a protective serum effect against cellular death, in agreement with previous evidences [61]. More in detail, in the absence of serum monocytes, macrophages and lymphocytes were very and similarly susceptible to SiO_2-NPs (LD50 3, 5, and 4 μg/ml respectively), while HeLa cells were significantly more resistant (LD50 83 μg/ml). This trend was maintained at low serum concentrations (0.5-2-5), while at 10% FCS (a dose typically used in cellular cultures) and at higher doses (20%, 40%) lymphocytes became much less sensitive to SiO_2-NPs (LD50 reached values comparable to Hela). On the contrary, FCS protective effect resulted sensibly less marked in the two phagocytic cells, in particular for macrophages (at 40% FCS, SiO_2-NPs LD50 was 32 μg/ml, 3 times lower than for monocytes (93 μg/ml)).

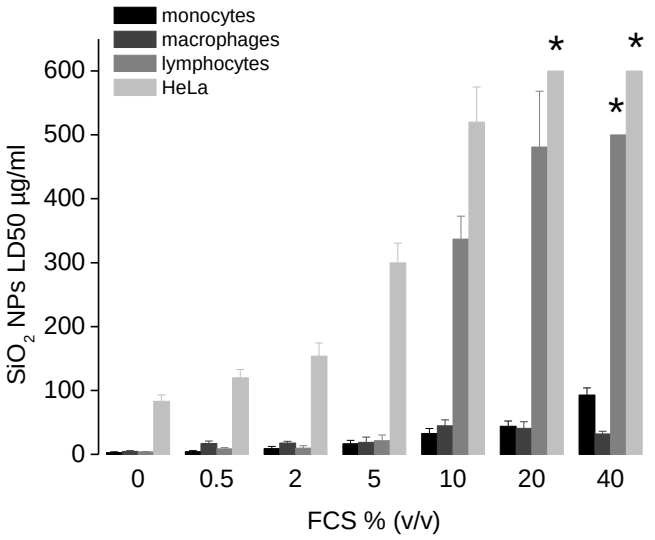

Figure 36: Effect of fetal calf serum on SiO_2-NPs induced cell death. Monocytes, macrophages, lymphocytes and HeLa were incubated for 18 h with increasing doses of Ludox TM40 NPs, in the presence of different amounts of FCS (0-40% v/v). Cellular mortality was determined as membrane permeabilization at flow cytometer (PI), and LD50 values were obtained from dose-response mortality curves. Data are the mean of four experiments run in triplicate. * Extrapolated values > 500 μg/ml.

3.4.3 Inflammatory response

As SiO_2-NPs cytotoxicity is shifted to higher NPs doses by serum increasing, I have investigated if also inflammatory response (that we have demonstrated being correlated to toxicity) was influenced by FCS %. Graphs reported in Figure 37 show that IL-1β, IL-6 and TNF-α production occurred above cytotoxicity threshold and, in parallel with toxicity, was shifted to higher NPs doses with the increment of serum. This almost perfect coincidence of the beginning of cellular death with the detection of inflammatory mediators at any serum percentage robustly confirms that SiO_2-NPs cytotoxicity and induction of inflammation are strictly correlated. Another interesting observation is that, for the same mortality, at higher serum doses the levels of cytokines are major, probably because in the presence of more nutrients and grow factors cellular metabolism is more efficient. As previously reported, at any serum percentage monocytes produced more cytokines than macrophages, and IL-1β resulted to be the most abundant.

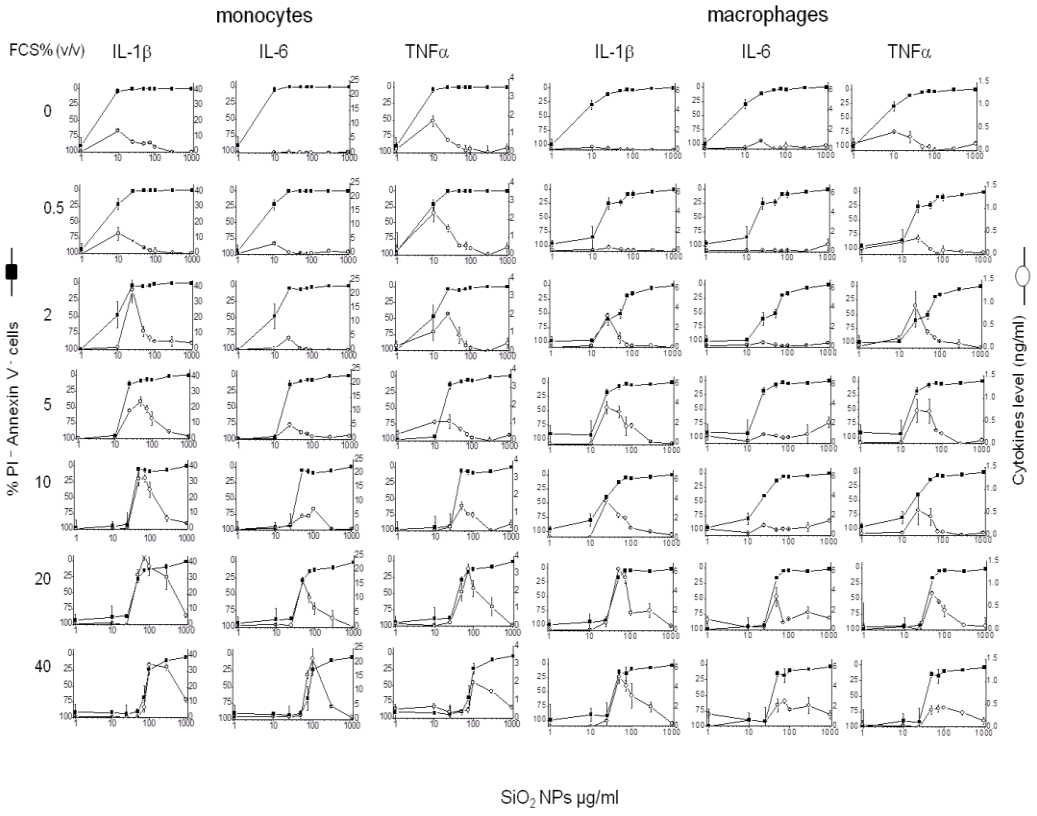

Figure 37: Effect of fetal calf serum on SiO_2-NPs induced death and inflammatory response in monocytes and macrophages. Indicated cells were incubated for 18 h with increasing doses of Ludox TM40 SiO_2-NPs, in the presence of different amounts of FCS (0-40% v/v). Cellular viability (determined at flow cytometer) and IL-1β, IL-6 and TNF-α production are represented in the same graph. Data are the mean from triplicate samples.

3.4.4 Cellular association

To evaluate the effect of serum on NPs cellular association, monocytes, macrophages, lymphocytes and HeLa were treated for 1 and 5 h with fluorescent Stöber NPs at low doses (≤ 50 μg/ml) to minimize cytotoxicity, in the presence of increasing FCS amounts (Figure 38). Preliminary spectrofluorimetric measures excluded any influence of serum on NPs fluorescence (Figure 17a). Confirming data obtained in paragraph 3.2.1, SiO_2-NPs mostly associated to macrophages, followed by HeLa, monocytes and lymphocytes. In non phagocytic cells, the presence of serum clearly decreased 10-20 times NPs cellular association at any time and NPs dose, depending on FCS % (10 < 2 < 0). In addition, at the three FCS concentrations, NPs association reached the maximal value already after 1 h, suggesting that NPs-cell interaction is mediated by an easy rapid process (it's no accident that in lymphocytes, less phagocytic than HeLa, this non-time dependent trend was more pronounced). On the contrary, monocytes and macrophages presented (at any FCS % and NPs dose) an evident time-dependence of NPs association, compatible with a slower and more sophisticated interaction mechanism (possibly phagocytosis). In phagocytic cells (in particular macrophages), NPs cellular association was less inhibited by the presence of serum, decreasing only 2-4 times at 10% FCS compared to 0% FCS. This well correlates with the protective effect of serum in the two cellular categories (strong in non-phagocytes and moderate in phagocytes), suggesting that, in such way, cellular death might depend on NPs cellular association.

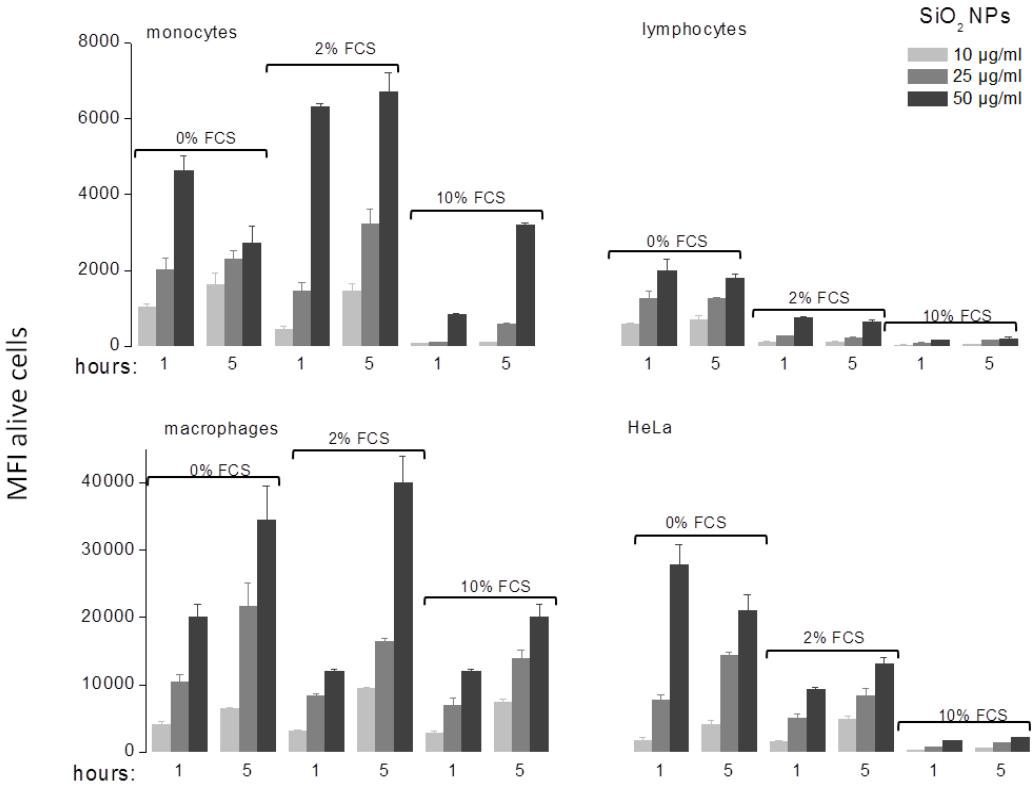

Figure 38: Effect of fetal calf serum on SiO_2-NPs association to monocytes, macrophages, lymphocytes and HeLa cells. Indicated cells were incubated for 1h and 5h with Stöber SiO_2-NPs at increasing concentrations in the presence of 0-2-10% FCS, and NPs cellular association was evaluated at flow cytometer. Data are the mean from three experiments run in duplicate.

To better understand the link between NPs cellular association and cellular viability we compared in parallel and in the same cell population the amount of alive cell-associated SiO_2-NPs with the degree of cell cytotoxic effect, in dose/time dependent experiments at different FCS concentrations (Figure 39).

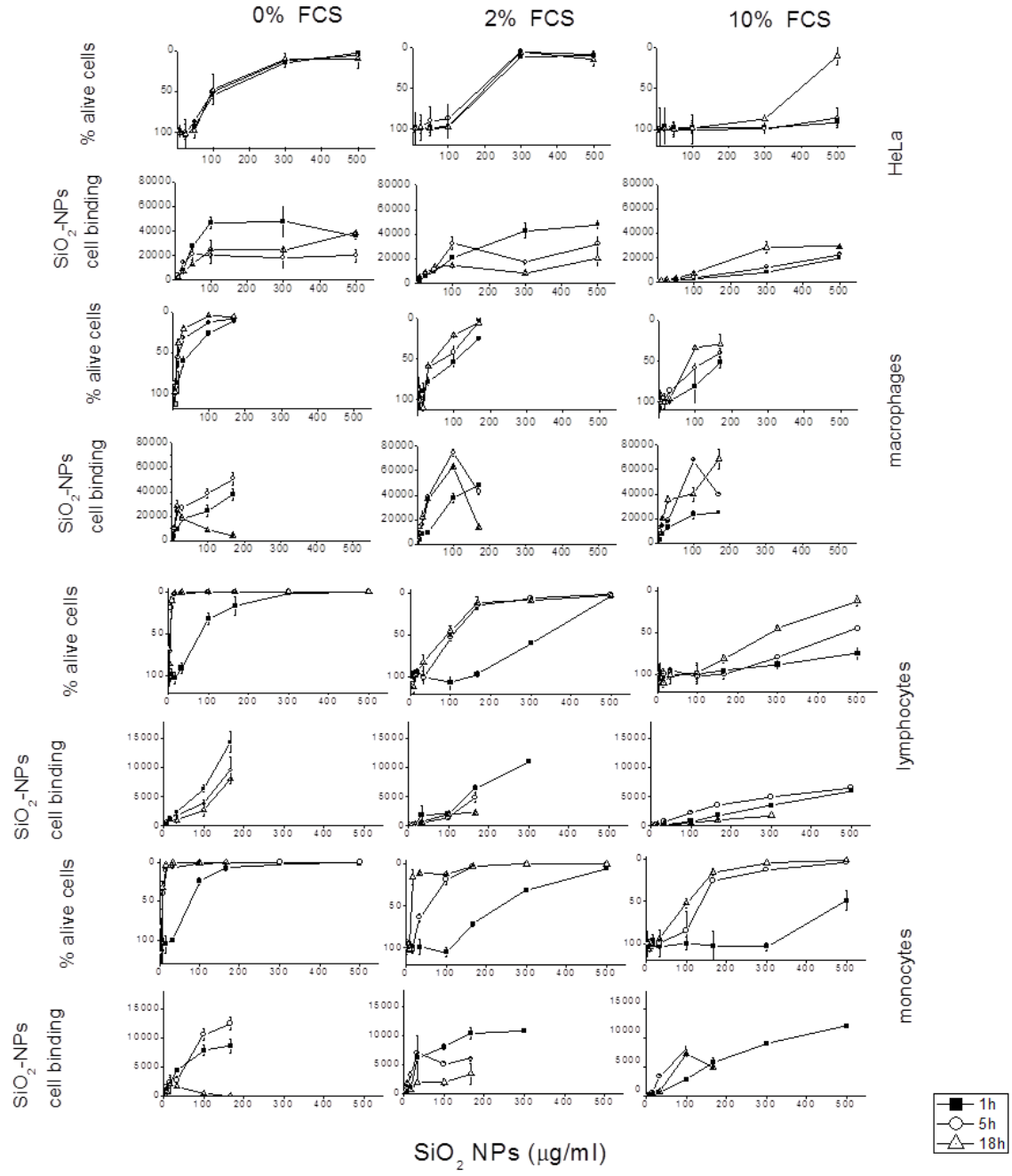

Figure 39: Correlation of SiO_2-NPs-induced cell death with cell association in different doses, incubation times and serum concentrations. HeLa, macrophages, lymphocytes and monocytes were treated with increasing doses of Stöber SiO_2-NPs for 1h, 5h and 18h in the presence of 0-2-10% FCS, and NPs cytotoxicity/cellular association were evaluated by cytofluorimetric analysis. Where the number of alive cells was < 100 fluorescence data concerning NPs-associated mean fluorescence intensity were considered not reliable ant not reported. Data are from one representative experiment out of two.

As shown above, SiO_2-NPs cytotoxicity was dose-time dependent in all considered cells, and was shifted to higher NPs concentrations at increasing serum (more evidently in non phagocytes compared to phagocytes). At the same time, signal of SiO_2-NPs associated to

alive cells was strongly decreased in lymphocytes and HeLa in the presence of serum, while in monocytes and macrophages it resulted less affected and, interestingly, in some cases (e.g. after 18 h SiO_2-NPs treatment in 0-2% FCS) it reached a plateau and eventually decreased above a certain NPs concentration, suggesting that there may be a maximal amount of NPs associated with cells compatible with physiological balance. We investigated this aspect concentrating on HeLa and macrophages, first because they similarly interacted with NPs and, second, after cellular death they were still detectable in the cellular system (monocytes and lymphocytes got disaggregated and disappeared), allowing a comparison between MFI of total, alive (PI negative) and death (PI positive) cells by cytofluorimetric analysis (Figure 40). We found in both cell types that, either in the absence or in the presence of serum, NPs associated to alive cells in a dose dependent way until reaching a maximal cell load (horizontal arrows), coincident with cytotoxicity threshold (vertical arrows). Conversely, NPs signal associated to permeabilized cells was found to linearly increase also above such threshold. Our result suggested that cells can interact with a maximal amount of NPs without compromising viability but, once reached this maximum load, they undergo death. Consequently, NPs increased signal became attributed to permeabilized cells (keeping in mind that fluorescence may be augmented also by the dissipation of lysosomal pH after leakage and by some non-specific interactions of particles to intracellular structures after membrane rupture), while the one of alive cells remains constant at the maximal loading value. In particular, in HeLa at 0% FCS the cytotoxicity threshold was ~ 100 μg/ml and maximal cellular load was ~ 130,000 MFI, while at 10% FCS threshold was shifted to ~ 300 μg/ml and, surprising, cellular load was lower (~ 35,000 MFI), indicating that the small amount of NPs associated in these conditions were more toxic. In macrophages, either cytotoxicity thresholds (10 μg/ml at 0% FCS, 25 μg/ml at 10% FCS) and maximal NPs cellular loads (~ 20,000 MFI at 0% FCS, ~ 40,000 MFI at 10% FCS) were lower than in HeLa cells in the same circumstances, consistently with macrophages major sensitivity to SiO_2-NPs.

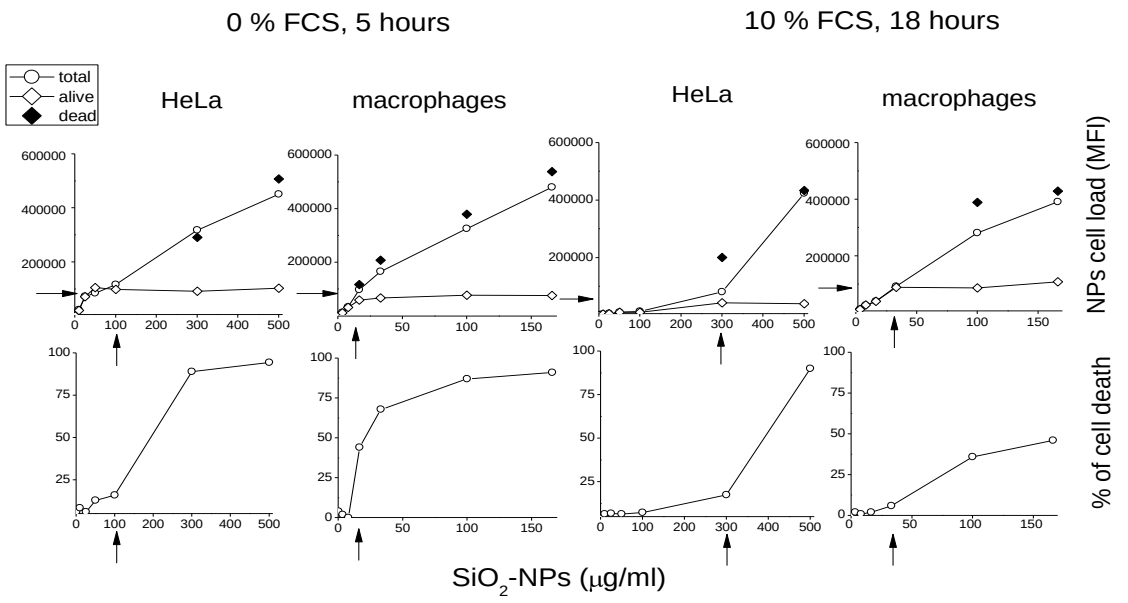

Figure 40: Relationship between SiO_2-NPs cytotoxicity threshold and NPs cell load in macrophages and HeLa. Indicated cells were incubated for 5h in serum free medium or for 18h in medium plus 10% FCS with increasing doses of Stöber SiO_2-NPs. Percentage cell death (lower panels) and mean fluorescence intensity due to NPs associated to total, alive and dead cells (upper panels) were quantified at flow cytometer. Vertical arrows are drawn to emphasize the correspondence between cytotoxicity threshold and the maximal cellular NPs amounts in alive cells, in turn marked by horizontal arrows in upper panels. Data are from a representative experiment out of four.

3.4.5 Cellular localization

To get morphological information also on the SiO_2-NPs cellular distribution in different serum conditions I analyzed unfixed cells incubated for 2.5 h with Stöber SiO_2-NPs in the presence of increasing serum amounts at confocal microscopy.

In HeLa cells (Figure 41a) at 0% FCS SiO_2-NPs accumulated on well defined clusters on plasma membrane at low doses (50 µg/ml), distributing on the entire membrane surface at high doses (at 500 µg/ml fluorescence signal was interrupted in correspondence of big membrane bleps, visible from contrast phase picture and indicative of strong toxicity). At intermediate FCS percentages (0.5-2%), SiO_2-NPs were still mostly localized on plasma membrane, forming large aggregates with serum proteins at 300-500 µg/ml (aggregates are present not only in correspondence of cells but also in the surrounding medium, and are consequent to serum defect, as explained in paragraph 3.4.1). At 10% FCS, NPs associated signal was reduced compared to null-low serum % (according to cytofluorimetric data) and, again, mainly localized on plasma membrane, even if fine

dispersed intracellular vesicles within the cytoplasm were visible. Large NPs-serum proteins aggregates were absent because, at 10% concentration, serum is not defective compared to NPs. Phase contrast pictures showed that serum deprivation *per se* influenced HeLa morphology, with a transition from the classic stretched form in 10% FCS to a round apoptotic-like aspect at 0% FCS. However, SiO_2-NPs toxicity appeared to be stronger in the absence of serum (cellular plasma membrane degenerated in big bleps and cytoplasm became non homogeneous) than in complete medium (treated cells maintained the same aspect of control cells), confirming serum protective effect presented in paragraph 3.4.2.

In monocytes (Figure 41b), in no or few serum (0-2%), SiO_2-NPs distributed on the plasma membrane, often forming a cap on one pole of cell surface, but also in intracellular compartments. As for HeLa, serum-NPs aggregates were visible, associated to cells or dispersed in the medium. At 10% FCS, SiO_2-NPs signal clearly localized in intracellular vesicles sparse in the cell cytoplasm with poor membrane staining, indicating that serum presence is necessary for NPs phagocytosis in monocytes. Phase contrast pictures highlighted a strong SiO_2-NPs toxicity at 0, 0.5 and 2% FCS (monocytes appeared completely disrupted or with large cytosolic vacuoles), while at 10% FCS cellular morphology was not affected by SiO_2-NPs, indicating a minor sensitivity.

In macrophages (Figure 41c), in serum free medium SiO_2-NPs were irregularly dispersed into the cytoplasm, denoting the ability to internalize uncoated SiO_2-NPs (contrary to HeLa and monocytes). However, in the presence of serum intracellular SiO_2-NPs signal appeared more homogeneous and accumulated in compartments resembling typical phagosomes/phagolysosomes, suggesting as for monocytes that serum promotes NPs internalization. Phase contrast pictures showed completely death cells at 0% FCS, highly vacuolizated cells at 0.5-2% FCS and normal cells at 10% FCS after SiO_2-NPs treatment.

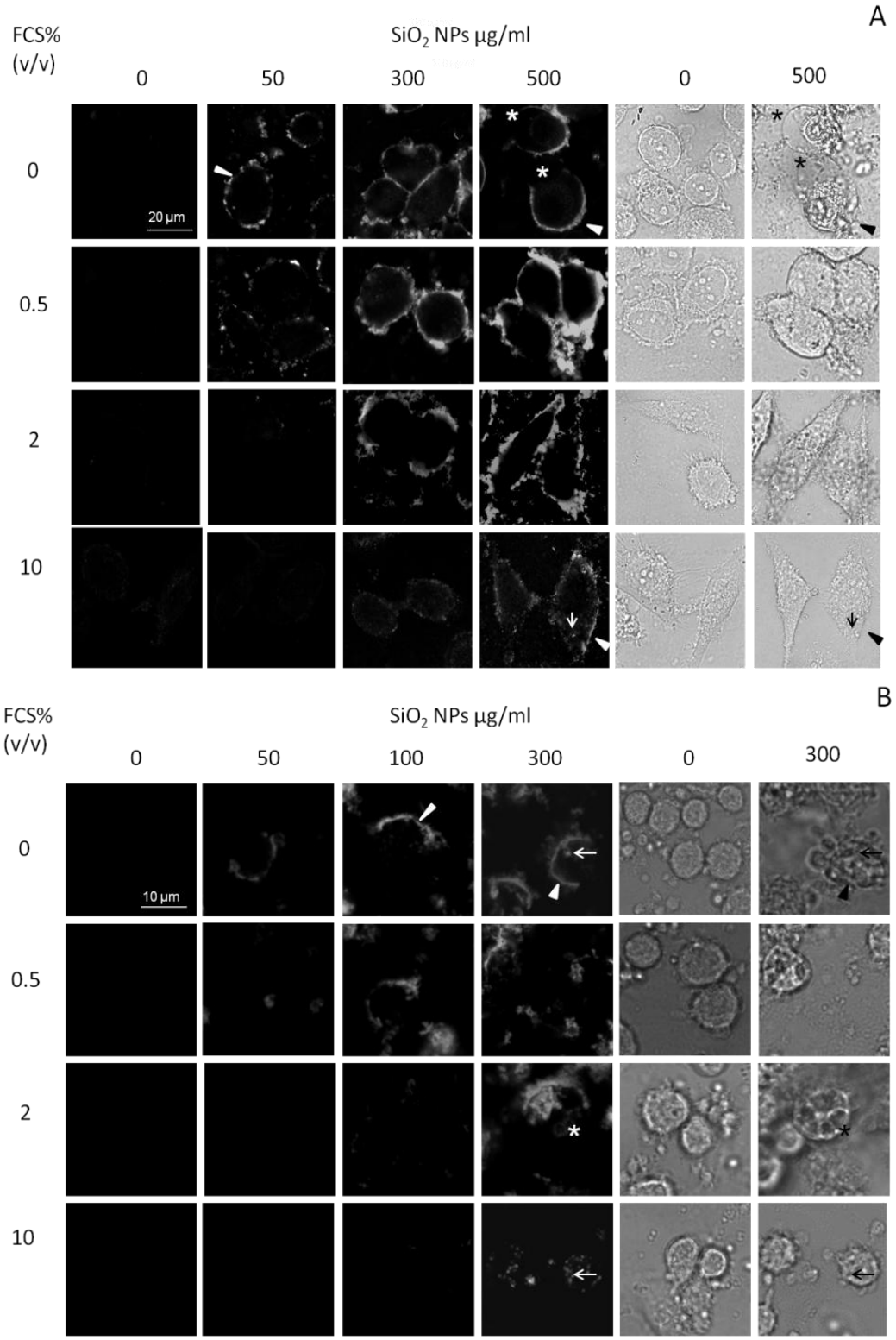
A
FCS%
(v/v)
SiO2 NPs µg/ml
0
50
300
500
0
500
0
0.5
2
10
20 µm
B
FCS%
(v/v)
SiO2 NPs µg/ml
0
50
100
300
0
300
0
0.5
2
10
10 µm

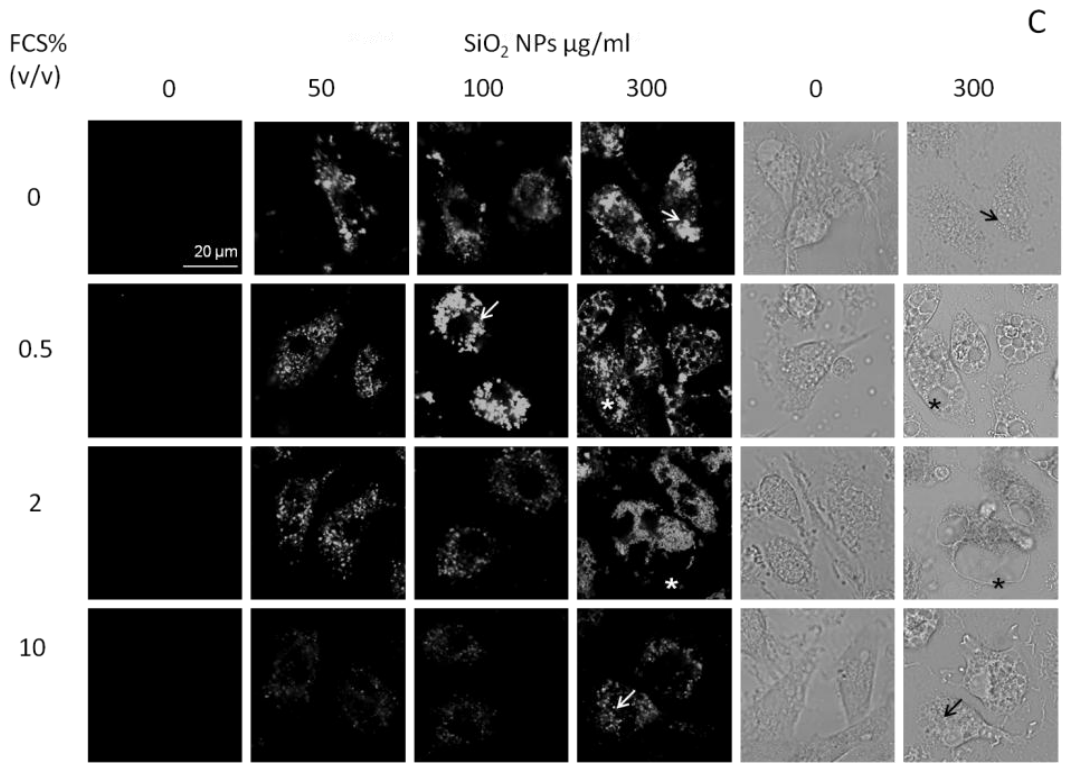

Figure 41: Effect of fetal calf serum on SiO_2-NPs cellular localization in HeLa cells (a), monocytes (b) and macrophages (c). Fluorescence and corresponding phase-contrast fields of one representative experiment from five are shown. Arrowheads indicate plasma membrane, arrows point to intracellular vesicles and asterisks show membrane swelling in HeLa cells and large cytoplasmic vacuoles in monocytes and macrophages.

Quantitative information on the actual efficacy of different cell types to internalize bound SiO_2-NPs as a function of serum were obtained by exploiting the ability of the membrane impermeant bio-compatible dye Trypan Blue (TB) to quench the fluorescence of the FITC-labeled Stöber SiO_2-NPs in flow cytofluorimetric assays. Trypan blue adsorbs light in the range from 475-675 nm [153] which covers the wavelength of fluorescein fluorescence emission (519 nm), so that FITC fluorescence is efficiently quenched by the dye. In preliminary experiments, we estimated the quenching efficacy of 3 mg/ml TB of fully membrane bound or fully internalized Stöber SiO_2-NPs, respectively incubating monocytes with SiO_2-NPs at 4°C and binding SiO_2-NPs to monocytes membrane as before, extensively washing and performing a chase for 24 h at 37°C. Extracellular signal quenching resulted to be ~ 60% , probably because the dye was not able to reach all fluorophore molecules within NPs matrix, whereas intracellular signal was quenched of ~ 16%, due to a filtering effect of TB solution layer around the cell. Similar observations on TB fluorescence quenching potential have been obtained by Nuutila *et* al. [154].

Considering such parameters, the relative amount of internalized SiO_2-NPs as % of total cell associated was estimated, as described in paragraph 2.5.

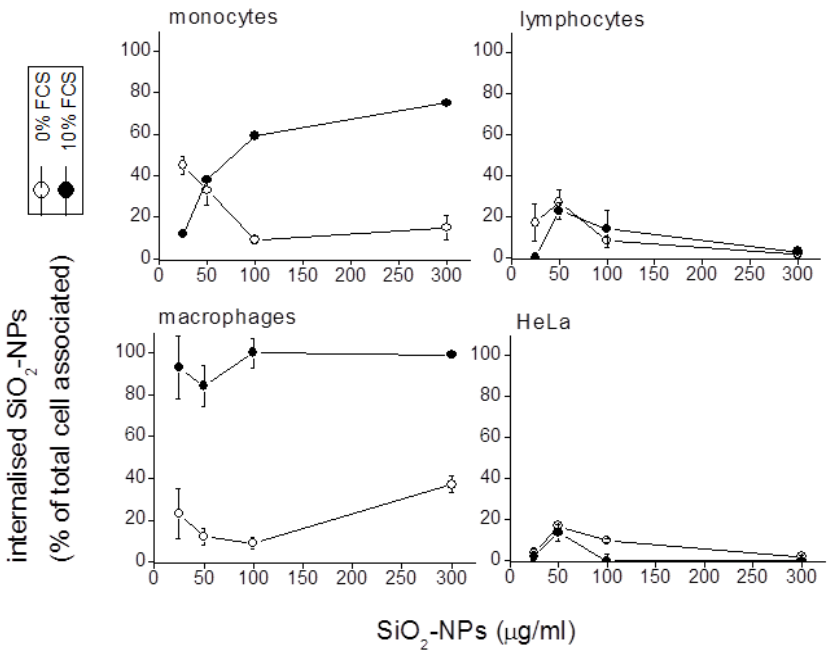

Figure 42: Extimation of cellular distribution of SiO_2-NPs in monocytes, macrophages, lymphocytes and HeLa cells. Indicated cells were incubated for 1.5 h with increasing doses of Stöber SiO_2-NPs, in the presence of 0-10% FCS. Then, samples were analyzed at flow cytometer with or without Trypan Blue 3 mg/ml to estimate the amount of internalized NPs.

In the absence of serum, ~ 20-30% of SiO_2-NPs associated to cells were internalized at relative low doses (25-50 µg/ml); at higher doses (100-300 µg/ml) signal associated to intracellular NPs decreased in monocytes, lymphocytes and HeLa (respectively, to 20, 0 and 0%) while it remained almost unchanged in macrophages (Figure 42). In the presence of 10% FCS, the percentage of SiO_2-NPs internalized by cells did not change compared to 0% FCS in the two non-phagocytic models (lymphocytes and HeLa), while it was significantly enhanced in phagocytes. Indeed, in monocytes intracellular signal increased at higher SiO_2-NPs doses reaching 80% of total cell load at 300 µg/ml, whereas in macrophages it was maximal already at 25 µg/ml (~ 100% endocytosis). Summarizing, TB experiments confirmed and provided a more quantitative view of confocal microscopy analysis, underlining the relevance of serum for SiO_2-NPs uptake by phagocytic cells and, in opposition, the poor phagocytic ability of lymphocytes and HeLa in the absence either in the presence of FCS.

3.4.6 Hemolytic activity

To get more information on SiO_2-NPs cytotoxicity mechanism and the possible influence of FCS and pH, we checked NPs ability to induce red blood cells lysis (hemolysis) in the absence or in the presence of FCS 10% and at acidic (5) and neutral (7.2) pH (Figure 43). Hemolysis was time dependent at both 0% and 10% FCS and, as for cytotoxicity, was reduced by the presence of serum (Figure 43). Interestingly, at 0% FCS acidic pH strongly increased hemolytic activity of NPs at both times, in fact after 1h treatment EC50 (NPs dose producing 50% of the hemolytic effect) was 32.9 µg/ml at pH 5 and 65.7 µg/ml at pH 7.2, and after 4h it was 26.9 µg/ml at pH 5 and 55.8 µg/ml at pH 7.2. This result is in accord with the reduction of hemolysis at alkaline pH documented by Shi *et al*. [155], and can be explained by the increased ionization (negative charge) of silanol groups at basic pH and the consequent stronger repulsion between net negatively charged red blood cells and SiO_2-NPs. On the contrary, in the presence of 10% FCS the effect of pH was significantly lower and, at the times tested, pH 5 and pH 7.2 curves showed minimal differences (only after 4h treatment EC50 at pH 5 (347 µg/ml) was slightly lower than at pH 7.2 (357 µg/ml)).

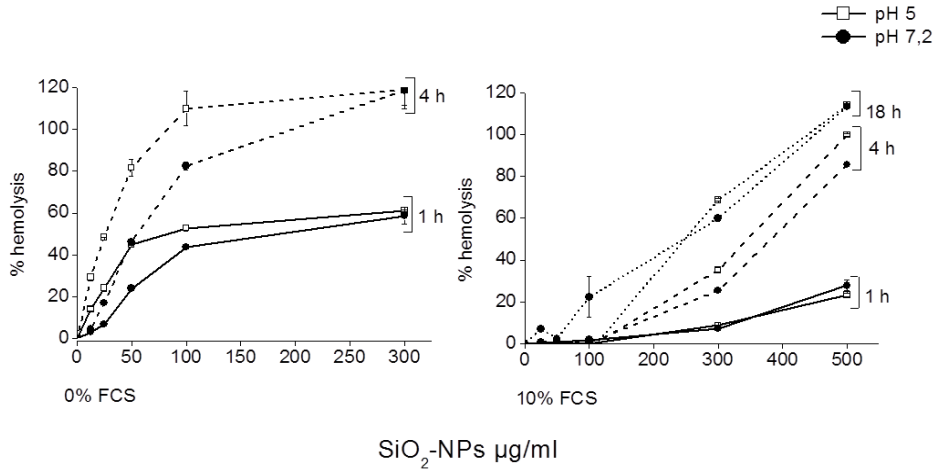

Figure 43: Dose-time dependent hemolytic activity of SiO_2-NPs, in different serum (0% and 10%) and pH (5, 7.2) conditions. PBS-washed red blood cells were incubated for indicated times with increasing doses of Ludox TM40 NPs, in 0 or 10% FCS and at pH 5 or 7.2. After brief centrifugation, the release of hemoglobin in the supernatant was evaluated spectrophotometrically at 450 nm. Data are the means of three experiments.

3.4.7 The effect of caspase 1 inhibition and acidic compartments neutralization in no serum media

To investigate if SiO_2-NPs induced cellular toxicity and inflammatory response in the absence of serum were influenced by caspase-1 inhibition and lysosomes neutralization similarly to standard conditions (10% FCS), I have performed experiments stimulating monocytes and macrophages for 4 and 18 h in serum free medium supplemented with Nutridoma (Figure 44).

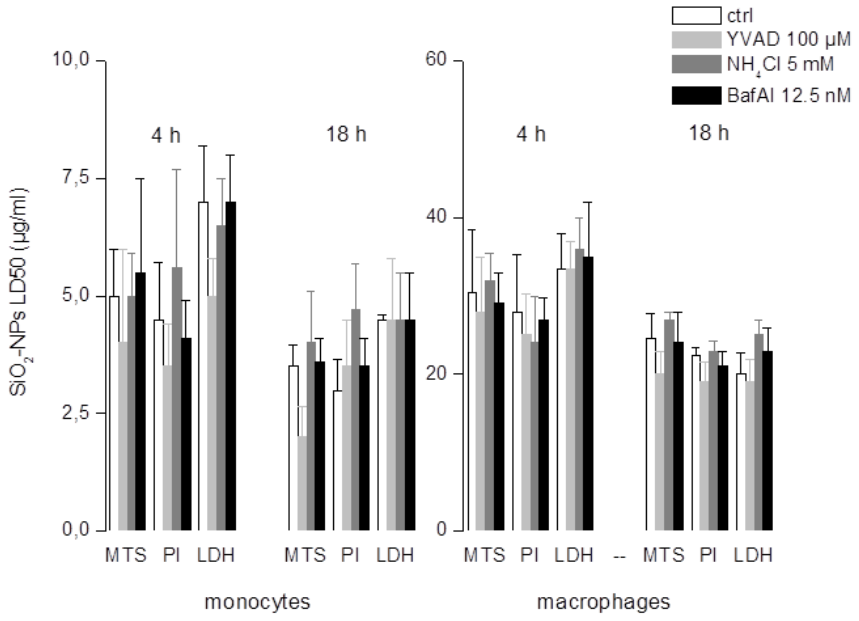

Figure 44: Effect of acidic compartments neutralization and caspase 1 inhibition on SiO_2-NPs induced cellular death in monocytes and macrophages in serum free condition. After pre-incubation for 1h with medium (ctrl), YVAD 100 µM, NH_4Cl 10 mM or BafAI 12.5 nM, indicated cells were treated for 4h or 18h with increasing doses of Ludox TM40 NPs. Cellular mortality was evaluated as mitochondrial damage (MTS), membrane permeabilization (PI) and cellular lysis (LDH). Data are the means of three experiments.

In monocytes, SiO_2-NPs LD50 (measured by MTS, PI and LDH assays) was ~ 10 times lower than in the presence of 10% FCS (5-7.5 µg/ml versus 50-100 µg/ml at 4 h; 3-4 µg/ml versus 25 µg/ml at 20 h), while in macrophages the difference between the two serum conditions was less marked (at 4 h, LD50 was ~ 30 µg/ml (0% FCS) vs ~ 40 µg/ml (10% FCS); at 20 h, LD50 was ~ 20 µg/ml (0% FCS) vs 30 µg/ml (10% FCS)). This result confirmed our preliminary observation that SiO_2-NPs effects are less influenced by serum in macrophages compared to monocytes. In the presence of 10% FCS, we have found that SiO_2-NPs toxicity was significantly reduced after caspase 1 inhibition and

lysosomes neutralization in monocytes, while in macrophages it was poorly affected (see paragraphs 3.3.5 and 3.3.6). Surprising, in the absence of serum neither YVAD, NH_4Cl and BafAI were able to diminish SiO_2-NPs toxicity in both cellular types at 4 h and 20 h (as revealed by the three cytotoxicity assays performed). The loss of protective effect provided by caspase 1 inhibition and lysosomal neutralization in monocytes suggests that, in the absence of serum, SiO_2-NPs may kill cells by a mechanism different from the one observed at 10% FCS, more similar to macrophages (that even in 10% FCS were less dependent on caspase 1 activity and lysosomes acidic pH). Inflammatory cytokines measured in parallel (IL-1β and TNF-α) resulted inhibited in the presence of YVAD, NH_4Cl and BafAI (Figure 45), although cellular death was not affected by these agonists.

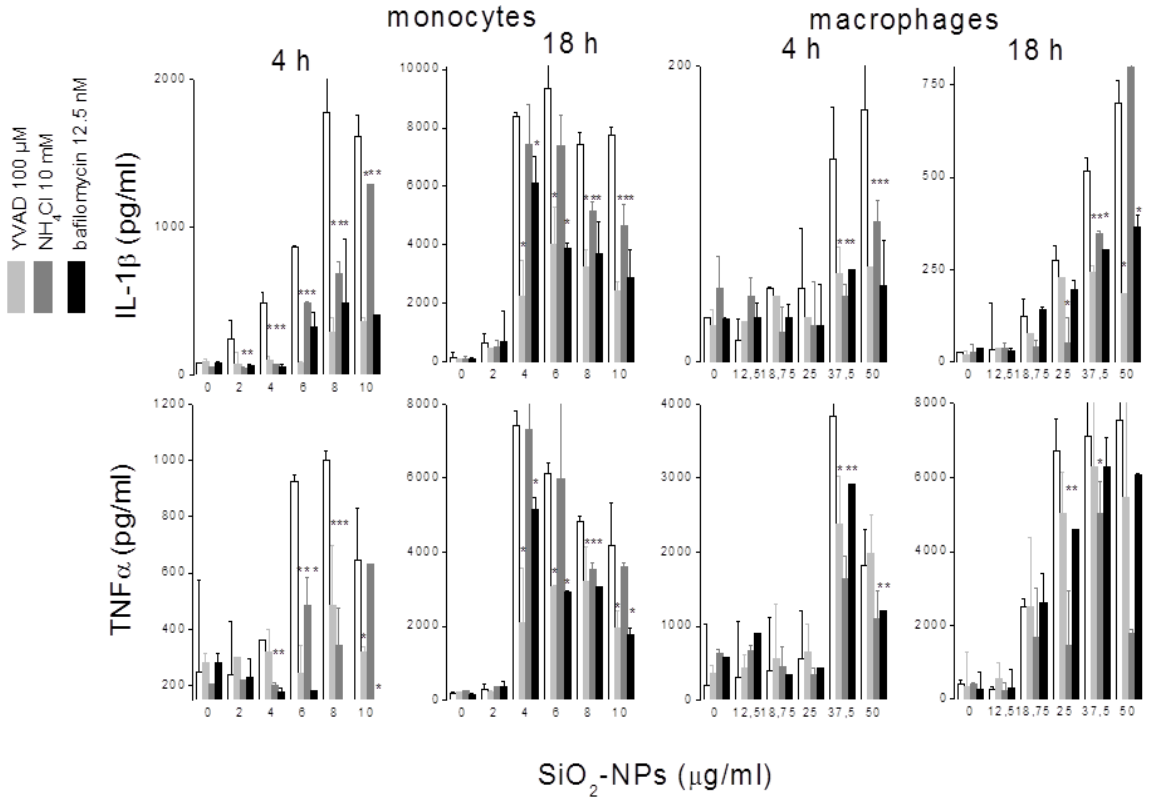

Figure 45: Effect of acidic compartments neutralization and caspase 1 inhibition on SiO_2-NPs induced inflammatory response in monocytes and macrophages, in serum free conditions. After pre-incubation for 1h with medium (ctrl), YVAD 100 µM, NH_4Cl 10 mM or BafAI 12.5 nM, indicated cells were treated for 4h or 18h with increasing doses of Ludox TM40 NPs. IL-1β, TNF-α and IL-6 levels were measured in cellular medium by ELISA assay. Data are from one representative experiment out of two. Significance of differences with respect to ctrl (no YVAD, NH_4Cl and BafAI) are indicated by * ($p<0.05$).

3.5 SiO_2-NPs protein corona

Once demonstrated that serum (an ubiquitous component of cellular media for the maintenance/stimulation of most cellular models for *in vitro* assays) largely influences several aspects of cellular response to NPs, I have concentrated on the characterization of serum proteins binding to SiO_2-NPs surface (the so called "NPs corona"). First, I have determined the protein pattern bound to Ludox TM40 NPs in the standard conditions of biological assays (in the presence of 10% FCS at 37°C), using SiO_2-NPs at 300 µg/ml as representative dose. NPs adsorbed proteins were visualized by Coomassie or silver staining and identified by mass spectrometry analysis. As represented in Figure 46, the two coloration methods revealed a very similar protein pattern. We found that the main FCS proteins adsorbed to NPs surface were plasminogen, albumin, apolipoprotein AI (ApoAI), hemoglobin and apolipoprotein AII (ApoAII). Plasminogen is the inactive precursor of plasmin, a serine protease responsible of fibrinolysis process through the regulated cleavage of fibrin (the protein forming blood clots) [156,157]. Albumin (the most abundant serum protein), presents several functions, such as maintaining the colloid osmotic pressure, transporting low water-soluble substances to site of action, metabolism or excretion, and providing a pool of amino acids for protein synthesis [158]. Hemoglobin, responsible of oxygen transport, is not a circulating protein because it's normally present inside red blood cells. Since FCS is obtained after blood coagulation, we think that this process may have induced hemolysis, releasing hemoglobin in serum and so allowing the binding to NPs (in fact, this protein is not present in the pattern obtained after incubation of NPs with human plasma, directly taken from a volunteer (see paragraph 3.5.3). Apolipoproteins AI and AII constitute respectively 70% and 20% of high density lipoproteins (HDL) protein mass [159,160]. HDL are small lipoproteins responsible of cholesterol transport from peripheral cells to the liver (where it will be catabolized), preventing its deposition within arteries and lowering the risk of cardiovascular diseases [161]. Briefly, after HDL secretion from the liver and intestine in a "lipid-free" form, they acquire phospholipids and free cholesterol from peripheral cells through ABCA1 transporter (ATP-binding cassette transporter AI). Subsequently, free cholesterol is esterified by LCAT (lecithin: cholesterol acyltransferase), through the transfer of a fatty acid from lecithin to the free hydroxyl residue of cholesterol. Finally, SR-BI (scavenger receptor BI) mediates HDL-CE (HDL-cholesteryl ester) accumulation in the liver, where they undergo to catabolism [160,162-165]. In this context, ApoAI and

ApoAII are HDL-associated proteins enriched in amphipathic helices (that probably mediate the interaction with the lipid component) [159,166], and their principal functions are LCAT activator (ApoAI) and HDL structural component (ApoAII) [164,166].

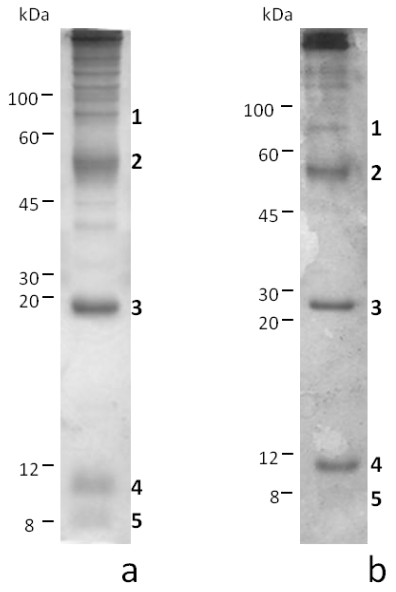

Protein	MW (kDa)	pI
1- plasminogen	88.4	7.39
2- albumin	66.4	5.71
3- apolipoprotein AI	27.5	5.36
4- hemoglobin fetal subunit β	15.8	6.51
5- apolipoprotein AII	8.7	5.34

c

Figure 46: Fetal calf serum proteins pattern bound to SiO_2-NPs. 300 μg of Ludox TM40 NPs were incubated at 37°C for 15' with 10% FCS and, after NPs recovery by ultracentrifugation, washing and solubilization in sample buffer, samples were loaded onto a 12% non reducing polyacrilamide gel and stained by Colloidal Coomassie G250 (a) or silver nitrate (b). Indicated bands from gel (a) were excised and identified by mass spectrometry. (c) Table summarizing molecular weight (MW) and isoelectric point (pI) of identified proteins. Values refer to the mature (secreted) proteins and were determined using ProtParam program.

After this preliminary identification of the components of NPs corona, we investigated proteins distribution on increasing amounts of NPs, incubating Ludox TM40 at different doses (0-1000 μg/ml) with 10% FCS at 37°C (miming the conditions of biological assays). For a better comprehension of the result, SDS-PAGE were performed by loading equal volumes of resuspended NPs (different quantities) (Figure 47a) and equal quantities of resuspended NPs (different volumes, Figure 47b).

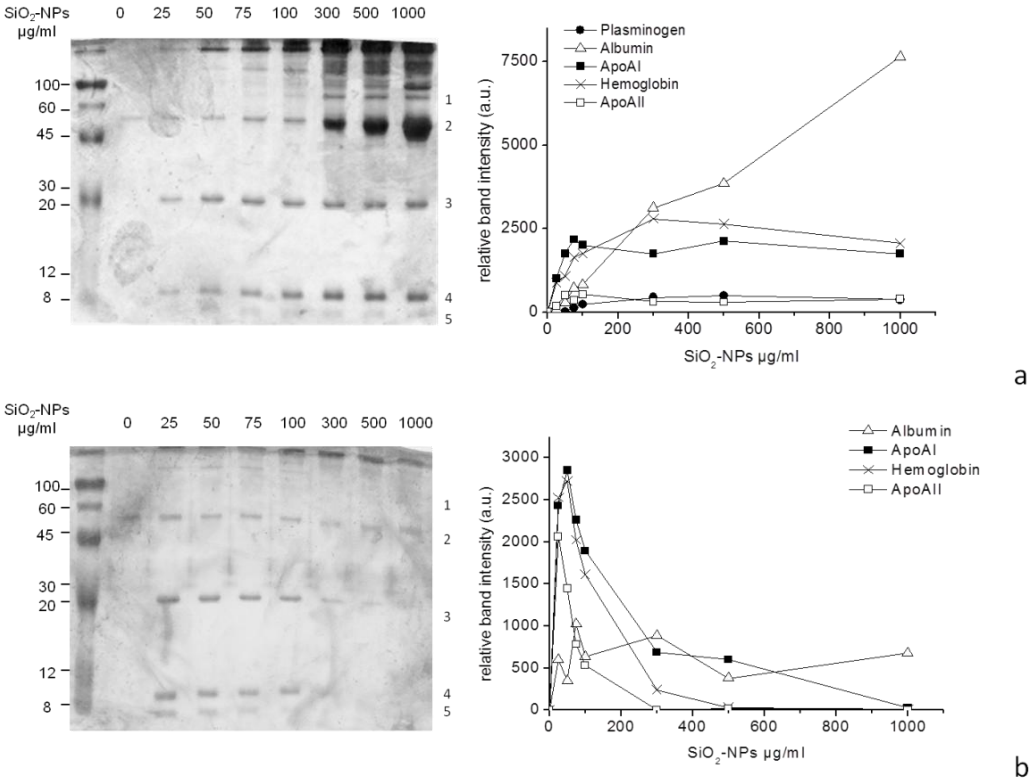

Figure 47: Influence of SiO_2-NPs dose on fetal calf serum proteins pattern bound to NPs surface. Increasing concentrations of Ludox TM40 SiO_2-NPs were incubated for 15' at 37°C with 10% FCS. After NPs recovery by ultracentrifugation, washing and solubilization in sample buffer, equal volumes (20 µl) (a) or equal amounts (3.3 µg) (b) of solubilized NPs were loaded onto a non reducing 12% polyacrylamide gel and stained with silver nitrate. Graphs on the right represent signal quantification of bands. 1: plasminogen, 2: albumin, 3: ApoAI, 4: hemoglobin, 5: ApoAII. Data are from one representative experiment out of three.

Figure 47a shows that SiO_2-NPs-attached plasminogen, apolipoproteins (AI and AII) and hemoglobin amount increased with the increment of NPs doses until ~ 100 µg/ml (plasminogen, apolipoproteins) or ~ 300 µg/ml (hemoglobin), while at higher concentrations their level remained constant, indicating that no more proteins were available for the binding to NPs because they have been completely exhausted from serum. On the contrary, albumin (the most abundant serum protein) poorly binds to SiO_2-NPs at concentrations < 100 µg/ml (suggesting a possible lower affinity for the surface then other proteins). However, in the correspondence of plasminogen, apolipoproteins and hemoglobin depletion, albumin started to adsorb in good amounts, proportionally to NPs dose. By loading an equal quantity of NPs (3.3 µg) in the gel it is possible to better appreciate the visible reduction of apolipoproteins and hemoglobin per SiO_2-NPs mass

unit at concentrations > 100 µg/ml, whereas albumin (as present in excess) remains constant at all NPs doses (Figure 47b).

3.5.1 The influence of FCS concentration

Serum proteins adsorption on NPs surface depends not only on their abundance but also on their affinity for a particular nanostructure (determined by factors as charge, hydrophobicity, dimensions and shape). Recently, the terms "soft corona" and "hard corona" have been introduced to distinguish respectively low affinity proteins that loosely bind to NPs and high affinity proteins that tightly bind to NPs. To investigate which proteins have the highest affinity for SiO_2-NPs surface, 0 (as control) or 300 µg/ml Ludox TM40 were incubated at 37°C with increasing serum concentrations (2-10-40%) (Figure 48). In the absence of NPs, a trace of albumin was found to precipitate into the tube after ultracentrifugation (probably because of its huge amount), but it didn't compromise our result because it was considered as "blank" and subtracted to other samples. Interestingly, we found a different pattern of proteins bound to NPs in diverse serum conditions. At 2% FCS, albumin was the main polypeptide associated, and it was also present as dimer (band correspondent to 100 kDa). At upper FCS concentrations, albumin amount clearly decreased (visible from either the monomeric and dimeric form), while plasminogen, apolipoproteins and hemoglobin (undetectable at 2% FCS) appeared in the pattern, proportionally to serum concentration. This serum dependent trend suggested us a possible explanation of what occurred at NPs / serum interface. In the presence of few FCS (2%) albumin, as the most abundant serum protein, reaches still relevant concentration values (0.5-1 mg/ml) and is favored in SiO_2-NPs binding over other proteins (that, as less abundant, at 2% FCS are almost negligible). The fact that increasing serum results in albumin displacement to the detriment of other proteins suggests that the latter (e.g. at 10-40% FCS) reach a concentration sufficient to compete with albumin for NPs binding and, thanks to their probable higher affinity, they occupy the majority of places on NPs surface (increment) leaving to albumin few or no places (decrease).

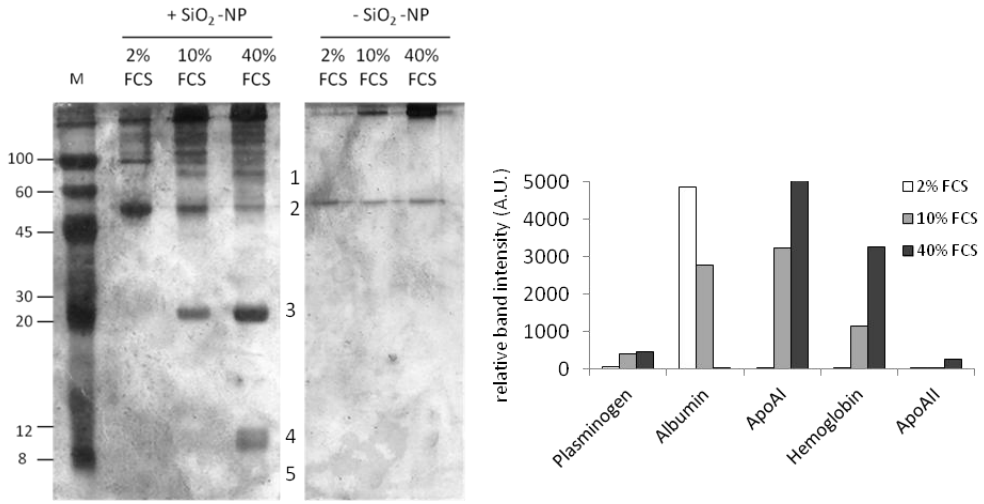

Figure 48: Influence FCS concentration on proteins pattern bound to SiO_2-NPs surface. 0 µg (- SiO_2 NPs) or 300 µg (+ SiO_2 NPs) of SiO_2 NPs were incubated for 15' at 37°C with 2-10-40 % FCS and, after NPs recovery by ultracentrifugation, washing and solubilization in sample buffer, samples were loaded onto a 12% non reducing polyacrilamide gel and stained with silver nitrate. Histograms on the right represent signal quantification of bands. 1: plasminogen, 2: albumin, 3: ApoAI, 4: hemoglobin, 5: ApoAII. Data are from one representative experiment out of three.

3.5.2 The influence of pH

In paragraph 3.3.6 we have demonstrated that lysosomal pH is important in determining SiO_2-NPs cellular toxicity and inflammatory response. Since NPs coated of serum proteins are internalized in phagolysosomes in monocytes and macrophages (see paragraph 3.3.2), we investigated if NPs "corona" might change from extracellular medium/cytosolic environment (pH 7.2-7.4) to cellular acidic compartments (pH 5). To this, Ludox TM40 NPs (0-50-100-300 µg) were incubated at 37°C with 10% FCS pH 5 or pH 7.2, and then standard experimental procedure was followed. In the absence of NPs, a non-specific protein signal was visible with 10% FCS pH 5, probably because at low pH (non physiological condition) serum proteins are more prone to precipitate. However, samples without NPs were considered as blank and subtracted to the others for band quantification. According to previous paragraph, at both pH NPs-bound plasminogen and albumin amount increased at higher SiO_2-NPs doses while apolipoproteins and hemoglobin levels remained almost constant (in particular between 100 and 300 µg/ml NPs). Furthermore, we found that plasminogen and albumin significantly decreased at pH 7.2 compared to pH 5 (respectively of 85% at the three NPs doses and of 66% at 300 µg/ml NPs), whereas hemoglobin and apolipoproteins were not subjected to relevant

changes (Figure 49). This result shows that SiO_2-NPs bound proteins do not undergo substantial modifications upon NPs uptake in lysosomes (only albumin and plasminogen present in the NPs bio-interface but not yet bound to the surface tend to absorb more), suggesting that toxicity mechanisms occurring in these compartments are not related to a simple pH-dependent rearrangement of the corona. This result is in accord also with the almost unchanged hemolytic activity of SiO_2-NPs in the presence of serum at acidic (pH 5) or neutral pH (pH 7.2) (paragraph 3.4.6).

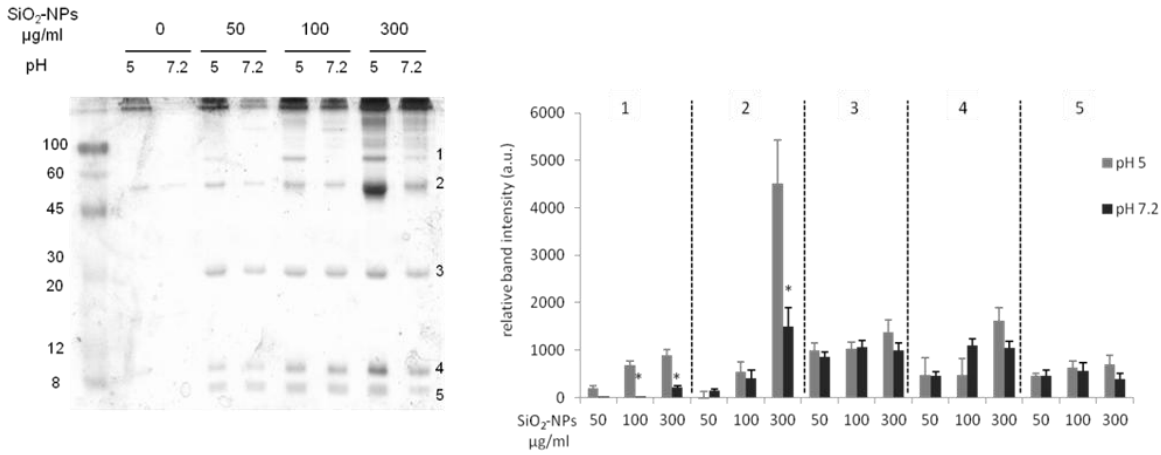

Figure 49: Influence of pH on proteins pattern bound to SiO_2-NPs surface. 0, 50, 100 and 300 µg/ml of Ludox TM40 NPs were incubated for 15' at 37°C with 10% FCS at two different pH (5 and 7.2). After NPs recovery by ultracentrifugation, washing and solubilization in sample buffer, samples were loaded onto a 12% non reducing polyacrilamide gel and stained with silver nitrate. Histograms on the right represent signal quantification of bands and are the means of three experiments. 1: plasminogen, 2: albumin, 3: ApoAI, 4: hemoglobin, 5: ApoAII. Significance of differences with respect to samples at pH 5 are indicated by * ($p<0.05$).

3.5.3 Fetal calf serum *vs* human plasma

Once characterized at different levels the interaction of fetal calf serum proteins with SiO_2-NPs (FCS was used as model system of *in vitro* condition), we wanted to identify the principal proteins of human plasma (HP) binding SiO_2-NPs surface, simulating a possible *in vivo* condition. Indeed, NPs used as drug carriers/imaging agents are mostly injected into the bloodstream, where they are coated by a series of plasma proteins that mediate cellular response to the foreign material. The experiment (performed with 2 mg SiO_2-NPs incubated with 10% HP at 37°C) was carried out in parallel with 10% FCS incubation, to compare proteins adsorbed to NPs in the two situations.

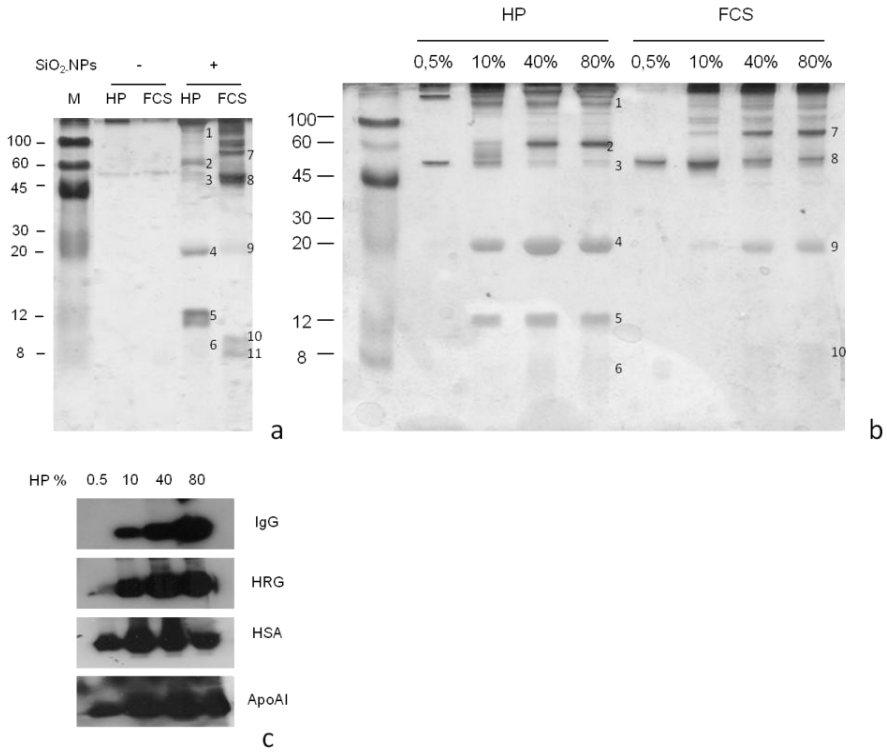

Protein	MW (kDa)	pI	Plasma concentration (mg/ml)
1- Immunoglobulin G	150	-	5-10
2- Histidine rich glycoprotein	57,6	7	0.15
3- Albumin	66,4	5,67	50-60
4- Apolipoprotein AI	28,0	5,27	1-1.5
5- Apolipoprotein AII	8,7	5,05	0.3-0.5
6- Apolipoprotein CIII	8,8	4,72	0.12-0.14

d

Figure 50: Comparison between SiO_2-NPs bound proteins derived from human plasma (HP) or fetal calf serum (FCS). 0 (-) or 2 mg (+) of Ludox TM40 NPs were incubated for 15' at 37°C with 10% HP or FCS (a), or with increasing HP or FCS percentages (0, 10, 40, 80) (b). After NPs recovery by ultracentrifugation, washing and solubilization in sample buffer, samples were loaded onto a 12% non reducing polyacrilamide gel and stained with silver nitrate. (c) Detection of IgG, HRG, HSA and ApoAI by Western Blot on HP samples of (b). Data are from one representative experiment out of four. (d) Table summarizing molecular weight (MW), isoelectric point (pI) and plasma concentration of identified proteins. Values refer to the mature (secreted) proteins and were determined using ProtParam program.

Interestingly, we found a different protein pattern in the presence of human plasma or bovine serum (Figure 50a). In fact, at 10% FCS the main proteins adsorbed were

plasminogen (7), albumin (8), ApoAI (9), hemoglobin (10) and ApoAII (11), confirming our previous data. In 10% HP, we identified by mass spectrometry Immunoglobulin G (IgG), Histidine rich glycoprotein (HRG), albumin (HSA), Apolipoprotein AI (ApoAI), Apolipoprotein AII (ApoAII) and Apolipoprotein CIII (ApoCIII). Further, some of them were recognized by specific antibodies in Western Blot analysis (Figure 50c). Histidine rich glycoprotein is a multidomain protein able to interact with several ligands and involved in the regulation of numerous biologic processes. In particular, Poon *et al*. found that HRG copurifies with immunoglobulins, which are necessary for HRG-mediated clearance of necrotic cells by phagocytes [167]. Consistently, Gorgani *et al*. demonstrated than HRG promotes macrophages FcγRI-dependent ingestion of apoptotic cells by binding naked DNA exposed on membrane bleps [168]. In addition, HRG is also a regulator of angiogenesis, coagulation, cellular adhesion and proliferation [169-171]. ApoCIII belongs to VLDL (very low density lipoprotein) complexes (~ 50% of the protein fraction) and, contrary to ApoAI and ApoAII, is poorly present in HDL (~ 2% of the protein fraction). ApoCIII has inhibitory functions in the catabolism of triglyceride rich lipoproteins (VLDL), indeed it inhibits lipoprotein lipase and hepatic lipase (responsible of the hydrolysis of triglycerides into free fatty acids) and blocks also the clearance of lipoproteins by hepatic receptors [166]. For this reasons, ApoCIII overproduction is often associated to hypertrigliceridemia.

Curiously, in the same conditions (e.g. 10% FCS) albumin and apolipoproteins were present in both patterns but in different quantities (HSA predominated in bovine serum while ApoAI, ApoAII and ApoCIII were more abundant in plasma), consistent with the fact that lipoproteins concentration is higher in plasma than in FCS [172]. Similarly to bovine serum, also HP protein pattern was modified at increasing plasma concentrations (Figure 50b), with a loss of NPs bound albumin and the concomitant increase of IgG, HRG, ApoAI, ApoAII and ApoCIII, suggesting that also human albumin, although it is the most abundant plasma protein, at high plasma concentrations is displaced by polypeptides less represented but with an higher affinity for SiO_2-NPs.

We subsequently performed functional assays to evaluate if SiO_2-NPs may induce different cytotoxic/inflammatory effects in the presence of bovine serum either human plasma (as they bind different proteins). After 20 h macrophages incubation with SiO_2-NPs, we found that cytotoxicity and induction of inflammatory cytokines (IL-1β and

TNF-α) occurring in the presence of FCS were significantly inhibited/abolished in the presence of HP (Figure 51), indicating that, in such way, plasma is a more protective environment against SiO_2-NPs cytotoxicity. Since the one of the main differences between proteins adsorbed on SiO_2-NPs surface after incubation with HP or FCS was the much higher amount of apolipoproteins present in the first case, we investigated if they could play a role in protecting cells against SiO_2-NPs adverse effects by treating macrophages with SiO_2-NPs in the presence of normal FCS or "lipoproteins-depleted" FCS. Serum delipidation was obtained incubating FCS with increasing concentrations of SiO_2-NPs that, as represented in Figure 47, at doses > 300 μg/ml exhaust almost all the lipoproteins (while more abundant proteins, such as albumin, still remain in the system).

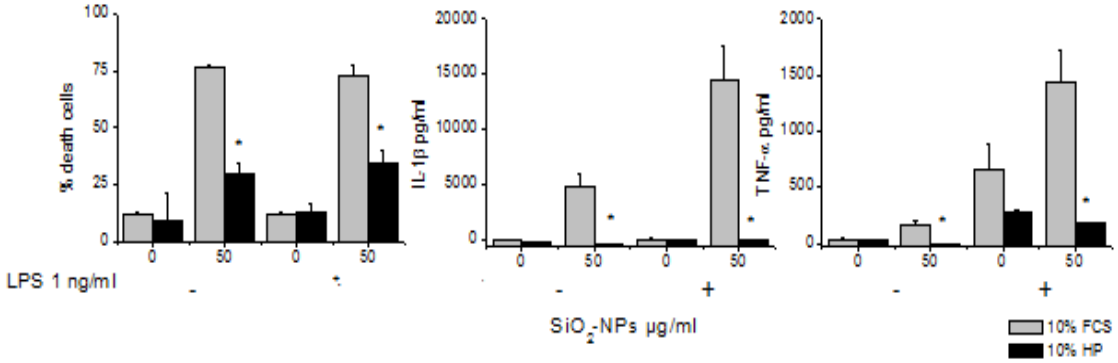

Figure 51: Comparison between SiO_2-NPs cytotoxicity/inflammatory response in the presence of FCS or HP in macrophages. Cells were incubated for 18 h with Ludox TM40 SiO_2-NPs (with or without LPS), in the presence of FCS or HP. Cellular mortality was evaluated by cytofluorimetric analysis (PI), while IL-1β and TNF-α levels released in extracellular medium were quantified by ELISA assay. Significance of differences with respect to FCS is indicated by * ($p<0.05$). Data are from one representative experiment out of three.

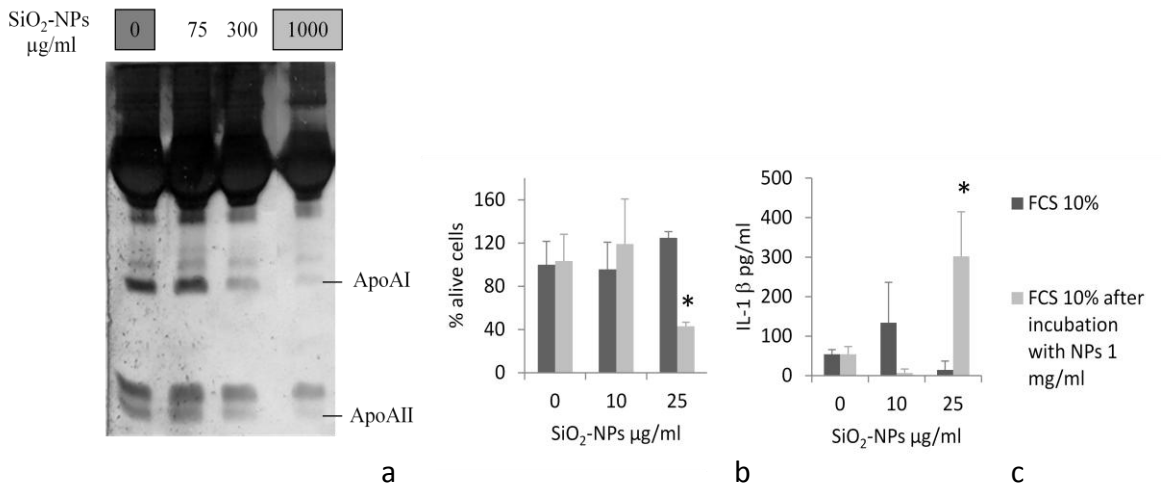

Figure 52: Comparison between SiO_2-NPs cytotoxicity/inflammatory response in the presence of normal or delipidated FCS. (a) Medium + 10% FCS was incubated at 37°C for 20' with increasing doses of Ludox TM40 NPs (0-75-300-1000 µg/ml). After ultracentrifugation to precipitate NPs, supernatant was collected, loaded onto a 12% non reducing polyacrilamide gel and stained by silver nitrate. (b, c): Macrophages were incubated for 18 h with Ludox TM40 NPs, in the presence of normal or delipidated 10% FCS obtained as described in (a). Cellular mortality was evaluated by cytofluorimetric analysis (PI), while IL-1β levels released in extracellular medium were quantified by ELISA assay. Significance of differences with respect to normal 10% FCS is indicated by * ($p<0.05$).

Figure 52a shows that SiO_2-NPs at a concentration of 1 mg/ml deplete serum from the majority of ApoAI and ApoAII, without exhausting plasminogen, albumin and hemoglobin. Macrophages incubated with apolipoproteins-deficient serum clearly resulted more sensitive to SiO_2-NPs treatment than in the presence of normal FCS (Figure 52b). Indeed, at 25 µg/ml NPs cellular viability was decreased from 100% (normal FCS) to 45% (depleted FCS) and, in the latter condition, a significant production of IL-1β was observed (Figure 52c). Our result might support the hypothesis of a possible protective effect of apolipoproteins, documented also by Barrett *et al*. [173].

3.5.4 Functional assays with isolated plasma proteins

In the last part of my thesis, I will present preliminary data concerning the influence of isolated plasma proteins on cellular response to SiO_2-NPs. This is an important point because the knowledge of the role of single proteins adsorbed to NPs would allow the design of nanoconstructs that, for example, bind to proteins protective against cellular toxicity.

First, histidine rich glycoprotein was successfully purified from human plasma by the cation exchange resin phosphocellulose (Figure 53a, b). As reported in literature, immunoglobulins (IgG2) co-purified with HRG, as they participate to HRG-dependent clearance of necrotic cells by phagocytes [167]. Incubation with *Staphylococcus Aureus* Protein A allowed the removal of IgG from HRG preparation (Figure 53c); however, both protein purification from plasma and IgG precipitation need to be improved for future work.

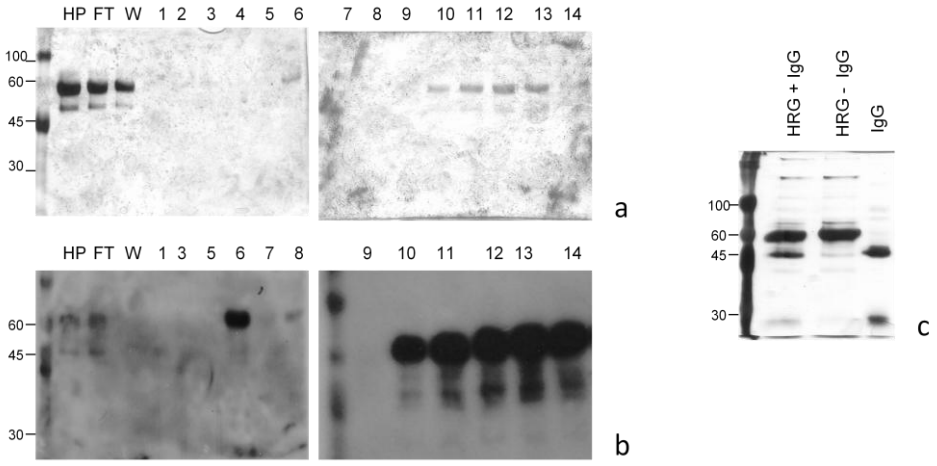

Figure 53: Histidine rich glycoprotein purification from human plasma. After purification procedure of HRG by the cation exchange phosphocellulose resin P11, 20 µl of human plasma 1:100 (HP), 20 µl of flow through 1:100 (FT), 20 µl of wash 1:2 (W) and 20 µl elution fractions were loaded onto a reducing 12% polyacrilamyde gel and stained with silver nitrate (a) or with anti-HRG antibody by Western Blot (b). (c) IgG were removed from HRG positive fractions by incubation with sepharose beads conjugated to *Staphylococcus Aureus* Protein A. Whole fraction (HRG + IgG), IgG depleted fraction (HRG – IgG) and detached IgG (IgG) were loaded onto a 12% reducing polyacrylamide gel and stained by silver nitrate.

Then, monocytes were incubated with Stöber NPs for 18 h in serum free medium, in the presence of some single proteins added at a concentration corresponding to 2% HP (IgG: 140 µg/ml, ApoAI: 24 µg/ml, HSA: 1.2 mg/ml, HDL: 50 µg/ml, HRG: 3 µg/ml), and cellular viability/alive cells fluorescence were evaluated at flow cytometer (Figure 54). IgG and HRG (co-purified with immunoglobulins) did not protect significantly cells from SiO_2-NPs cytotoxicity (LD50 no proteins: 4.85 ± 0.2 µg/ml; LD50 IgG: 9.85 ± 4.3 µg/ml), while NPs cellular association was enhanced by IgG, consistently with the hypothesis that in phagocytic cells NPs uptake can be mediated by the binding of adsorbed immunoglobulins to Fc receptors [174]. ApoAI showed a little protective effect (LD50 ApoAI: 15.65 ± 4,3 µg/ml), and NPs cellular association didn't undergo

significant changes. Interestingly, both HSA and HDL clearly enhanced cellular viability in the presence of SiO_2-NPs, with a stronger effect of HDL (LD50 HSA: 44.2 μg/ml, LD50 HDL: > 80 μg/ml) and, in parallel, alive cells MFI values were similarly decreased in comparison to cells treated in the absence of proteins (Figure 54).

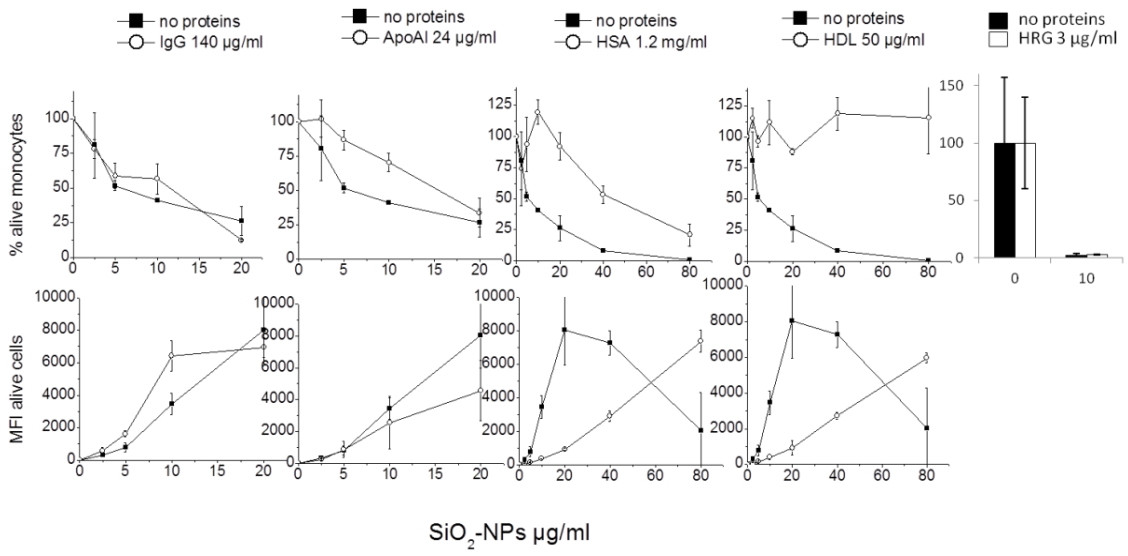

Figure 54: Effect of single plasma proteins on SiO_2-NPs cytotoxicity and cellular association in monocytes. Cells were incubated with Ludox TM40 NPs for 18h in serum free medium (no proteins) or medium supplemented with indicated proteins. Cellular viability and NPs cellular association were evaluated at flow cytometer. Data are the mean of two experiments.

Concentrating on the two protective proteins (HDL and HSA), we further investigated if they similarly influenced SiO_2-NPs membrane toxicity by hemolysis experiments performed in serum free medium or in the presence of HDL or HSA (Figure 55). After short time incubation (1h), NPs were strongly hemolytic at relatively low doses (< 50 μg/ml) in the absence of serum, no hemolytic in the presence of albumin and 50% hemolytic at 300 μg/ml in the presence of HDL. The lower protective activity of HDL at high NPs doses could be attributed to their unability to cover the entire NPs surface (as they have been completely depleted from serum as shown in figure 47), leaving part of NPs uncoated and highly interacting with membrane. On the contrary, the more plentiful protein albumin can saturate all the NPs superficies and apparently protect cells from lysis. Interestingly, at longer incubation times (4h and, more evidentely, at 18h), HDL were still protective against hemolysis until 100 μg/ml NPs, while in the presence of albumin NPs showed a hemolytic activity linearly dependent on NPs dose and incubation time, resulting, in some cases, more dangerous than in the presence of HDL. Such result

suggests a less efficiency of albumin in preventing membrane damage in comparison to HDL, and can partially justify the lower HSA protective effect reported in Figure 54.

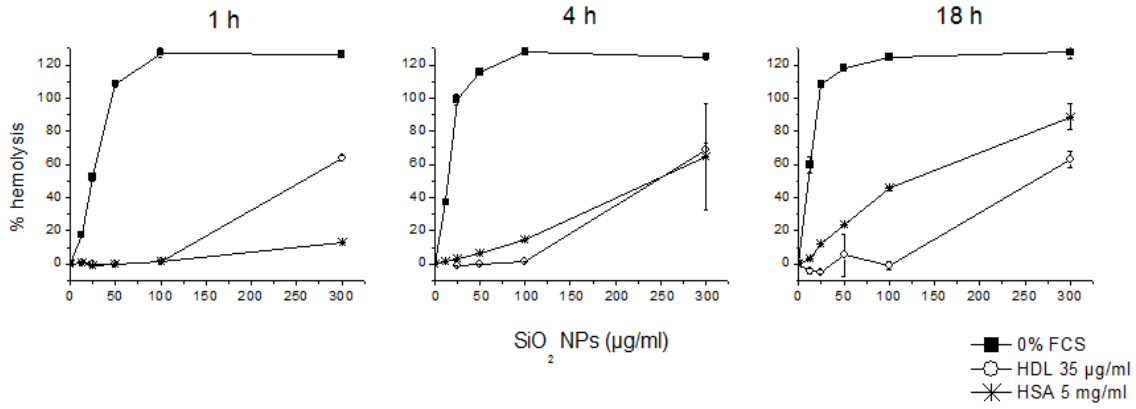

Figure 55: Effect of single plasma proteins on SiO_2-NPs hemolytic activity. PBS-washed red blood cells were incubated for indicated times with increasing doses of Ludox TM40 NPs, in the absence of serum (0% FCS) and in the presence of HDL 35 µg/ml or HSA 5 mg/ml. After brief centrifugation, the release of hemoglobin in the supernatant was evaluated spectrophotometrically at 450 nm. Data are from one representative experiment out of three.

4. Discussion and conclusions

In this PhD thesis several aspects concerning environmental or anthropogenic NPs interaction with human cells have been investigated, using as nanomaterial model synthetic amorphous silica nanoparticles and as cellular models two categories of populations (phagocytic and non phagocytic cells) exemplificative of the ones mostly interacting with nanoparticles. In particular, SiO_2-NPs cytotoxic and pro-inflammatory mechanisms have been largely characterized, focusing the attention on how they could be influenced by the presence of serum and, in a more detailed and functional analysis, by specific serum/plasma proteins. In this last section, a critical summary of the main results obtained and a possible integrated view of them will be presented and discussed. The first relevant finding is that in the presence of serum (a condition closer to the physiological context of NPs in contact with blood) phagocytic cells (monocytes and macrophages) are ~ 10 fold more sensitive to SiO_2-NPs than non phagocytic cells (lymphocytes and HeLa). In addition, in the correspondence of cytotoxicity they undergo a strong pro inflammatory cytokines secretion (TNF-α, IL-6 and, over all, IL-1β), in agreement with another our result indicating that SiO_2-NPs induce necrosis/oncosis (an inflammatory death) but not apoptosis in monocytes and macrophages. This points the attention on the fact that, upon NPs introduction into the organism, the most affected cellular populations may be the circulating (monocytes) or resident (macrophages) cells of RES/MPS system. These cells may be subjected to a catastrophic death with the activation of intracellular pathways like the NLRP3 inflammasome and the release of inflammatory mediators that may cause additional adverse effects in the surrounding environment. These already critical effects might be worsened if blood contains traces of endotoxin (~ 1 ng/ml), scarcely pro-inflammatory *per se* but able to synergize with SiO_2-NPs in the production of pro inflammatory mediators. We purpose, as a possible explanation of this higher sensitivity of phagocytes compared to non phagocytes, their better ability to internalize NPs-serum protein complexes, because of their peculiar endocytic mechanism (phagocytosis, mostly mediated by a plethora of receptors such as Fc receptors, Complement receptors and Scavenger receptors) [42] allowing a rapid and very efficient uptake of particles of large size (> 0.5 μM) (as can be viruses, bacteria and cellular debris). On the contrary, non phagocytic cells (in our case lymphocytes and HeLa) in the majority of cases internalize external objects through pinocytosis, engulfing

extracellular fluid containing small molecules or solutes in vesicles with a maximal cut-off of 90-120 nm. Such dimensional limit of the objects that can be uptaken by phagocytes or non phagocytes is important in our experimental context, as we have found that SiO_2-NPs (whose monodispersed size is 25-32 nm) upon contact with serum form larger structures (big aggregates of 200-500 nm diameter when serum is defective and small aggregates of 40-80 nm diameter when serum in excess), so that they are still easily engulfed by monocytes and macrophages (localizing into acidic endo-phagosomes) but minimally captured by lymphocytes and HeLa cells (accumulating on the plasma membrane). In the case of a serum free condition, the difference between phagocytic and non phagocytic cells appears less pronounced, as NPs are present only in their small monodispersed form. However, our data suggest that phagocytes (in particular macrophages) internalize SiO_2-NPs better then HeLa cells, and are therefore more sensitive to their effects. In conclusion we found that serum influence on SiO_2-NPs biological effects is much more relevant (that is *protective*) for non phagocytic cells than for phagocytes, as the latter can still internalize large nanoparticles-serum protein complexes via phagocytosis and may possibly still interact with a silicon surface through serum proteins-independent mechanisms (for example, by the scavenger receptor MARCO as reported in [175,176]) that allow NPs storage into intracellular compartments. We also found that alive cells can accumulate into acidic endo-lysosomes a maximal amount of NPs (defined "critical intracellular load"), above which cytotoxicity and pro-inflammatory events initiate leading to a catastrophic cellular death. Phagocytes may reach this "critical load" at lower NPs doses (as they have a better ability to uptake particles) than non phagocytes, and so result more sensitive to NPs treatment (Figure 56).

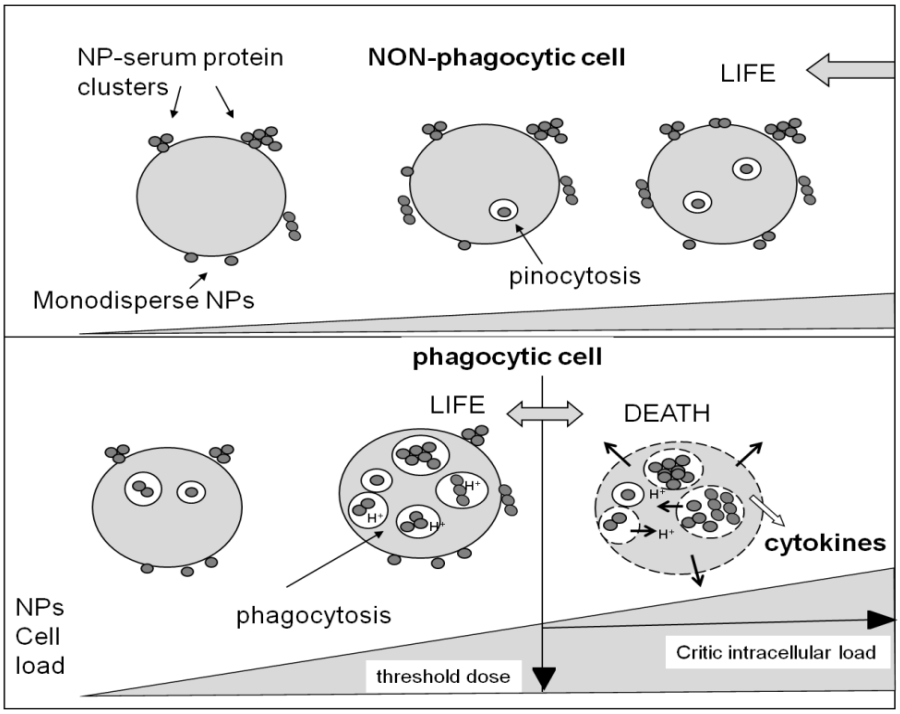

Figure 56: Model of differential interaction/cytotoxicity of SiO_2-NPs/serum proteins complexes in non phagocytes (lymphocytes and HeLa) and phagocytes (monocytes and macrophages).

To understand the link between NPs accumulation in endo-lysosomal vesicles and the cytotoxicity/pro-inflammatory responses occurring in phagocytes we started from the literature. It is in fact reported that, for example, silica crystals accumulation in acidic compartments can induce their destabilization and rupture, leading to the release into the cytosol of several lytic enzymes -proteases, hydrolases, lipases- able to dismantle the cell and to activate inflammatory pathway (e.g., NLRP3 inflammasome) [56]. We tried to better characterize this process using our two phagocytic models and found unexpected and interesting differences. We initially discovered that, in the correspondence of SiO_2-NPs cytotoxicity threshold, endo-lysosomal compartments containing NPs undergo disruption (confirming data already present in literature). An additional result was that, in the presence of serum, endo-lysosomal acidic pH is important in determining NPs cytotoxic potential in monocytes, in fact in the presence of neutralizing agents (NH_4Cl and BafAI) SiO_2 -NPs LD50s were shifted to higher values, indicating a protective effect. This could be due to a possible rearrangement of the protein corona of NPs at pH values (4-5) lower than in normal condition (7). Alternatively, an enhanced activation and activity of lytic enzymes at acidic pH may determine not only a more efficient disruption of cellular structures but also a rapid degradation of NPs corona with the consequent exposure of the nude silicon surface, able to exert adverse effects simply “by contact”.

Our data, indicating that nor protein pattern bound to SiO_2-NPs nor that the rough activity of NPs on cells (intended as plasma membrane activity and evaluated by hemolysis assays in the presence of 10% FCS) change significantly between acidic (5) and neutral (7.2) pH, highlight the major importance of proteases activation by acidic pH for NPs cytotoxicity. Interestingly, the dependence of SiO_2-NPs cytotoxicity on acidic pH is much less pronounced in macrophages. This could be due to several still unidentified aspects, such as additional SiO_2-NPs cytotoxicity mechanisms not dependent on pH or to a different binding and internalization route on NPs-protein complexes in comparison to monocytes, attributed to the different expression levels of some membrane receptors (e.g., the scavenger receptor B1, implicated in HDL uptake) recognizing proteins present in SiO_2 NPs corona. Another interesting result was that in both cellular types the SiO_2 NPs – induction of pro inflammatory cytokines was partially inhibited by acidic compartments neutralization, despite this poorly interferes with monocytes/macrophages activation by the classical agonist LPS. Focusing on IL-1β (as the main pro-inflammatory mediator induced by particulate structures upon NLRP3 inflammasome activation), it has to be reminded that its production requires a "priming step" (throughout pro-IL1β mRNA is synthesized by a transcriptional step and pro-IL1β is produced by a translational step), and an "activation step" (in which NLRP3 inflammasome is assembled and activated through a mechanism either dependent on ROS generation, ATP binding to its receptor or lysosomal proteases activity), resulting in caspase 1 mediated processing of pro IL-1β into IL-1β, that is released extracellularly. Our previous results (not presented in this thesis) demonstrated by Real Time PCR analysis that SiO_2-NPs induce IL-1β mRNA transcription. Here we firstly show by Western Blot analysis that IL-1β mRNA is translated into IL-1β immature form and subsequently cleaved into mature IL-1β by caspase 1 (in fact, the blockage of caspase 1 through the inhibitor YVAD strongly reduces this process). Since caspase 1 activation is, according to the literature, the last event before IL-1β production, we investigated possible steps occurring "upstream", important for the NLRP3 activation. The fact that acidic compartments neutralization partially reduces IL-1β levels clearly indicates that the lysosomal proteases most likely released upon lysosomal rupture could process a hypothetical substrate able to activate NLRP3. However, as the IL-1β inhibition was not complete, we studied other possible mechanisms involved in inflammasome activation, in particular the binding of ATP to its membrane receptor P2X7. We found that also by preventing the binding of ATP to P2X7

through a competitor (oATP) IL-1β levels were partially diminished, indicating that also this pathway contributes to SiO_2-NPs NALP3 activation. In future experiments, it would be interesting to evaluate how acidic compartments neutralization and P2X7 blockage could influence caspase 1 activation, since it is supposed that they act upstream.

With the aim to link the cytotoxic and pro inflammatory events, we investigated if caspase 1 and P2X7 inhibition could affect also cellular death, thinking about a possible pyroptotic mortality mechanism or about a paracrine-endocrine danger signal constituted by extracellular ATP. Curiously, as for acidic compartments neutralization, SiO_2-NPs LD50 was lowered by the presence of YVAD (strong reduction) or oATP (poor reduction) in monocytes after treatment for a long time (20 h), while in macrophages any important effect was observed at any time. This result reinforced the hypothesis that SiO_2-NPs treatment induces different death modalities in monocytes and macrophages. In particular, in monocytes a more complex mechanism similar to pyroptosis (blocked by caspase 1 inhibition) and depending on endo-lysosomal acidic pH is initiated, while in macrophages cellular death appears to be due to a simpler oncotic mechanism. Such dissimilarity between the two cellular models is less evident looking at pro-inflammatory cytokines production (resulting always reduced after treatment with YVAD, oATP or acidic compartments neutralizers), probably because in such way these agonists interfere with inflammasome activation by SiO_2-NPs.

In addition to the NPs endocytosis-dependent cellular death described up to here, SiO_2-NPs can kill cells also by simply interacting with plasma membrane, for example, in a serum free condition or when target cells are completely unable to internalize external entities (such as erythrocytes). Amorphous silica is known to effectively bind biological membranes, as its silanol groups (SiOH) exposed on the surface can form H bonds with the oxygens of PO_4^- groups of phospholipids and, alternatively, deprotonated negatively charged silanols (SiO^-) can establish an electrostatic interaction with the positively charged quaternary ammonium moiety of phospholipids (like phosphatidylcholine) [177]. Such direct binding causes a rapid and strong cellular disruption, as demonstrated by all our experiments carried out in the absence of serum. For a better comprehension of this cytotoxicity mechanism, we firstly choose the model of red blood cells lysis to investigate if silanols protonation state could modify SiO_2-NPs membranolytic effect. We found that at neutral pH (7.2) cellular lysis occurred at higher NPs doses than at acidic pH (5), consistently with the idea of a reduced interaction between silica surface and biological

membrane components by increasing pH values. We also found that, in the absence of serum, both monocytes and macrophages were not protected by lysosomal compartments neutralization and caspase 1 inhibition. A plausible explanation of this result could be that, since in a serum free condition SiO_2-NPs are mainly located on the plasma membrane without being internalized into the cells, the cytotoxicity mechanism is no more dependent on events occurring intracellularly (as caspase 1 or lysosomal proteases activation) registered in particular in monocytes in the presence of 10% FCS. On the other hand, contrary to hemolysis carried out at pH 5.2 or 7, treatment with NH_4Cl or Bafilomycin AI does not show any protective effect as this two neutralizer agents act at intracellular vesicles level, without affecting silanol groups protonation state when NPs remain in the medium. However, also in serum free condition SiO_2-NPs – induced pro inflammatory cytokines were partially inhibited in the presence of YVAD, NH_4Cl and BafAI, indicating that before the complete cellular lysis some dangerous signals such as ATP secretion (able to bind its membrane receptor) or ROS production (possibly leading to lysosomal destabilization through membrane lipids peroxidation) may be activated, with the consequent recruitment and switching on of NLRP3. So, in general we can conclude that SiO_2-NPs cytotoxic event is always associated to the secretion of pro inflammatory mediators, but they don't necessary strictly and "linearly" depend on the same pathway (in fact in the presence of various inhibitors they behave differently).

After defining the main differences between SiO_2-NPs cytotoxicity mechanism in our two myeloid phagocytic cellular models in the presence or in the absence of serum, we concentrated on the first condition as it is more representative of a possible *in vivo* situation (referring to NPs injected into the blood stream as drug carriers or imaging agents). It is universally accepted that NPs exert their biological effects on cellular populations they come in contact with not as entities *per se* but dressed with macromolecules (over all proteins) present in the surrounding environment. Hence, we identified the main serum/plasma proteins absorbed to SiO_2-NPs surface and we correlated them with NPs biological activity. The first main finding emerging was that SiO_2-NPs bind to proteins with different affinities, with an higher propensity for Apolipoproteins (AI and AII, components of HDL complexes) and a low preference for albumin, despite this is the most plentiful serum/plasma protein. This result (evident from experiments carried out with both FCS and HP) is in agreement with the literature [31,32,178] and probably due to a general specific lipoproteins-NPs interaction driven by

their similar size/curvature. In addition, other proteins forming SiO_2-NPs corona have been identified (IgG, HRG and ApoCIII for HP, plasminogen and hemoglobin for FCS). Concentrating on HDL and albumin, we found multiple evidences suggesting that they differentially contribute to NPs biological activity, with a higher protection against cytotoxicity of HDL. First, in a condition of HDL excess (HP *vs* FCS and FCS *vs* delipidated FCS) SiO_2-NPs adverse effects were strongly reduced. Second, in the presence of certain FCS concentration (e.g.10%), SiO_2-NPs cytotoxicity was null/minimal at concentrations in which the protein corona was mainly constituted by HDL with low albumin (below 50-75 μg/ml), while at increasing doses NPs exerted their toxic potential despite their surface was still completely coated (this time, by high albumin and low HDL, because high affinity lipoproteins have been depleted from serum and the additional places on NPs surface could be occupied by the more plentiful albumin). Moreover, we also noted that SiO_2-NPs cytotoxicity (in monocytes) resembles the one of endo-lysosomal/pyroptotic pathway (partially prevented by lysosomal neutralization and caspase 1 blockage) when nanoparticles were administered at doses in which protein corona was still composed by high HDL/low BSA (50-75 μg/ml), while at higher doses (in which albumin is the predominant absorbed protein) cytotoxicity occurred through a membrane-dependent mechanism (not prevented by agonists). These hypotheses were confirmed by some experiments. First, in monocytes SiO_2-NPs LD50 was higher in the presence of medium + HDL than of medium + albumin (however, NPs toxicity was strongly reduced by both proteins if compared to a serum free condition). The fact that NPs similarly associated to cells if incubated with either HDL or BSA excluded that this different sensitivity could be simply due to a differential NPs intracellular load, suggesting a more complex mechanism differently dependent on the two specific proteins. In the matter of this, additional hemolysis experiments (representative of a membrane toxicity) clearly indicated that HDL coated NPs lack membranolytic activity (occurring only when HLD are defective leaving nude spaces on NPs surface), while albumin coated NPs can damage plasma membrane, supporting our initial hypothesis of an endocytic pathway for HDL-NPs, and a membrane action for albumin-NPs. Since NPs coated with albumin showed a hemolytic activity similar, although occurring with a slower kinetics, to nude ones we supposed that its binding to NPs surface could be less stable due to its low affinity, possibly leaving unprotected sites (nude surface) able to exert a membranolytic activity. This latter hypothesis is congruent with our DLS

measurements in 10% FCS, clearly evidencing a drastic increment of the dimension of SiO_2-NPs-serum proteins aggregates in the correspondence of the switch from a NPs corona mostly formed by HDL to a corona in which albumin is predominant (at NPs concentrations > 100 μg/ml), suggesting that low affinity proteins (even if present at doses still able to saturate total NPs surface) interact disorderly with NPs, forming less compact and more dispersed aggregates of large size and leaving unoccupied places onto the surface. A schematic summary of the hypothetical different modality of SiO_2-NPs cytotoxic/pro inflammatory mechanism is illustrated in Figure 57. To get more information and to validate this model, however, additional experiments must be done, for example by investigating NPs cellular localization and testing acidic compartments neutralizer and caspase 1 inhibitor protective effects in the presence of HDL and albumin. It would be interesting to perform this type of analysis on both our phagocytic cellular models (monocytes and macrophages), in order to better understand also their different response to SiO_2-NPs.

In addition to HDL and albumin, we also started a preliminary characterization of the influence on cellular SiO_2-NPs effects by other proteins absorbed on silica surface, preferring the ones from HP to better mimic a putative *in vivo* situation. In particular, we found that IgG and HRG did not protect cells from NPs cytotoxicity (contrary to HDL and albumin) and that, on the contrary, IgG incremented NPs cellular association. So, it would be interesting to analyze the mechanism of NPs cellular interaction driven by these "bad" proteins, paying particular attention on the possible role of receptors, like Fc receptors, normally involved in the phagocytosis of opsonized particles during immune response. Moreover it is interesting to investigate if HRG acts *per se* or by the mediation of IgG (naturally bound to its N terminal). The final aim of this functional analysis of single plasma proteins absorbed on NPs surface would be to design more biocompatible nanoparticles (characterized by low cytotoxic/pro inflammatory potential and stealth properties), by favoring the binding of "protective" proteins and limiting the one of "bad" proteins after their injection into the bloodstream or in other biological fluids. In principle, this might be obtained by synthesizing NPs exposing on their surface different chemical groups able to bind different proteins that can differently modulate NPs biological activity. Encouraging results recently obtained in our laboratory indicate that ORMOSIL-NPs are less toxic/pro-inflammatory than amorphous SiO_2-NPs and, in line with our hypothesis of a differential influence of surface-bound proteins, their protein

corona is mainly composed by apolipoproteins (putative “good” proteins) with a minimal trace of IgG and HRG (putative “bad” proteins adsorbed in a good amount on amorphous SiO_2 NPs surface). In conclusion, despite amorphous SiO_2-NPs (thanks to their cheapness and large availability) are useful for a preliminary characterization of the role of single absorbed proteins in modulating cellular response to nanomaterials, futures studies for the design of a nanoparticle model suitable for nanotheranostic should be performed using ORMOSIL-NPs. First, because they are more biocompatible than SiO_2-NPs (with less cytotoxic/pro-inflammatory and procoagulant effects) [179] and, second, because, due to their synthesis procedure and chemical nature (in particular the presence organic groups), they can be easily modified with different superficial groups, hopefully conferring a higher biocompatibility.

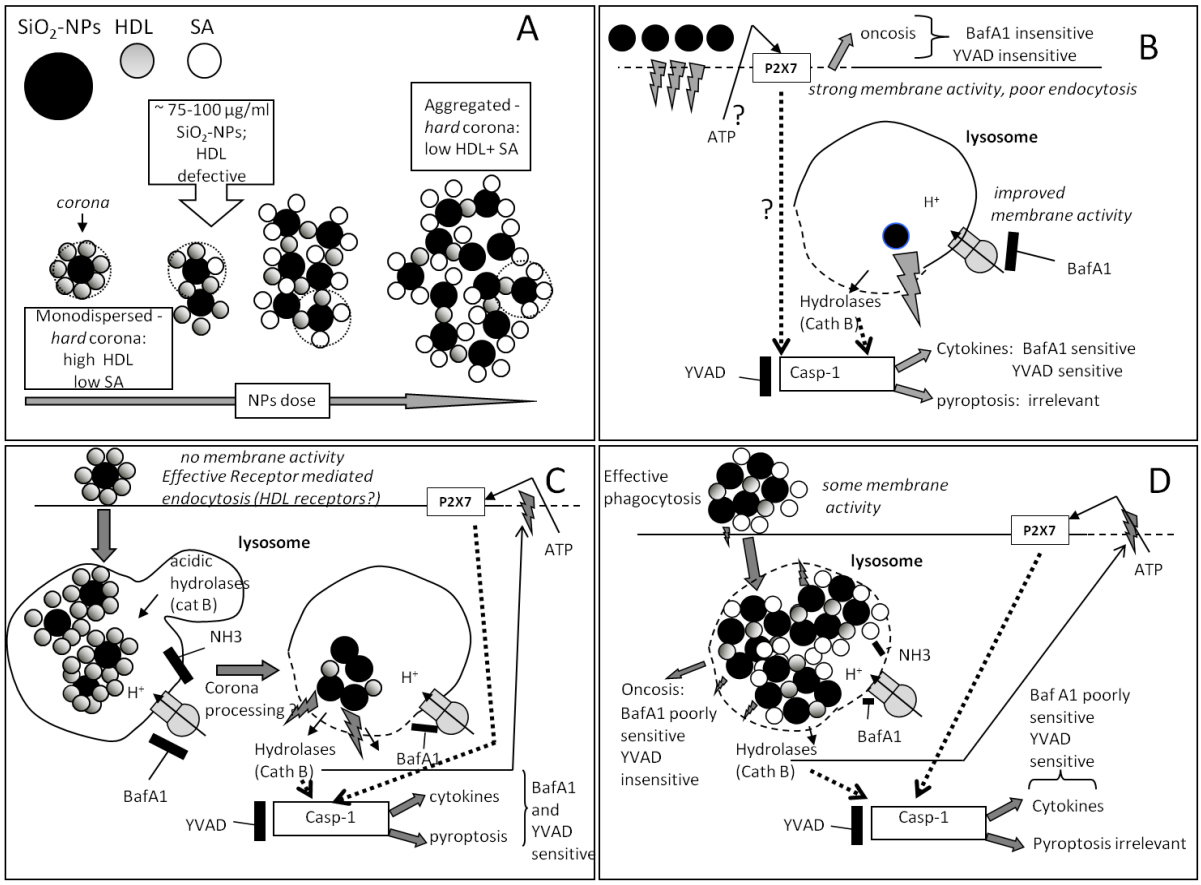

Figure 57: Proposed models of cytotoxic and pro-inflammatory mechanism of SiO_2-NPs in the presence of different NPs-serum proteins complexes in monocytes. (a) different types of nanoagglomerates formed at increasing NPs doses in the same serum concentration (e.g., in 10% FCS). Low NPs concentrations: NPs corona is mainly constituted by HDL; NPs-serum proteins complexes are monodispersed or poorly aggregated and very compact. From the point "HDL defective" (high NPs concentrations): NPs corona is composed by HDL and serum albumin (SA); NPs serum proteins complexes are more dispersed and bigger. The evolution of the NPs corona composition around single particles, as a function of NPs concentration, is highlighted by the dotted line circles. (b) Serum free condition: uncoated NPs directly interact with plasma membrane, causing its damage, the release of danger signals such as ATP, the activation of pro inflammatory pathways and finally an oncotic death. The few NPs endocytosed can destroy endo-lysosomes, with the consequent release of proteases contributing to inflammasome activation. (c) Monodispersed-HDL coated unit condition: NPs-HDL complexes (lacking membrane activity) are endocytosed into endo-lysosomes, where we postulate that the protein corona is processed by acidic proteases/hydrolases with the consequent exposure of nude NPs surface, lysosomal rupture and release of the proteases that activate cell death and inflammatory pathways. (d) Aggregated HDL/SA coated unit condition: large NPs-HDL-SA complexes display some direct membrane activity and are also phagocytized into endo-lysosomes in which they continue to induce an acidic independent membrane damage and the release of proteases activating inflammatory pathways and inducing cellular death. In b, c and d the pathways of NALP3 inflammasome activation are indicated by dotted lines.

5. References

1. Krug HF, Wick P: Nanotoxicology: an interdisciplinary challenge. *Angew. Chem. Int. Ed Engl.* 50(6), 1260-1278 (2011).

2. Buzea C, Pacheco II, Robbie K: Nanomaterials and nanoparticles: sources and toxicity. *Biointerphases* 2(4), MR17-71 (2007).

3. Oberdorster G, Oberdorster E, Oberdorster J: Nanotoxicology: an emerging discipline evolving from studies of ultrafine particles. *Environ. Health Perspect.* 113(7), 823-839 (2005).

4. Buzea C, Pacheco II, Robbie K: Nanomaterials and nanoparticles: sources and toxicity. *Biointerphases* 2(4), MR17-71 (2007).

5. Brulle T, Ju W, Niedermayr P *et al.*: Size-dependent electrocatalytic activity of gold nanoparticles on HOPG and highly boron-doped diamond surfaces. *Molecules* 16(12), 10059-10077 (2011).

6. Chaudhry Q, Scotter M, Blackburn J *et al.*: Applications and implications of nanotechnologies for the food sector. *Food Addit Contam. Part A. Chem. Anal. Control. Expo. Risk Assess.* 25(3), 241-258 (2008).

7. Moghimi SM, Hunter AC, Murray JC: Nanomedicine: current status and future prospects. *FASEB J.* 19(3), 311-330 (2005).

8. Rawat M, Singh D, Saraf S, Saraf S: Nanocarriers: promising vehicle for bioactive drugs. *Biol. Pharm. Bull.* 29(9), 1790-1798 (2006).

9. Zhang L, Gu FX, Chan JM, Wang AZ, Langer RS, Farokhzad OC: Nanoparticles in medicine: therapeutic applications and developments. *Clin. Pharmacol. Ther.* 83(5), 761-769 (2008).

10. Jain KK: Nanomedicine: application of nanobiotechnology in medical practice. *Med. Princ Pract.* 17(2), 89-101 (2008).

11. Drummond DC, Zignani M, Leroux J: Current status of pH-sensitive liposomes in drug delivery. *Prog. Lipid Res.* 39(5), 409-460 (2000).

12. Moghimi SM, Hunter AC, Murray JC: Long-circulating and target-specific nanoparticles: theory to practice. *Pharmacol. Rev.* 53(2), 283-318 (2001).

13. Donaldson K, Stone V, Tran CL, Kreyling W, Borm PJ: Nanotoxicology. *Occup. Environ. Med.* 61(9), 727-728 (2004).

14. Arora S, Rajwade JM, Paknikar KM: Nanotoxicology and in vitro studies: the need of the hour. *Toxicol. Appl. Pharmacol.* 258(2), 151-165 (2012).

15. Oberdorster G, Oberdorster E, Oberdorster J: Nanotoxicology: an emerging discipline evolving from studies of ultrafine particles. *Environ. Health Perspect.* 113(7), 823-839 (2005).

16. Ferin J: Pulmonary retention and clearance of particles. *Toxicol. Lett.* 72(1-3), 121-125 (1994).

17. Oldfors A, Fardeau M: The permeability of the basal lamina at the neuromuscular junction. An ultrastructural study of rat skeletal muscle using particulate tracers. *Neuropathol. Appl. Neurobiol.* 9(6), 419-432 (1983).

18. Warheit DB, Hill LH, George G, Brody AR: Time course of chemotactic factor generation and the corresponding macrophage response to asbestos inhalation. *Am. Rev. Respir. Dis.* 134(1), 128-133 (1986).

19. Warheit DB, Hartsky MA: Role of alveolar macrophage chemotaxis and phagocytosis in pulmonary clearance responses to inhaled particles: comparisons among rodent species. *Microsc. Res. Tech.* 26(5), 412-422 (1993).

20. Toll R, Jacobi U, Richter H, Lademann J, Schaefer H, Blume-Peytavi U: Penetration profile of microspheres in follicular targeting of terminal hair follicles. *J. Invest. Dermatol.* 123(1), 168-176 (2004).

21. Tinkle SS, Antonini JM, Rich BA *et al.*: Skin as a route of exposure and sensitization in chronic beryllium disease. *Environ. Health Perspect.* 111(9), 1202-1208 (2003).

22. Poon VK, Burd A: In vitro cytotoxity of silver: implication for clinical wound care. *Burns* 30(2), 140-147 (2004).

23. Yamago S, Tokuyama H, Nakamura E *et al.*: In vivo biological behavior of a water-miscible fullerene: 14C labeling, absorption, distribution, excretion and acute toxicity. *Chem. Biol.* 2(6), 385-389 (1995).

24. Peters R, Kramer E, Oomen AG *et al.*: Presence of nano-sized silica during in vitro digestion of foods containing silica as a food additive. *ACS Nano* 6(3), 2441-2451 (2012).

25. Aggarwal P, Hall JB, McLeland CB, Dobrovolskaia MA, McNeil SE: Nanoparticle interaction with plasma proteins as it relates to particle biodistribution, biocompatibility and therapeutic efficacy. *Adv. Drug Deliv. Rev.* 61(6), 428-437 (2009).

26. Lynch I, Cedervall T, Lundqvist M, Cabaleiro-Lago C, Linse S, Dawson KA: The nanoparticle-protein complex as a biological entity; a complex fluids and surface science challenge for the 21st century. *Adv. Colloid Interface Sci.* 134-135, 167-174 (2007).

27. Nel AE, Madler L, Velegol D *et al.*: Understanding biophysicochemical interactions at the nano-bio interface. *Nat. Mater.* 8(7), 543-557 (2009).

28. Anderson NL, Polanski M, Pieper R *et al.*: The human plasma proteome: a nonredundant list developed by combination of four separate sources. *Mol. Cell. Proteomics* 3(4), 311-326 (2004).

29. Walkey CD, Chan WC: Understanding and controlling the interaction of nanomaterials with proteins in a physiological environment. *Chem. Soc. Rev.* 41(7), 2780-2799 (2012).

30. Hellstrand E, Lynch I, Andersson A *et al.*: Complete high-density lipoproteins in nanoparticle corona. *FEBS J.* 276(12), 3372-3381 (2009).

31. Allemann E, Gravel P, Leroux JC, Balant L, Gurny R: Kinetics of blood component adsorption on poly(D,L-lactic acid) nanoparticles: evidence of complement C3 component involvement. *J. Biomed. Mater. Res.* 37(2), 229-234 (1997).

32. Goppert TM, Muller RH: Adsorption kinetics of plasma proteins on solid lipid nanoparticles for drug targeting. *Int. J. Pharm.* 302(1-2), 172-186 (2005).

33. Vroman L, Adams AL, Fischer GC, Munoz PC: Interaction of high molecular weight kininogen, factor XII, and fibrinogen in plasma at interfaces. *Blood* 55(1), 156-159 (1980).

34. Tenzer S, Docter D, Rosfa S *et al.*: Nanoparticle size is a critical physicochemical determinant of the human blood plasma corona: a comprehensive quantitative proteomic analysis. *ACS Nano* 5(9), 7155-7167 (2011).

35. Lundqvist M, Stigler J, Elia G, Lynch I, Cedervall T, Dawson KA: Nanoparticle size and surface properties determine the protein corona with possible implications for biological impacts. *Proc. Natl. Acad. Sci. U. S. A.* 105(38), 14265-14270 (2008).

36. Cedervall T, Lynch I, Foy M *et al.*: Detailed identification of plasma proteins adsorbed on copolymer nanoparticles. *Angew. Chem. Int. Ed Engl.* 46(30), 5754-5756 (2007).

37. Dell'Orco D, Lundqvist M, Oslakovic C, Cedervall T, Linse S: Modeling the time evolution of the nanoparticle-protein corona in a body fluid. *PLoS One* 5(6), e10949 (2010).

38. Chakraborti S, Chatterjee T, Joshi P *et al.*: Structure and activity of lysozyme on binding to ZnO nanoparticles. *Langmuir* 26(5), 3506-3513 (2010).

39. Xu Z, Liu XW, Ma YS, Gao HW: Interaction of nano-TiO2 with lysozyme: insights into the enzyme toxicity of nanosized particles. *Environ. Sci. Pollut. Res. Int.* 17(3), 798-806 (2010).

40. Deng ZJ, Liang M, Monteiro M, Toth I, Minchin RF: Nanoparticle-induced unfolding of fibrinogen promotes Mac-1 receptor activation and inflammation. *Nat. Nanotechnol* 6(1), 39-44 (2011).

41. Owens DE,3rd, Peppas NA: Opsonization, biodistribution, and pharmacokinetics of polymeric nanoparticles. *Int. J. Pharm.* 307(1), 93-102 (2006).

42. Aderem A, Underhill DM: Mechanisms of phagocytosis in macrophages. *Annu. Rev. Immunol.* 17, 593-623 (1999).

43. Gref R, Luck M, Quellec P *et al.*: 'Stealth' corona-core nanoparticles surface modified by polyethylene glycol (PEG): influences of the corona (PEG chain length and surface density) and of the core composition on phagocytic uptake and plasma protein adsorption. *Colloids Surf. B Biointerfaces* 18(3-4), 301-313 (2000).

44. He Q, Zhang J, Shi J *et al.*: The effect of PEGylation of mesoporous silica nanoparticles on nonspecific binding of serum proteins and cellular responses. *Biomaterials* 31(6), 1085-1092 (2010).

45. Rio-Echevarria IM, Tavano R, Causin V, Papini E, Mancin F, Moretto A: Water-soluble peptide-coated nanoparticles: control of the helix structure and enhanced differential binding to immune cells. *J. Am. Chem. Soc.* 133(1), 8-11 (2011).

46. Segat D, Tavano R, Donini M *et al.*: Proinflammatory effects of bare and PEGylated ORMOSIL-, PLGA- and SUV-NPs on monocytes and PMNs and their modulation by f-MLP. *Nanomedicine (Lond)* 6(6), 1027-1046 (2011).

47. Ogawara K, Furumoto K, Nagayama S *et al.*: Pre-coating with serum albumin reduces receptor-mediated hepatic disposition of polystyrene nanosphere: implications for rational design of nanoparticles. *J. Control. Release* 100(3), 451-455 (2004).

48. Michaelis K, Hoffmann MM, Dreis S *et al.*: Covalent linkage of apolipoprotein e to albumin nanoparticles strongly enhances drug transport into the brain. *J. Pharmacol. Exp. Ther.* 317(3), 1246-1253 (2006).

49. Kim HR, Gil S, Andrieux K *et al.*: Low-density lipoprotein receptor-mediated endocytosis of PEGylated nanoparticles in rat brain endothelial cells. *Cell Mol. Life Sci.* 64(3), 356-364 (2007).

50. Napierska D, Thomassen LC, Lison D, Martens JA, Hoet PH: The nanosilica hazard: another variable entity. *Part Fibre Toxicol.* 7(1), 39 (2010).

51. Arriagada FJ, Osseo-Asare K: Synthesis of Nanosize Silica in a Nonionic Water-in-Oil Microemulsion: Effects of the Water/Surfactant Molar Ratio and Ammonia Concentration. *J. Colloid Interface Sci.* 211(2), 210-220 (1999).

52. Park EJ, Park K: Oxidative stress and pro-inflammatory responses induced by silica nanoparticles in vivo and in vitro. *Toxicol. Lett.* 184(1), 18-25 (2009).

53. Cassel SL, Eisenbarth SC, Iyer SS *et al.*: The Nalp3 inflammasome is essential for the development of silicosis. *Proc. Natl. Acad. Sci. U. S. A.* 105(26), 9035-9040 (2008).

54. Hornung V, Bauernfeind F, Halle A *et al.*: Silica crystals and aluminum salts activate the NALP3 inflammasome through phagosomal destabilization. *Nat. Immunol.* 9(8), 847-856 (2008).

55. Castranova V, Vallyathan V: Silicosis and coal workers' pneumoconiosis. *Environ. Health Perspect.* 108 Suppl 4, 675-684 (2000).

56. Hornung V, Bauernfeind F, Halle A *et al.*: Silica crystals and aluminum salts activate the NALP3 inflammasome through phagosomal destabilization. *Nat. Immunol.* 9(8), 847-856 (2008).

57. Mossman BT, Churg A: Mechanisms in the pathogenesis of asbestosis and silicosis. *Am. J. Respir. Crit. Care Med.* 157(5 Pt 1), 1666-1680 (1998).

58. Chang JS, Chang KL, Hwang DF, Kong ZL: In vitro cytotoxicitiy of silica nanoparticles at high concentrations strongly depends on the metabolic activity type of the cell line. *Environ. Sci. Technol.* 41(6), 2064-2068 (2007).

59. Liu X, Sun J: Endothelial cells dysfunction induced by silica nanoparticles through oxidative stress via JNK/P53 and NF-kappaB pathways. *Biomaterials* 31(32), 8198-8209 (2010).

60. Costantini LM, Gilberti RM, Knecht DA: The phagocytosis and toxicity of amorphous silica. *PLoS One* 6(2), e14647 (2011).

61. Drescher D, Orts-Gil G, Laube G *et al.*: Toxicity of amorphous silica nanoparticles on eukaryotic cell model is determined by particle agglomeration and serum protein adsorption effects. *Anal. Bioanal Chem.* 400(5), 1367-1373 (2011).

62. Ye Y, Liu J, Chen M, Sun L, Lan M: In vitro toxicity of silica nanoparticles in myocardial cells. *Environ. Toxicol. Pharmacol.* 29(2), 131-137 (2010).

63. Waters KM, Masiello LM, Zangar RC *et al.*: Macrophage responses to silica nanoparticles are highly conserved across particle sizes. *Toxicol. Sci.* 107(2), 553-569 (2009).

64. Lu X, Qian J, Zhou H *et al.*: In vitro cytotoxicity and induction of apoptosis by silica nanoparticles in human HepG2 hepatoma cells. *Int. J. Nanomedicine* 6, 1889-1901 (2011).

65. Sun L, Li Y, Liu X *et al.*: Cytotoxicity and mitochondrial damage caused by silica nanoparticles. *Toxicol. In. Vitro.* 25(8), 1619-1629 (2011).

66. Lin W, Huang YW, Zhou XD, Ma Y: In vitro toxicity of silica nanoparticles in human lung cancer cells. *Toxicol. Appl. Pharmacol.* 217(3), 252-259 (2006).

67. Ye Y, Liu J, Xu J, Sun L, Chen M, Lan M: Nano-SiO2 induces apoptosis via activation of p53 and Bax mediated by oxidative stress in human hepatic cell line. *Toxicol. In. Vitro.* 24(3), 751-758 (2010).

68. Rabolli V, Thomassen LC, Uwambayinema F, Martens JA, Lison D: The cytotoxic activity of amorphous silica nanoparticles is mainly influenced by surface area and not by aggregation. *Toxicol. Lett.* 206(2), 197-203 (2011).

69. Mohamed BM, Verma NK, Prina-Mello A *et al.*: Activation of stress-related signalling pathway in human cells upon SiO2 nanoparticles exposure as an early indicator of cytotoxicity. *J. Nanobiotechnology* 9, 29 (2011).

70. Herd HL, Malugin A, Ghandehari H: Silica nanoconstruct cellular toleration threshold in vitro. *J. Control. Release* 153(1), 40-48 (2011).

71. Dostert C, Petrilli V, Van Bruggen R, Steele C, Mossman BT, Tschopp J: Innate immune activation through Nalp3 inflammasome sensing of asbestos and silica. *Science* 320(5876), 674-677 (2008).

72. Yazdi AS, Guarda G, Riteau N *et al.*: Nanoparticles activate the NLR pyrin domain containing 3 (Nlrp3) inflammasome and cause pulmonary inflammation through release of IL-1alpha and IL-1beta. *Proc. Natl. Acad. Sci. U. S. A.* 107(45), 19449-19454 (2010).

73. Sandberg WJ, Lag M, Holme JA *et al.*: Comparison of non-crystalline silica nanoparticles in IL-1beta release from macrophages. *Part Fibre Toxicol.* 9, 32-8977-9-32 (2012).

74. Morishige T, Yoshioka Y, Inakura H *et al.*: The effect of surface modification of amorphous silica particles on NLRP3 inflammasome mediated IL-1beta production, ROS production and endosomal rupture. *Biomaterials* 31(26), 6833-6842 (2010).

75. Corbalan JJ, Medina C, Jacoby A, Malinski T, Radomski MW: Amorphous silica nanoparticles trigger nitric oxide/peroxynitrite imbalance in human endothelial cells: inflammatory and cytotoxic effects. *Int. J. Nanomedicine* 6, 2821-2835 (2011).

76. Martinon F, Mayor A, Tschopp J: The inflammasomes: guardians of the body. *Annu. Rev. Immunol.* 27, 229-265 (2009).

77. Schroder K, Tschopp J: The inflammasomes. *Cell* 140(6), 821-832 (2010).

78. Bauernfeind F, Ablasser A, Bartok E *et al.*: Inflammasomes: current understanding and open questions. *Cell Mol. Life Sci.* 68(5), 765-783 (2011).

79. Khare S, Luc N, Dorfleutner A, Stehlik C: Inflammasomes and their activation. *Crit. Rev. Immunol.* 30(5), 463-487 (2010).

80. Fujihara M, Muroi M, Tanamoto K, Suzuki T, Azuma H, Ikeda H: Molecular mechanisms of macrophage activation and deactivation by lipopolysaccharide: roles of the receptor complex. *Pharmacol. Ther.* 100(2), 171-194 (2003).

81. Miyake K: Innate recognition of lipopolysaccharide by Toll-like receptor 4-MD-2. *Trends Microbiol.* 12(4), 186-192 (2004).

82. Akashi S, Saitoh S, Wakabayashi Y *et al.*: Lipopolysaccharide interaction with cell surface Toll-like receptor 4-MD-2: higher affinity than that with MD-2 or CD14. *J. Exp. Med.* 198(7), 1035-1042 (2003).

83. Dagenais M, Skeldon A, Saleh M: The inflammasome: in memory of Dr. Jurg Tschopp. *Cell Death Differ.* 19(1), 5-12 (2012).

84. Martinon F, Burns K, Tschopp J: The inflammasome: a molecular platform triggering activation of inflammatory caspases and processing of proIL-beta. *Mol. Cell* 10(2), 417-426 (2002).

85. Stutz A, Golenbock DT, Latz E: Inflammasomes: too big to miss. *J. Clin. Invest.* 119(12), 3502-3511 (2009).

86. Agostini L, Martinon F, Burns K, McDermott MF, Hawkins PN, Tschopp J: NALP3 forms an IL-1beta-processing inflammasome with increased activity in Muckle-Wells autoinflammatory disorder. *Immunity* 20(3), 319-325 (2004).

87. Netea MG, Simon A, van de Veerdonk F, Kullberg BJ, Van der Meer JW, Joosten LA: IL-1beta processing in host defense: beyond the inflammasomes. *PLoS Pathog.* 6(2), e1000661 (2010).

88. Eder C: Mechanisms of interleukin-1beta release. *Immunobiology* 214(7), 543-553 (2009).

89. Dinarello CA: Immunological and inflammatory functions of the interleukin-1 family. *Annu. Rev. Immunol.* 27, 519-550 (2009).

90. Rubartelli A, Cozzolino F, Talio M, Sitia R: A novel secretory pathway for interleukin-1 beta, a protein lacking a signal sequence. *EMBO J.* 9(5), 1503-1510 (1990).

91. MacKenzie A, Wilson HL, Kiss-Toth E, Dower SK, North RA, Surprenant A: Rapid secretion of interleukin-1beta by microvesicle shedding. *Immunity* 15(5), 825-835 (2001).

92. Qu Y, Franchi L, Nunez G, Dubyak GR: Nonclassical IL-1 beta secretion stimulated by P2X7 receptors is dependent on inflammasome activation and correlated with exosome release in murine macrophages. *J. Immunol.* 179(3), 1913-1925 (2007).

93. Brough D, Rothwell NJ: Caspase-1-dependent processing of pro-interleukin-1beta is cytosolic and precedes cell death. *J. Cell. Sci.* 120(Pt 5), 772-781 (2007).

94. Lopez-Castejon G, Brough D: Understanding the mechanism of IL-1beta secretion. *Cytokine Growth Factor Rev.* 22(4), 189-195 (2011).

95. Earnshaw WC, Martins LM, Kaufmann SH: Mammalian caspases: structure, activation, substrates, and functions during apoptosis. *Annu. Rev. Biochem.* 68, 383-424 (1999).

96. Kostura MJ, Tocci MJ, Limjuco G *et al.*: Identification of a monocyte specific pre-interleukin 1 beta convertase activity. *Proc. Natl. Acad. Sci. U. S. A.* 86(14), 5227-5231 (1989).

97. Wilson KP, Black JA, Thomson JA *et al.*: Structure and mechanism of interleukin-1 beta converting enzyme. *Nature* 370(6487), 270-275 (1994).

98. Thornberry NA, Bull HG, Calaycay JR *et al.*: A novel heterodimeric cysteine protease is required for interleukin-1 beta processing in monocytes. *Nature* 356(6372), 768-774 (1992).

99. Miao EA, Rajan JV, Aderem A: Caspase-1-induced pyroptotic cell death. *Immunol. Rev.* 243(1), 206-214 (2011).

100. Zychlinsky A, Prevost MC, Sansonetti PJ: Shigella flexneri induces apoptosis in infected macrophages. *Nature* 358(6382), 167-169 (1992).

101. Fink SL, Cookson BT: Caspase-1-dependent pore formation during pyroptosis leads to osmotic lysis of infected host macrophages. *Cell. Microbiol.* 8(11), 1812-1825 (2006).

102. Fink SL, Cookson BT: Apoptosis, pyroptosis, and necrosis: mechanistic description of dead and dying eukaryotic cells. *Infect. Immun.* 73(4), 1907-1916 (2005).

103. Kepp O, Galluzzi L, Zitvogel L, Kroemer G: Pyroptosis - a cell death modality of its kind? *Eur. J. Immunol.* 40(3), 627-630 (2010).

104. Bergsbaken T, Fink SL, Cookson BT: Pyroptosis: host cell death and inflammation. *Nat. Rev. Microbiol.* 7(2), 99-109 (2009).

105. Fink SL, Bergsbaken T, Cookson BT: Anthrax lethal toxin and Salmonella elicit the common cell death pathway of caspase-1-dependent pyroptosis via distinct mechanisms. *Proc. Natl. Acad. Sci. U. S. A.* 105(11), 4312-4317 (2008).

106. Brennan MA, Cookson BT: Salmonella induces macrophage death by caspase-1-dependent necrosis. *Mol. Microbiol.* 38(1), 31-40 (2000).

107. Hilbi H, Moss JE, Hersh D *et al.*: Shigella-induced apoptosis is dependent on caspase-1 which binds to IpaB. *J. Biol. Chem.* 273(49), 32895-32900 (1998).

108. Mariathasan S, Weiss DS, Dixit VM, Monack DM: Innate immunity against Francisella tularensis is dependent on the ASC/caspase-1 axis. *J. Exp. Med.* 202(8), 1043-1049 (2005).

109. Reisetter AC, Stebounova LV, Baltrusaitis J *et al.*: Induction of inflammasome-dependent pyroptosis by carbon black nanoparticles. *J. Biol. Chem.* 286(24), 21844-21852 (2011).

110. Li H, Willingham SB, Ting JP, Re F: Cutting edge: inflammasome activation by alum and alum's adjuvant effect are mediated by NLRP3. *J. Immunol.* 181(1), 17-21 (2008).

111. Halle A, Hornung V, Petzold GC *et al.*: The NALP3 inflammasome is involved in the innate immune response to amyloid-beta. *Nat. Immunol.* 9(8), 857-865 (2008).

112. Mariathasan S, Weiss DS, Newton K *et al.*: Cryopyrin activates the inflammasome in response to toxins and ATP. *Nature* 440(7081), 228-232 (2006).

113. Cassel SL, Joly S, Sutterwala FS: The NLRP3 inflammasome: a sensor of immune danger signals. *Semin. Immunol.* 21(4), 194-198 (2009).

114. Kahlenberg JM, Dubyak GR: Mechanisms of caspase-1 activation by P2X7 receptor-mediated K+ release. *Am. J. Physiol. Cell. Physiol.* 286(5), C1100-8 (2004).

115. Kahlenberg JM, Lundberg KC, Kertesy SB, Qu Y, Dubyak GR: Potentiation of caspase-1 activation by the P2X7 receptor is dependent on TLR signals and requires NF-kappaB-driven protein synthesis. *J. Immunol.* 175(11), 7611-7622 (2005).

116. Petrilli V, Papin S, Dostert C, Mayor A, Martinon F, Tschopp J: Activation of the NALP3 inflammasome is triggered by low intracellular potassium concentration. *Cell Death Differ.* 14(9), 1583-1589 (2007).

117. Yamin TT, Ayala JM, Miller DK: Activation of the native 45-kDa precursor form of interleukin-1-converting enzyme. *J. Biol. Chem.* 271(22), 13273-13282 (1996).

118. Walev I, Reske K, Palmer M, Valeva A, Bhakdi S: Potassium-inhibited processing of IL-1 beta in human monocytes. *EMBO J.* 14(8), 1607-1614 (1995).

119. Fitz JG: Regulation of cellular ATP release. *Trans. Am. Clin. Climatol. Assoc.* 118, 199-208 (2007).

120. Ferrari D, Pizzirani C, Adinolfi E *et al.*: The P2X7 receptor: a key player in IL-1 processing and release. *J. Immunol.* 176(7), 3877-3883 (2006).

121. Di Virgilio F, Chiozzi P, Ferrari D *et al.*: Nucleotide receptors: an emerging family of regulatory molecules in blood cells. *Blood* 97(3), 587-600 (2001).

122. Marina-Garcia N, Franchi L, Kim YG *et al.*: Pannexin-1-mediated intracellular delivery of muramyl dipeptide induces caspase-1 activation via cryopyrin/NLRP3 independently of Nod2. *J. Immunol.* 180(6), 4050-4057 (2008).

123. Pelegrin P, Surprenant A: Pannexin-1 mediates large pore formation and interleukin-1beta release by the ATP-gated P2X7 receptor. *EMBO J.* 25(21), 5071-5082 (2006).

124. Tschopp J, Schroder K: NLRP3 inflammasome activation: The convergence of multiple signalling pathways on ROS production? *Nat. Rev. Immunol.* 10(3), 210-215 (2010).

125. Allison AC, Harington JS, Birbeck M: An examination of the cytotoxic effects of silica on macrophages. *J. Exp. Med.* 124(2), 141-154 (1966).

126. Zhou R, Tardivel A, Thorens B, Choi I, Tschopp J: Thioredoxin-interacting protein links oxidative stress to inflammasome activation. *Nat. Immunol.* 11(2), 136-140 (2010).

127. Fettucciari K, Rosati E, Scaringi L *et al.*: Group B Streptococcus induces apoptosis in macrophages. *J. Immunol.* 165(7), 3923-3933 (2000).

128. Netea MG, Nold-Petry CA, Nold MF *et al.*: Differential requirement for the activation of the inflammasome for processing and release of IL-1beta in monocytes and macrophages. *Blood* 113(10), 2324-2335 (2009).

129. Yang H, Rivera Z, Jube S *et al.*: Programmed necrosis induced by asbestos in human mesothelial cells causes high-mobility group box 1 protein release and resultant inflammation. *Proc. Natl. Acad. Sci. U. S. A.* 107(28), 12611-12616 (2010).

130. Trump BF, Berezesky IK, Chang SH, Phelps PC: The pathways of cell death: oncosis, apoptosis, and necrosis. *Toxicol. Pathol.* 25(1), 82-88 (1997).

131. Schultz DR, Harrington WJ,Jr: Apoptosis: programmed cell death at a molecular level. *Semin. Arthritis Rheum.* 32(6), 345-369 (2003).

132. Majno G, Joris I: Apoptosis, oncosis, and necrosis. An overview of cell death. *Am. J. Pathol.* 146(1), 3-15 (1995).

133. Gozal E, Ortiz LA, Zou X, Burow ME, Lasky JA, Friedman M: Silica-induced apoptosis in murine macrophage: involvement of tumor necrosis factor-alpha and nuclear factor-kappaB activation. *Am. J. Respir. Cell Mol. Biol.* 27(1), 91-98 (2002).

134. Thibodeau MS, Giardina C, Knecht DA, Helble J, Hubbard AK: Silica-induced apoptosis in mouse alveolar macrophages is initiated by lysosomal enzyme activity. *Toxicol. Sci.* 80(1), 34-48 (2004).

135. van Engeland M, Nieland LJ, Ramaekers FC, Schutte B, Reutelingsperger CP: Annexin V-affinity assay: a review on an apoptosis detection system based on phosphatidylserine exposure. *Cytometry* 31(1), 1-9 (1998).

136. Vermes I, Haanen C, Steffens-Nakken H, Reutelingsperger C: A novel assay for apoptosis. Flow cytometric detection of phosphatidylserine expression on early apoptotic cells using fluorescein labelled Annexin V. *J. Immunol. Methods* 184(1), 39-51 (1995).

137. Ohkuma S, Poole B: Fluorescence probe measurement of the intralysosomal pH in living cells and the perturbation of pH by various agents. *Proc. Natl. Acad. Sci. U. S. A.* 75(7), 3327-3331 (1978).

138. Holian A, Kelley K, Hamilton RF,Jr: Mechanisms associated with human alveolar macrophage stimulation by particulates. *Environ. Health Perspect.* 102 Suppl 10, 69-74 (1994).

139. Beamer CA, Holian A: Silica suppresses Toll-like receptor ligand-induced dendritic cell activation. *FASEB J.* 22(6), 2053-2063 (2008).

140. Laliberte RE, Eggler J, Gabel CA: ATP treatment of human monocytes promotes caspase-1 maturation and externalization. *J. Biol. Chem.* 274(52), 36944-36951 (1999).

141. Piccini A, Carta S, Tassi S, Lasiglie D, Fossati G, Rubartelli A: ATP is released by monocytes stimulated with pathogen-sensing receptor ligands and induces IL-1beta and

IL-18 secretion in an autocrine way. *Proc. Natl. Acad. Sci. U. S. A.* 105(23), 8067-8072 (2008).

142. Murgia M, Hanau S, Pizzo P, Rippa M, Di Virgilio F: Oxidized ATP. An irreversible inhibitor of the macrophage purinergic P2Z receptor. *J. Biol. Chem.* 268(11), 8199-8203 (1993).

143. Miggin SM, Palsson-McDermott E, Dunne A *et al.*: NF-kappaB activation by the Toll-IL-1 receptor domain protein MyD88 adapter-like is regulated by caspase-1. *Proc. Natl. Acad. Sci. U. S. A.* 104(9), 3372-3377 (2007).

144. Li P, Allen H, Banerjee S *et al.*: Mice deficient in IL-1 beta-converting enzyme are defective in production of mature IL-1 beta and resistant to endotoxic shock. *Cell* 80(3), 401-411 (1995).

145. Meunier E, Coste A, Olagnier D *et al.*: Double-walled carbon nanotubes trigger IL-1beta release in human monocytes through Nlrp3 inflammasome activation. *Nanomedicine* 8(6), 987-995 (2012).

146. Poole B, Ohkuma S: Effect of weak bases on the intralysosomal pH in mouse peritoneal macrophages. *J. Cell Biol.* 90(3), 665-669 (1981).

147. Ohkuma S, Poole B: Fluorescence probe measurement of the intralysosomal pH in living cells and the perturbation of pH by various agents. *Proc. Natl. Acad. Sci. U. S. A.* 75(7), 3327-3331 (1978).

148. Bowman EJ, Siebers A, Altendorf K: Bafilomycins: a class of inhibitors of membrane ATPases from microorganisms, animal cells, and plant cells. *Proc. Natl. Acad. Sci. U. S. A.* 85(21), 7972-7976 (1988).

149. Beyenbach KW, Wieczorek H: The V-type H+ ATPase: molecular structure and function, physiological roles and regulation. *J. Exp. Biol.* 209(Pt 4), 577-589 (2006).

150. Forgac M: Vacuolar ATPases: rotary proton pumps in physiology and pathophysiology. *Nat. Rev. Mol. Cell Biol.* 8(11), 917-929 (2007).

151. Arata Y, Nishi T, Kawasaki-Nishi S, Shao E, Wilkens S, Forgac M: Structure, subunit function and regulation of the coated vesicle and yeast vacuolar (H(+))-ATPases. *Biochim. Biophys. Acta* 1555(1-3), 71-74 (2002).

152. Jang CH, Choi JH, Byun MS, Jue DM: Chloroquine inhibits production of TNF-alpha, IL-1beta and IL-6 from lipopolysaccharide-stimulated human monocytes/macrophages by different modes. *Rheumatology (Oxford)* 45(6), 703-710 (2006).

153. Wang R, Kovalchin JT, Muhlenkamp P, Chandawarkar RY: Exogenous heat shock protein 70 binds macrophage lipid raft microdomain and stimulates phagocytosis, processing, and MHC-II presentation of antigens. *Blood* 107(4), 1636-1642 (2006).

154. Nuutila J, Lilius EM: Flow cytometric quantitative determination of ingestion by phagocytes needs the distinguishing of overlapping populations of binding and ingesting cells. *Cytometry A.* 65(2), 93-102 (2005).

155. Shi J, Hedberg Y, Lundin M, Odnevall Wallinder I, Karlsson HL, Moller L: Hemolytic properties of synthetic nano- and porous silica particles: the effect of surface properties and the protection by the plasma corona. *Acta Biomater.* 8(9), 3478-3490 (2012).

156. Adams RL, Bird RJ: Review article: Coagulation cascade and therapeutics update: relevance to nephrology. Part 1: Overview of coagulation, thrombophilias and history of anticoagulants. *Nephrology (Carlton)* 14(5), 462-470 (2009).

157. Norris LA: Blood coagulation. *Best Pract. Res. Clin. Obstet. Gynaecol.* 17(3), 369-383 (2003).

158. Nicholson JP, Wolmarans MR, Park GR: The role of albumin in critical illness. *Br. J. Anaesth.* 85(4), 599-610 (2000).

159. Davidson WS, Thompson TB: The structure of apolipoprotein A-I in high density lipoproteins. *J. Biol. Chem.* 282(31), 22249-22253 (2007).

160. Rader DJ: Molecular regulation of HDL metabolism and function: implications for novel therapies. *J. Clin. Invest.* 116(12), 3090-3100 (2006).

161. Hersberger M, von Eckardstein A: Modulation of high-density lipoprotein cholesterol metabolism and reverse cholesterol transport. *Handb. Exp. Pharmacol.* (170)(170), 537-561 (2005).

162. Lewis GF, Rader DJ: New insights into the regulation of HDL metabolism and reverse cholesterol transport. *Circ. Res.* 96(12), 1221-1232 (2005).

163. Kwiterovich PO,Jr: The metabolic pathways of high-density lipoprotein, low-density lipoprotein, and triglycerides: a current review. *Am. J. Cardiol.* 86(12A), 5L-10L (2000).

164. Mahley RW, Innerarity TL, Rall SC,Jr, Weisgraber KH: Plasma lipoproteins: apolipoprotein structure and function. *J. Lipid Res.* 25(12), 1277-1294 (1984).

165. Zannis VI, Chroni A, Krieger M: Role of apoA-I, ABCA1, LCAT, and SR-BI in the biogenesis of HDL. *J. Mol. Med. (Berl)* 84(4), 276-294 (2006).

166. Bolanos-Garcia VM, Miguel RN: On the structure and function of apolipoproteins: more than a family of lipid-binding proteins. *Prog. Biophys. Mol. Biol.* 83(1), 47-68 (2003).

167. Poon IK, Hulett MD, Parish CR: Histidine-rich glycoprotein is a novel plasma pattern recognition molecule that recruits IgG to facilitate necrotic cell clearance via FcgammaRI on phagocytes. *Blood* 115(12), 2473-2482 (2010).

168. Gorgani NN, Smith BA, Kono DH, Theofilopoulos AN: Histidine-rich glycoprotein binds to DNA and Fc gamma RI and potentiates the ingestion of apoptotic cells by macrophages. *J. Immunol.* 169(9), 4745-4751 (2002).

169. Blank M, Shoenfeld Y: Histidine-rich glycoprotein modulation of immune/autoimmune, vascular, and coagulation systems. *Clin. Rev. Allergy Immunol.* 34(3), 307-312 (2008).

170. Jones AL, Hulett MD, Parish CR: Histidine-rich glycoprotein: A novel adaptor protein in plasma that modulates the immune, vascular and coagulation systems. *Immunol. Cell Biol.* 83(2), 106-118 (2005).

171. Poon IK, Patel KK, Davis DS, Parish CR, Hulett MD: Histidine-rich glycoprotein: the Swiss Army knife of mammalian plasma. *Blood* 117(7), 2093-2101 (2011).

172. Forte TM, Bell-Quint JJ, Cheng F: Lipoproteins of fetal and newborn calves and adult steer: a study of developmental changes. *Lipids* 16(4), 240-245 (1981).

173. Barrett EG, Johnston C, Oberdorster G, Finkelstein JN: Silica binds serum proteins resulting in a shift of the dose-response for silica-induced chemokine expression in an alveolar type II cell line. *Toxicol. Appl. Pharmacol.* 161(2), 111-122 (1999).

174. Leroux JC, De Jaeghere F, Anner B, Doelker E, Gurny R: An investigation on the role of plasma and serum opsonins on the internalization of biodegradable poly(D,L-lactic acid) nanoparticles by human monocytes. *Life Sci.* 57(7), 695-703 (1995).

175. Hamilton RF,Jr, Thakur SA, Mayfair JK, Holian A: MARCO mediates silica uptake and toxicity in alveolar macrophages from C57BL/6 mice. *J. Biol. Chem.* 281(45), 34218-34226 (2006).

176. Thakur SA, Hamilton R,Jr, Pikkarainen T, Holian A: Differential binding of inorganic particles to MARCO. *Toxicol. Sci.* 107(1), 238-246 (2009).

177. Sahai N: Biomembrane phospholipid-oxide surface interactions: crystal chemical and thermodynamic basis. *J. Colloid Interface Sci.* 252(2), 309-319 (2002).

178. Monopoli MP, Walczyk D, Campbell A *et al.*: Physical-chemical aspects of protein corona: relevance to in vitro and in vivo biological impacts of nanoparticles. *J. Am. Chem. Soc.* 133(8), 2525-2534 (2011).

179. Tavano R, Segat D, Reddi E *et al.*: Procoagulant properties of bare and highly PEGylated vinyl-modified silica nanoparticles. *Nanomedicine (Lond)* 5(6), 881-896 (2010).

180. Lynch I, Dawson Kennet A: Protein-nanoparticle interactions. *Nanotoday.* 3, 40-47 (2008).

181.Sanfins E, Dairou J, Rodrigues-Lima F, Dupret JM: Nanoparticle-protein interactions: from crucial plasma proteins to key enzymes. *Journal of physics.* (304), 1-6 (2011).

182. Barbè C, Bartlett J, Kong L, Finnie K, Lin H, Larkin M, Calleja S, Bush A, Calleja G: Silica particles: a novel drug delivery system. *Advanced Materials* 16(21), 1959-1966 (2004).

183. Stober W, Fink A, Bohn E: Controlled growth of monodisperse silica spheres in the micron size range. *J. Colloid Interface Sci*. 26, 62-69 (1968).

184. Yu K, Grabinski CM, Shrand AM, Murdock RC *et al*: Toxicity of amorphous silica nanoparticles in mouse keratinocytes. *J. Nanopart. Res.* 11, 15-24 (2009).

185. Iyer SS, Pulskens WP, Sadler JJ, Butter LM *et al*: Necrotic cells trigger a sterile inflammatory response through the Nlrp3 inflammasome. *PNAS* 106(48), 20388-20393 (2009).

186. Fedeli C, Selvestrel F, Tavano R, Segat D, Mancin F, Papini E: Catastrophic inflammatory death of monocytes and macrophages by overtaking of a critical dose of endocytosed synthetic amorphous silica nanoparticles/serum protein complexes. *Nanomedicine (London)*. Epub ahead of print (2012).